ECMWF COPERNICUS REPORT

Copernicus Climate Change Service

Product User Guide and Specification (PUGS) – Main document for Greenhouse Gas (GHG: CO_2 & CH_4) data set CDR 4 (2003-2019)

C3S_312b_Lot2_DLR – Atmosphere

Issued by: Michael Buchwitz, University of Bremen,

Institute of Environmental Physics (IUP)

Date: 17/09/2020

Ref: C3S_D312b_Lot2.3.2.3-v2.0_PUGS-GHG_MAIN_v4.0

Official reference number service contract: 2018/C3S_312b_Lot2_DLR/SC1

Contributors

INSTITUTE OF ENVIRONMENTAL PHYSICS (IUP), UNIVERSITY OF BREMEN, BREMEN, GERMANY
(IUP)
M. Buchwitz
M. Reuter
O. Schneising-Weigel

SRON NETHERLANDS INSTITUTE FOR SPACE RESEARCH, UTRECHT, THE NETHERLANDS
(SRON)
I. Aben
L. Wu
O. P. Hasekamp

UNIVERSITY OF LEICESTER, LEICESTER, UK
(UoL)
H. Boesch
A. Di Noia

CENTRE NATIONAL DE LA RECHERCHE SCIENTIFIQUE (CNRS), LABORATOIRE DE METEOROLOGIE DYNAMIQUE (LMD), PALAISEAU, FRANCE
(LMD/CNRS)
C. Crevoisier
R. Armante

Table of Contents

History of modifications

Version	Date	Description of modification	Chapters / Sections
1.3	20-October-2017	New document for data set CDR1 (temporal coverage: 2003-2016)	All
2.0	16-October-2018	Update for data set CDR2 (temporal coverage: 2003-2017)	All
3.0	12-August-2019	Update for data set CDR3 (temporal coverage: 2003-2018)	All
3.1	03-November-2019	Update after review by Assimila: Corrections of typos and broken links. Other modifications: Update of Figs. 1 and 2.	All
4.0 beta	18-August-2020	Update for data set CDR4 (temporal coverage: 2003-2019)	All
4.0	17-September-2020	Correction of typos and issues with numbering of tables and figures after review by Assimila	All

Related documents

Reference ID	Document
D1	**GCOS-154:** Global Climate Observing System (GCOS): SYSTEMATIC OBSERVATION REQUIREMENTS FOR SATELLITE-BASED DATA PRODUCTS FOR CLIMATE - 2011 Update - Supplemental details to the satellite-based component of the "Implementation Plan for the Global Observing System for Climate in Support of the UNFCCC (2010 Update)", December 2011, prepared by World Meteorological Organization (WMO), Intergovernmental Oceanographic Commission, United Nations Environment Programme (UNEP), International Council for Science, Doc.: GCOS 154, link: http://cci.esa.int/sites/default/files/gcos-154.pdf, 2011.
D2	**GCOS-200:** The Global Observing System for Climate: Implementation Needs, World Meteorological Organization (WMO), GCOS-200 (GOOS-214), pp. 325, link: http://unfccc.int/files/science/workstreams/systematic_observation/application/pdf/gcos_ip_10oct2016.pdf, 2016.
D3	**ESA-CCI-GHG-URDv2.1:** Chevallier, F., et al., User Requirements Document (URD), ESA Climate Change Initiative (CCI) GHG-CCI project, Version 2.1, 19 Oct 2016, 2016.
D4	**TRD GAD GHG, 2020:** Buchwitz, M., Aben, I., Armante, R., Boesch, H., Crevoisier, C., Hasekamp, O. P., Wu, L.., Reuter, M., Schneising-Weigel, O., Target Requirement and Gap Analysis Document, Copernicus Climate Change Service (C3S) project on satellite-derived Essential Climate Variable (ECV) Greenhouse Gases (CO_2 and CH_4) data products (project C3S_312b_Lot2), Version 2.11, 9-April-2020, pp. 80, 2020.
D5	**ATBD GHG, 2020:** Buchwitz, M., Aben, I., Boesch, H., Crevoisier, C., Hasekamp, O. P., Reuter, M., Schneising-Weigel, O., Wu, L.., Algorithm Theoretical Basis Document (ATBD) – Main document for Greenhouse Gas (GHG: CO_2 & CH_4) data set CDR 4 (2003-2019), C3S project C3S_312b_Lot2_DLR, v4.0, 2020.
D6	**PQAR GHG, 2020:** Buchwitz, M., Aben, I., J., Armante, R., Boesch, H., Crevoisier, C., Di Noia, A., Hasekamp, O. P., Reuter, M., Schneising-Weigel, O., Wu, L.., Product Quality Assessment Report (PQAR) – Main document for Greenhouse Gas (GHG: CO_2 & CH_4) data set CDR 4 (2003-2019), C3S project C3S_312b_Lot2_DLR, v4.0, 2020.

Acronyms

Acronym	Definition
AIRS	Atmospheric Infrared Sounder
AMSU	Advanced Microwave Sounding Unit
ATBD	Algorithm Theoretical Basis Document
BESD	Bremen optimal EStimation DOAS
CAR	Climate Assessment Report
C3S	Copernicus Climate Change Service
CCDAS	Carbon Cycle Data Assimilation System
CCI	Climate Change Initiative
CDR	Climate Data Record
CDS	(Copernicus) Climate Data Store
CMUG	Climate Modelling User Group (of ESA's CCI)
CRG	Climate Research Group
D/B	Data base
DOAS	Differential Optical Absorption Spectroscopy
EC	European Commission
ECMWF	European Centre for Medium Range Weather Forecasting
ECV	Essential Climate Variable
EMMA	Ensemble Median Algorithm
ENVISAT	Environmental Satellite (of ESA)
EO	Earth Observation
ESA	European Space Agency
EU	European Union
EUMETSAT	European Organisation for the Exploitation of Meteorological Satellites
FCDR	Fundamental Climate Data Record
FoM	Figure of Merit
FP	Full Physics retrieval method
FTIR	Fourier Transform InfraRed
FTS	Fourier Transform Spectrometer
GCOS	Global Climate Observing System
GEO	Group on Earth Observation
GEOSS	Global Earth Observation System of Systems
GHG	GreenHouse Gas
GOME	Global Ozone Monitoring Experiment
GMES	Global Monitoring for Environment and Security
GOSAT	Greenhouse Gases Observing Satellite
IASI	Infrared Atmospheric Sounding Interferometer
IMAP-DOAS (or IMAP)	Iterative Maximum A posteriori DOAS

IPCC	International Panel in Climate Change
IUP	Institute of Environmental Physics (IUP) of the University of Bremen, Germany
JAXA	Japan Aerospace Exploration Agency
JCGM	Joint Committee for Guides in Metrology
L1	Level 1
L2	Level 2
L3	Level 3
L4	Level 4
LMD	Laboratoire de Météorologie Dynamique
MACC	Monitoring Atmospheric Composition and Climate, EU GMES project
NA	Not applicable
NASA	National Aeronautics and Space Administration
NetCDF	Network Common Data Format
NDACC	Network for the Detection of Atmospheric Composition Change
NIES	National Institute for Environmental Studies
NIR	Near Infra Red
NLIS	LMD/CNRS *neuronal* network mid/upper tropospheric CO2 and CH4 retrieval algorithm
NOAA	National Oceanic and Atmospheric Administration
Obs4MIPs	Observations for Climate Model Intercomparisons
OCO	Orbiting Carbon Observatory
OE	Optimal Estimation
PBL	Planetary Boundary Layer
ppb	Parts per billion
ppm	Parts per million
PQAD	Product Quality Assurance Document
PQAR	Product Quality Assessment Report
PR	(light path) PRoxy retrieval method
PVIR	Product Validation and Intercomparison Report
QA	Quality Assurance
QC	Quality Control
REQ	Requirement
RMS	Root-Mean-Square
RTM	Radiative transfer model
SCIAMACHY	SCanning Imaging Absorption spectroMeter for Atmospheric ChartographY
SCIATRAN	SCIAMACHY radiative transfer model
SRON	SRON Netherlands Institute for Space Research
SWIR	Short Wava Infra Red
TANSO	Thermal And Near infrared Sensor for carbon Observation
TANSO-FTS	Fourier Transform Spectrometer on GOSAT

TBC	To be confirmed
TBD	To be defined / to be determined
TCCON	Total Carbon Column Observing Network
TIR	Thermal Infra Red
TR	Target Requirements
TRD	Target Requirements Document
TRD GAD	Target Requirements Document & Gap Analysis Document
WFM-DOAS (or WFMD)	Weighting Function Modified DOAS
UoL	University of Leicester, United Kingdom
URD	User Requirements Document
WMO	World Meteorological Organization
Y2Y	Year-to-year (bias variability)

General definitions

Table 1 lists some general definitions relevant for this document.

Table 1: General definitions.

Item	Definition
XCO_2	Column-average dry-air mixing ratio (mole fraction) of CO_2
XCH_4	Column-average dry-air mixing ratio (mole fraction) of CH_4
L1	Level 1 satellite data product: geolocated radiance (spectra)
L2	Level 2 satellite-derived data product: Here: CO_2 and CH_4 information for each ground-pixel
L3	Level 3 satellite-derived data product: Here: Gridded CO_2 and CH_4 information, e.g., 5 deg times 5 deg, monthly
L4	Level 4 satellite-derived data product: Here: Surface fluxes (emission and/or uptake) of CO_2 and CH_4

Scope of document

This document is the Product User Guide and Specification (PUGS) for the Copernicus Climate Change Service (C3S, https://climate.copernicus.eu/) component as covered by the greenhouse gas (GHG) activities of project C3S_312b_Lot2 led by DLR, Germany (a follow-on activity of project C3S_312a_Lot6 led by University of Bremen, Germany), in the following referred to as C3S/GHG project.

Within this project, satellite-derived atmospheric carbon dioxide (CO_2) and methane (CH_4) Essential Climate Variable (ECV) data products have been generated and delivered to ECMWF for inclusion into the Copernicus Climate Data Store (CDS), from where users can access these data products and the corresponding documentation.

These satellite-derived data products are (see also *Reuter et al., 2020*):

- Column-average dry-air mixing ratios (mole fractions) of CO_2 and CH_4, denoted XCO_2 (in parts per million, ppm) and XCH_4 (in parts per billion, ppb), respectively.
- Mid/upper tropospheric mixing ratios of CO_2 (in ppm) and CH_4 (in ppb).

An overview about the products is given in Table 2 for the CO_2 products and in Table 3 for the CH_4 products.

For an overview of the merged Level 2 data products XCO2_EMMA and XCH4_EMMA and of the merged Level 3 data products XCO2_OBS4MIPS and XCH4_OBS4MIPS see also *Reuter et al., 2020*.

Requirements on data quality are formulated in the corresponding Target Requirement Document (TRD) (Reference ID *D4*).

The main purpose of this document is to describe the satellite-derived CO_2 and CH_4 greenhouse gas (GHG) ECV data products for users of these data products.

Note that this document does not contain a description of the retrieval algorithms which have been used to generate these products. These algorithms are described in a separate document (Reference ID *D5*): Algorithm Theoretical Basis Document (ATBD).

Note also that this document does not contain detailed validation results. Detailed data quality and validation results are reported in a separate document (Reference ID *D6*): Product Quality Assessment Report (PQAR).

Table 2: Overview CO_2 products. "CRD#" indicates the Climate Data Record (CDR) Number. Level 2 (L2) products contains information for each individual satellite footprint (ground pixel) whereas Level 3 (L3) products are gridded /averaged spatially and temporally.

Product ID (Level)	Version	CDR#	Temporal coverage	Comments
CO2_SCI_BESD (L2)	02.01.02	1-4	01.2003 – 03.2012	XCO_2 from SCIAMACHY as retrieved with Univ. Bremen's BESD algorithm. Brokered from GHG-CCI.
CO2_SCI_WFMD (L2)	4.0	1-4	10.2002 – 04.2012	XCO_2 from SCIAMACHY as retrieved with Univ. Bremen's WFMD algorithm. Brokered from GHG-CCI.
CO2_GOS_OCFP (L2)	7.1 7.2 7.3	1 2-3 4	04.2009 – 12.2016 04.2009 – 12.2018 04.2009 – 12.2019	XCO_2 from GOSAT as retrieved with Univ. Leicester's OCFP algorithm.
CO2_GOS_SRFP (L2)	2.3.8	1-4	04.2009 – 12.2019	XCO_2 from GOSAT as retrieved with SRON's SRFP (RemoTeC) algorithm.
XCO2_EMMA (L2)	3.0 3.1 4.1 4.2	1 2 3 4	01.2003 – 12.2016 01.2003 – 12.2017 01.2003 – 12.2018 01.2003 – 12.2019	Merged L2 XCO_2 product using Univ. Bremen's EMMA algorithm.
XCO2_OBS4MIPS (L3)	3 3.1 4.1 4.2	1 2 3 4	01.2003 – 12.2016 01.2003 – 12.2017 01.2003 – 12.2018 01.2003 – 12.2019	Merged L3 XCO_2 product in OBS4MIPS format.
CO2_AIRS_NLIS (L2)	3.0	1-4	04.2003 – 07.2007	Mid-tropospheric CO_2 mixing ratios as retrieved from AIRS using LMD's NLIS algorithm. Brokered from GHG-CCI.
CO2_IASA_NLIS (L2)	8.0 9.1	1-3 4	7.2007 – 05.2015 7.2007 – 12.2019	Mid-tropospheric CO_2 mixing ratios as retrieved from IASI/Metop-A using LMD's NLIS algorithm.
CO2_IASB_NLIS (L2)	4.0 4.2 9.1	1 2-3 4	2.2013 – 12.2016 2.2013 – 12.2018 2.2013 – 12.2019	Mid-tropospheric CO_2 mixing ratios as retrieved from IASI/Metop-B using LMD's NLIS algorithm.

Table 3: Overview CH_4 products. “CRD#” indicates the Climate Data Record (CDR) Number. Level 2 (L2) products contains information for each individual satellite footprint (ground pixel) whereas Level 3 (L3) products are gridded /averaged spatially and temporally.

Product ID (Level)	Version	CDR#	Temporal coverage	Comments
CH4_SCI_WFMD (L2)	4.0	1-4	10.2002 – 12.2011	XCH_4 from SCIAMACHY as retrieved with Univ. Bremen’s WFMD algorithm. Brokered from GHG-CCI.
CH4_SCI_IMAP (L2)	7.2	1-4	01.2003 – 04.2012	XCH_4 from SCIAMACHY as retrieved with SRON/JPL’s IMAP algorithm. Brokered from GHG-CCI.
CH4_GOS_OCPR (L2)	7.0 7.2 7.3	1 2-3 4	04.2009 – 12.2016 04.2009 – 12.2018 04.2009 – 12.2019	XCH_4 from GOSAT as retrieved with Univ. Leicester’s OCPR algorithm.
CH4_GOS_SRPR (L2)	2.3.8 2.3.9	1 2-4	04.2009 – 12.2016 04.2009 – 12.2019	XCH_4 from GOSAT as retrieved with SRON’s SRPR (RemoTeC) algorithm.
CH4_GOS_OCFP (L2)	7.1 7.2 7.3	1 2-3 4	04.2009 – 12.2016 04.2009 – 12.2018 04.2009 – 12.2019	XCH_4 from GOSAT as retrieved with Univ. Leicester’s OCFP algorithm.
CH4_GOS_SRFP (L2)	2.3.8 2.3.8	1 2-4	04.2009 – 12.2016 04.2009 – 12.2019	XCH_4 from GOSAT as retrieved with SRON’s SRFP (RemoTeC) algorithm.
XCH4_EMMA (L2)	3.0 3.1 4.1 4.2	1 2 3 4	01.2003 – 12.2016 01.2003 – 12.2017 01.2003 – 12.2018 01.2003 – 12.2019	Merged L2 XCH_4 product using Univ. Bremen’s EMMA algorithm.
XCH4_OBS4MIPS (L3)	3 3.1 4.1 4.2	1 2 3 4	01.2003 – 12.2016 01.2003 – 12.2017 01.2003 – 12.2018 01.2003 – 12.2019	Merged L3 XCH_4 product in OBS4MIPS format.
CH4_IASA_NLIS (L2)	8.4 9.1	1-3 4	7.2007 – 05.2015 7.2007 – 05.2019	Mid-tropospheric CH_4 mixing ratios as retrieved from IASI/Metop-A using LMD’s NLIS algorithm.
CH4_IASB_NLIS (L2)	8.1 8.1 9.1	1 2-3 4	2.2013 – 12.2016 2.2013 – 12.2018 2.2013 – 12.2019	Mid-tropospheric CH_4 mixing ratios as retrieved from IASI/Metop-B using LMD’s NLIS algorithm.

Executive summary

In this document the satellite-derived atmospheric carbon dioxide (CO_2) and methane (CH_4) Climate Data Record (CDR) data products are described as generated via the C3S_312b_Lot2 project of the Copernicus Climate Change Service (C3S, https://climate.copernicus.eu/).

These satellite-derived data products are:

- Column-averag dry-air mixing ratios (mole fractions) of CO_2 and CH_4, denoted XCO_2 (in parts per million, ppm) and XCH_4 (in parts per billion, ppb), respectively.
- Mid/upper tropospheric mixing ratios of CO_2 (in ppm) and CH_4 (in ppb).

These data products are generated from the satellite instruments SCIAMACHY/ENVISAT and TANSO-FTS/GOSAT (XCO_2 and XCH_4 products) and AIRS and IASI (mid/upper troposphere products).

All data products are available as Level 2 (individual ground pixels) products in NetCDF format. The XCO_2 (Figure 1) and XCH_4 (Figure 2) Level 2 products are available for individual sensors but also as merged multi-sensor products. In addition, also merged Level 3 (i.e., gridded) products in OBS4MIPS format are available for the XCO_2 and XCH_4 products.

Figure 1 shows an overview about the XCO_2 products in terms of maps and time series. The maps top left show product CO2_SCI_BESD, i.e., XCO_2 from SCIAMACHY as retrieved with the BESD algorithm. The maps bottom right show product CO2_GOS_OCFP, i.e., XCO_2 from GOSAT as retrieved with the OCFP algorithm. The time series has been computed using product XCO2_OBS4MIPS, i.e., the merged Level 3 product obtained from merging the individual sensor products.

Figure 2 shows an overview about the XCH_4 products in terms of maps and time series. The maps top left show product CH4_SCI_WFMD, i.e., XCH_4 from SCIAMACHY as retrieved with the WFMD algorithm. The maps bottom right show product CH4_GOS_SRPR, i.e., XCH_4 from GOSAT as retrieved with the SRPR algorithm. The time series has been computed using product XCH4_OBS4MIPS, i.e., the merged Level 3 product obtained from merging the individual sensor products.

CO_2 and CH_4 are important climate-relevant atmospheric gases, so-called greenhouse gases (GHG). Because of their important role for climate, they are classified as Essential Climate Variables (ECVs). The ECV GHG as formulated by GCOS (Global Climate Observing System) is defined as: "Retrievals of greenhouse gases, such as CO_2 and CH_4, of sufficient quality to estimate regional sources and sinks" (*GCOS-154*). This definition contains already the main application of these atmospheric data products, namely to use them (in combination with appropriate modelling) to obtain (improved) information on their (primarily surface) sources and sinks.

Both gases, CO_2 and CH_4, have a long lifetime in the atmosphere. As a consequence of this fact and related human emissions, the atmospheric concentrations of these gases are relatively high (about 400 ppm for CO_2 and 1.8 ppm for CH_4) compared to other atmospheric trace gases. As a result of this even a moderate to strong (surface) source or sink typically only results in a relatively small local or regional change (enhancement or depletion relative to the surrounding region) in their vertical columns or their mid/upper tropospheric concentration. The observational requirements are therefore very demanding in particular with respect to random and systematic errors and stability.

Because of their long lifetime and atmospheric transport, elevated (or depleted) atmospheric CO_2 and CH_4 concentrations can be higher (or lower) relative to the background far away from the surface source (or sink), which has emitted (or taken up) these atmospheric gases. In order to obtain source/sink information from the atmospheric observations it is therefore required to take atmospheric transport (and in particular for methane also atmospheric chemistry) into account and to consider the exact time and location of the atmospheric observations. As a consequence, the most relevant data products are the Level 2 (L2) products, which contain detailed information (time, location, etc.) for each individual satellite ground pixel. The requirements as formulated in the Target Requirement Document (*D4*) are, therefore, mostly L2 requirements. However, for XCO_2 and XCH_4 also (gridded) Level 3 (L3) products have been generated (in OBS4MIPS format).

This C3S project is essentially the operational continuation of the research and development (R&D) pre-cursor project GHG-CCI of ESA's Climate Change Initiative (CCI). A goal of the C3S_312b_Lot2 project is to extend (in time) the data base of GHG-CCI pre-cursor data products.

The first C3S GHG data set - Climate Data Record 1 (CDR1) - covered the time period 2003-2016 and had been delivered to ECMWF in 2017. The second data set - Climate Data Record 2 (CDR2) - covered the time period 2003-2017 and has be made available for the C3S CDS in 2018. This document is an update for the latest version of this data set.

This document is the MAIN PUGS document. It provides and overview about the products by describing the data format and content which is relevant for all users. However, each product may also contain additional – typically algorithm specific – information, which may be useful for certain applications. Details on each product are provided in separate ANNEXes:

- **ANNEX A:** PUGS for products CO2_GOS_OCFP, CH4_GOS_OCFP, CH4_OCPR (University of Leicester's GOSAT products)
- **ANNEX B:** PUGS for products CO2_GOS_SRFP, CH4_GOS_SRFP (SRON's "full physics" GOSAT products)
- **ANNEX C:** PUGS for product CH4_GOS_SRPR (SRON's "proxy" GOSAT XCH_4 product)
- **ANNEX D:** PUGS for products XCO2_EMMA, XCH4_EMMA, XCO2_OBS4MIPS, XCH4_OBS4MIPS (University of Bremen's merged Level 2 and Level 3 products)
- **ANNEX E:** PUGS for IASI CO_2 and CH_4 products (LMD/CNRS's IASI products)

Figure 1 - Overview of the C3S XCO_2 product during 2003-2019 in terms of global maps and time series.

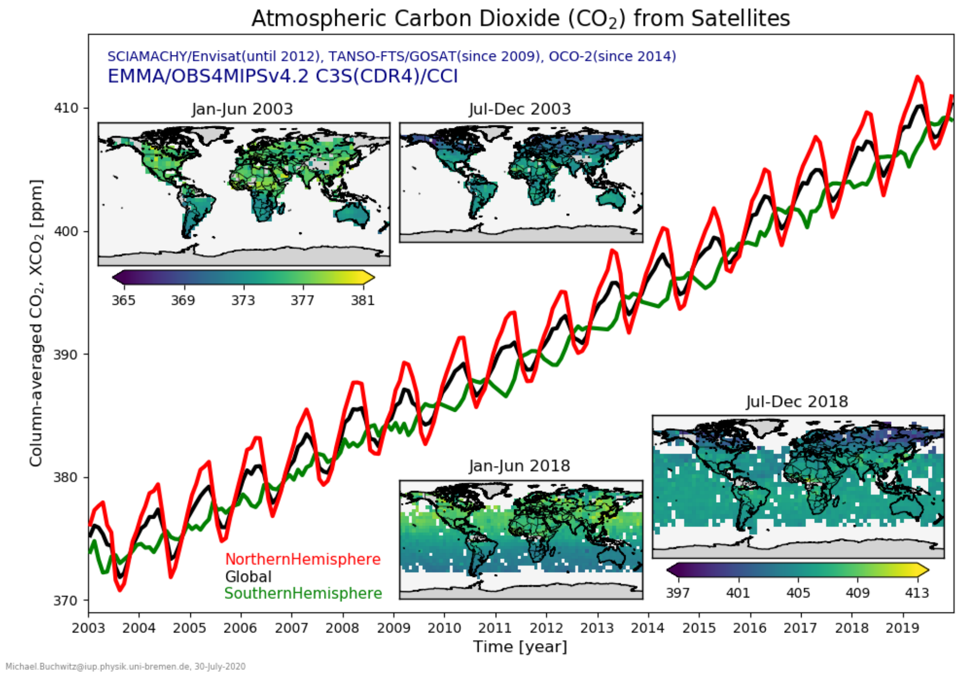

Figure 2 - Overview of the C3S XCH_4 product during 2003-2019 in terms of global maps and time series.

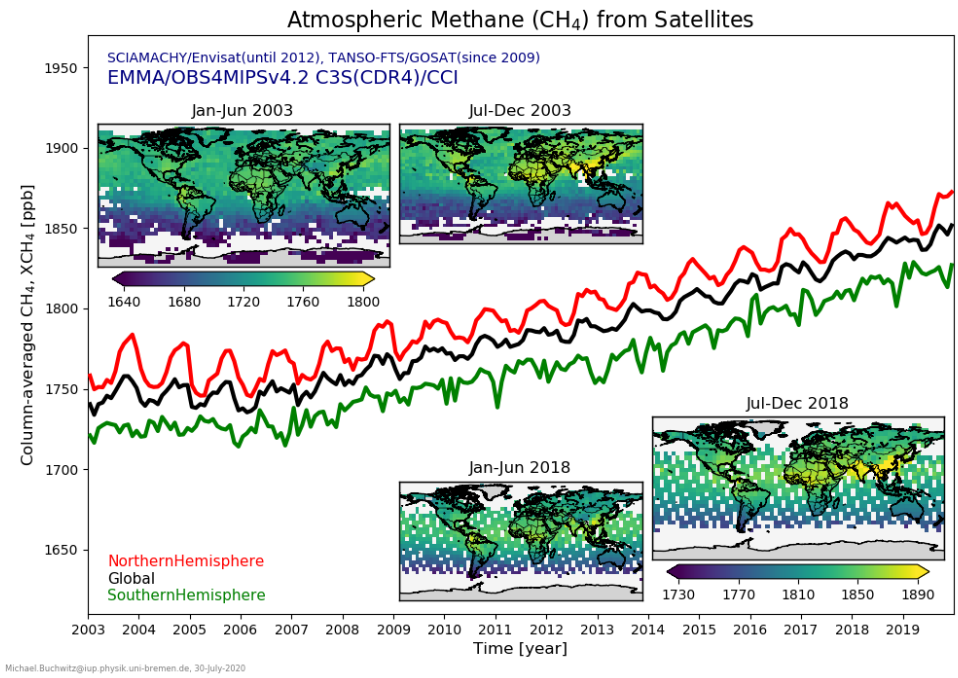

Finally a warning:

The data products have been generated as carefully as possible including appropriate quality filtering to (automatically) remove "bad data". Nevertheless, these are real data from real instruments and they contain (instrument related) features such as noise and systematic errors. The products have been validated by comparison with (mostly) ground-based observations (see *D6*, i.e., *PQAR GHG, 2020*) but these reference observations are sparse and do not cover all observational and geophysical conditions. Using these data products for scientific or other applications requires care and is not trivial.

Note in particular that the SCIAMACHY XCH_4 products suffer from detector degradation issues especially after October 2005 resulting in increased scatter and likely also increased systematic error. As a consequence also the merged multi-sensor (i.e., XCH4_EMMA and XCH4_OBS4MIPS) methane products suffer from this (Fig. 3). For XCO_2 no degradation has been identified (see Fig. 4).

Figure 3 – Time series of XCH_4 around Lamont, Oklahoma, USA (+/- 1°). Shown is product XCH4_EMMA (merged multi-sensor XCH_4 Level 2 product covering the time period 2003-2016 (CDR1)). The time series starts with SCIAMACHY/ENVISAT. TANSO-FTS/GOSAT XCH_4 is added in 2009 and after March 2010 the product only contains GOSAT data. As can be seen, the scatter (noise) of the SCIAMACHY data is much larger than GOSAT and it can also be seen that the scatter of the SCIAMACHY data increases with time. This needs to be considered when using this product (or other methane products based on SCIAMACHY) for scientific or other applications.

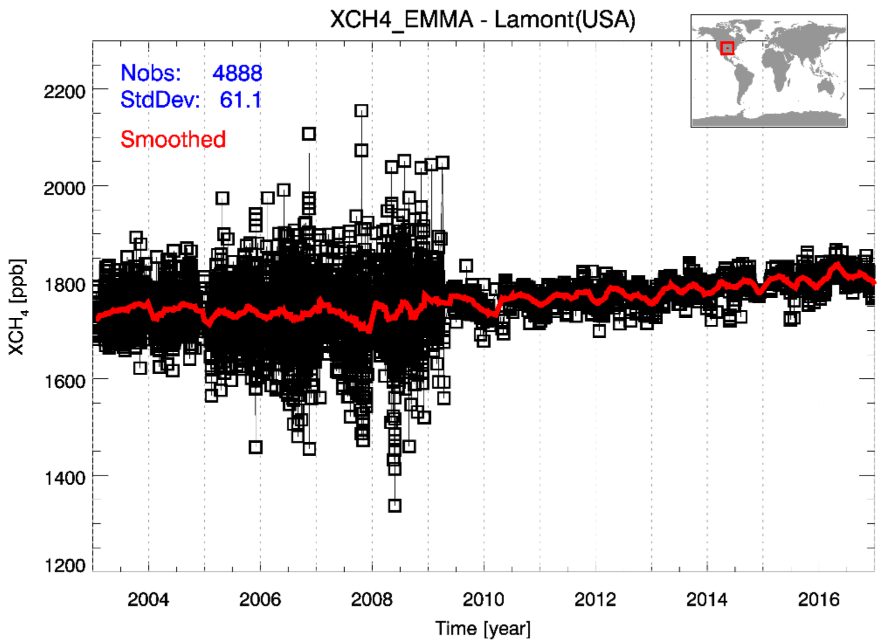

Figure 4 – As Figure 3 but for product XCO2_EMMA (data set CDR1, 2003-2016).

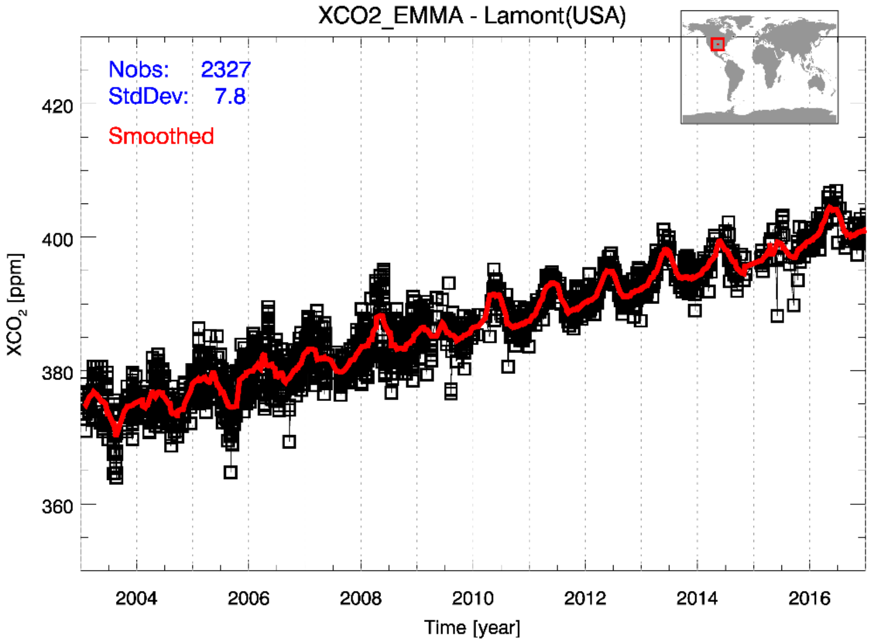

1. Overview data products and instruments

In this section an overview of the data products - specified in terms of variable, its property, processing level(s) and instrument(s) - is given.

The data products are (see also *Buchwitz et al., 2013b, 2016, 2017; Reuter et al., 2020*):

- Column-average dry-air mixing ratios (mole fractions) of CO_2 and CH_4, denoted XCO_2 (in parts per million, ppm) and XCH_4 (in parts per billion, ppb).
- Mid/upper tropospheric mixing ratios of CO_2 and CH_4.

Carbon dioxide and methane are important atmospheric greenhouse gases (e.g., *IPCC 2013*) but despite their importance our knowledge on their various and variable natural and anthropogenic sources and sinks has significant gaps (e.g., *IPCC 2013; Ciais et al., 2014; 2015; Kirschke et al., 2013; Nisbet et al., 2014*, and references given therein). A purpose of the satellite data products described in this document is to contribute to enhancing our knowledge on the CO_2 and CH_4 sources and sinks (via appropriate (inverse) modelling).

Carbon dioxide and methane are so-called Essential Climate Variables (ECVs) and the need to monitor them has been clearly identified including the definition of key requirements (e.g., *GCOS-154, GCOS-200*). In recent years several satellite-derived ECV data products have been generated in particular in the framework of the Climate Change Initiative (CCI) of ESA (e.g., *Hollmann et al., 2013*) including CO_2 and CH_4 (e.g., *Buchwitz et al., 2013a, 2016, 2017*).

Previous version of these satellite-derived CO_2 and CH_4 data products have been used for a number of (primarily scientific) applications, e.g.,

- to improve our knowledge on the various natural and anthropogenic (surface) sources and sinks of these important greenhouse gases (GHG) (see, e.g., *Alexe et al., 2015; Bergamaschi et al., 2015; Chevallier et al., 2014, 2016a, 2016b; Cressot et al, 2014; Detmers et al., 2015; Guerlet et al., 2013; Houweling et al., 2015; McNorton et al., 2016; Pandey et al., 2016; Reuter et al., 2014b, 2017; Schneising et al., 2014b; Turner et al., 2015, 2016,* and references given therein)
- to monitor the global distribution of CO_2 and CH_4 (e.g., *Buchwitz et al., 2007, 2016b; Schneising et al., 2011; Frankenberg et al., 2011; Massart et al., 2016*)
- to improve our knowledge on emission ratios, e.g., for biomass burning (e.g., *Ross et al., 2013; Parker et al., 2016*)
- for comparisons with (chemistry) climate models (e.g., *Shindell et al., 2013; Hayman et al., 2014; Lauer et al., 2017*) and other models (e.g., *Schneising et al., 2014a; Parker et al., 2016*)

In the following sub-sections an overview about the satellite-derived CO_2 and CH_4 data products is given.

1.1 Column-average mixing ratios of CO_2 and CH_4 (XCO_2 and XCH_4)

1.1.1 Overview

Satellite radiance observations in the Near Infrared / Short Wave Infrared (NIR/SWIR) spectral region in nadir (down looking) observation viewing mode are sensitive to atmospheric CO_2 and CH_4 concentration changes with good sensitivity down to the Earth's surface (because solar radiation reflected at the Earth's surface is observed). These measurements permit to obtain "total column information" but do not permit to obtain (detailed) information on the vertical profiles of CO_2 and CH_4. The CO_2 and CH_4 products derived from these satellites are column-averaged dry-air mixing ratios (more precisely: mole fractions) of CO_2 and CH_4 denoted XCO_2 (e.g., in ppm) and XCH_4 (e.g., in ppb).

In the following, several satellite instruments are shortly described which are used / can be used to generate XCO_2 and/or XCH_4 data products.

1.1.2 Instruments

The C3S data set has been primarily derived from the satellite instruments SCIAMACHY on ENVISAT and TANSO-FTS onboard GOSAT. In addition, XCO_2 from NASA's OCO-2 mission has been used for some products (EMMA and OBS4MIPS). These instruments are shortly described in the following. Other satellites, which are planned to be used for future versions of our data products, are also shortly mentioned.

1.1.2.1 SCIAMACHY/ENVISAT

SCIAMACHY (SCanning Imaging Absorption spectroMeter for Atmospheric ChartographY) was a spectrometer on ESA's ENVISAT satellite (2002-2012). SCIAMACHY (*Burrows et al., 2005; Bovensmann et al., 1999*) covers the spectral region from the ultra-violet to the SWIR spectral region (240 nm - 2380 nm) at moderate spectral resolution (0.2 nm - 1.5 nm) and observes the Earth's atmosphere in various viewing geometries (nadir, limb and solar and lunar occultation). For a good general overview on SCIAMACHY see also https://en.wikipedia.org/wiki/SCIAMACHY. SCIAMACHY permits the retrieval of XCO_2 (e.g., *Reuter et al., 2011; Schneising et al., 2011*) and XCH_4 (e.g., *Schneising et al., 2011; Frankenberg et al., 2011*) from the appropriate spectral regions in the SWIR (around 1.6 µm) and the NIR (O_2 A-band at 760 nm used to obtain the dry-air column using the known dry-air mixing ratio of atmospheric oxygen). The ground pixel size is typically 30 km along track times 60 km across track and the swath width is about 960 km. There are no across-track gaps between the ground pixels but there are gaps along-track as SCIAMACHY operates only part of the time (approx. 50%) in nadir observation mode.

1.1.2.2 TANSO-FTS/GOSAT

TANSO-FTS is a Fourier-Transform-Spectrometer (FTS) onboard the Japanese GOSAT satellite (*Kuze et al., 2009, 2014, 2016*). The Greenhouse Gases Observing Satellite "IBUKI" (GOSAT) is the world's first spacecraft in orbit dedicated to measure the concentrations of carbon dioxide and methane from space. The spacecraft was launched successfully on January 23, 2009, and has been operating properly since then. GOSAT covers the relevant CO_2, CH_4 and O_2 absorption bands in the NIR and SWIR spectral region as needed for accurate XCO_2 and XCH_4 retrieval (in addition GOSAT also covers a large part of the Thermal Infrared (TIR) spectral region). The spectral resolution of TANSO-FTS is much higher compared to SCIAMACHY and also the ground pixels are smaller (10 km compared to several 10 km for SCIAMACHY). However, in contrast to SCIAMACHY, the GOSAT scan pattern consists of non-consecutive individual ground pixels, i.e., the scan pattern is not gap-free.
For a general overview about GOSAT see also http://www.gosat.nies.go.jp/en/.

GOSAT-2 has been successfully launched on 29 October 2018. GOSAT-2 XCO_2 and XCH_4 retrievals are not yet included in the C3S GHG CDR.

1.1.2.3 OCO-2

NASA's Orbiting Carbon Observatory 2 (OCO-2) mission (*Crisp et al., 2004; Boesch et al., 2011*) has been successfully launched in July 2014. The OCO-2 Project primary science objective is to collect the first space-based measurements of atmospheric carbon dioxide with the precision, resolution and coverage needed to characterize its sources and sinks and quantify their variability over the seasonal cycle. OCO-2 flies in a sun-synchronous, near-polar orbit with a group of Earth-orbiting satellites with synergistic science objectives whose ascending node crosses the equator near 13:30 hours Mean Local Time (MLT). Near-global coverage of the sunlit portion of Earth is provided in this orbit over a 16-day (233-revolution) repeat cycle. OCO-2's single instrument incorporates three high-resolution grating spectrometers, designed to measure the near-infrared absorption of reflected sunlight by carbon dioxide and molecular oxygen. OCO-2 covers similar spectral bands as SCIAMACHY and GOSAT but OCO-2 has much smaller ground pixels (km scale) but the swath width is much smaller (approx. 10 km) compared to SCIAMACHY. OCO-2 delivers XCO_2 but not XCH_4. Details on OCO-2 are also given on https://oco.jpl.nasa.gov/.

1.1.2.4 TanSat

The Chinese TanSat satellite (https://en.wikipedia.org/wiki/TanSat) has been successfully launched in December 2016. The TanSat satellite and instrument is very similar as OCO-2. As OCO-2, TanSat delivers XCO_2 but not XCH_4. TanSat XCO_2 retrievals are not yet included in the C3S GHG CDR.

1.1.2.5 Sentinel-5-Precursor (S5P)

ESA's Sentinel-5-Precursor (S5P) mission (*Veefkind et al, 2012*) has been launched in October 2017. S5P permits XCH_4 retrievals (*Butz et al., 2012, Hu et al., 2018*) at about 7 km and using a wide swath of about 2600 km. Details on S5P can also be found on https://earth.esa.int/web/guest/missions/esa-future-missions/sentinel-5P. S5P XCH_4 retrievals are not yet included in the C3S GHG CDR.

1.1.2.6 Other instruments

Several other satellites are expected to be launched in the future, e.g., the active laser-based mission MERLIN (Methane Remote Sensing Lidar Mission, see https://de.wikipedia.org/wiki/Merlin_(Satellit)).

1.1.3 XCO_2

As explained, XCO_2 is the column-averaged dry-air mixing ratio (mole fraction) of atmospheric CO_2. A XCO_2 value of, for example, 400 ppm at a given location means that 400 CO_2 molecules are present in the atmosphere above that location per one million air molecules excluding water molecules.

XCO_2 can be retrieved from instruments such as SCIAMACHY/ENVISAT and TANSO-FTS/GOSAT using Optimal Estimation (*Rodgers, 2000*) or DOAS (*Buchwitz et al., 2000*) retrieval algorithms as shown in various publications (e.g., *Buchwitz et al., 2005; Butz et al., 2011; Cogan et al., 2011; Reuter et al., 2011; 2013; Schneising et al., 2011; Yoshida et al., 2013*). These products have been validated using Total Carbon Column Observing Network (TCCON) (*Wunch et al., 2010, 2011, 2015*) XCO_2 ground based observations (e.g., *Dils et al., 2014*). In this document, the latest versions of these data products are described.

Figure 5 shows time series of satellite-derived XCO_2. As can be seen, XCO_2 is increasing by about 2-3 ppm/year primarily due to burning of fossil fuels and shows a pronounced seasonal cycle, primarily due to uptake and release of CO_2 by the terrestrial biosphere.

Figure 5 – Satellite-derived northern mid-latitudes XCO_2 time series. Shown are four time series, each corresponding to one of the four individual satellite sensor Level 2 XCO_2 products, which are described in this document.

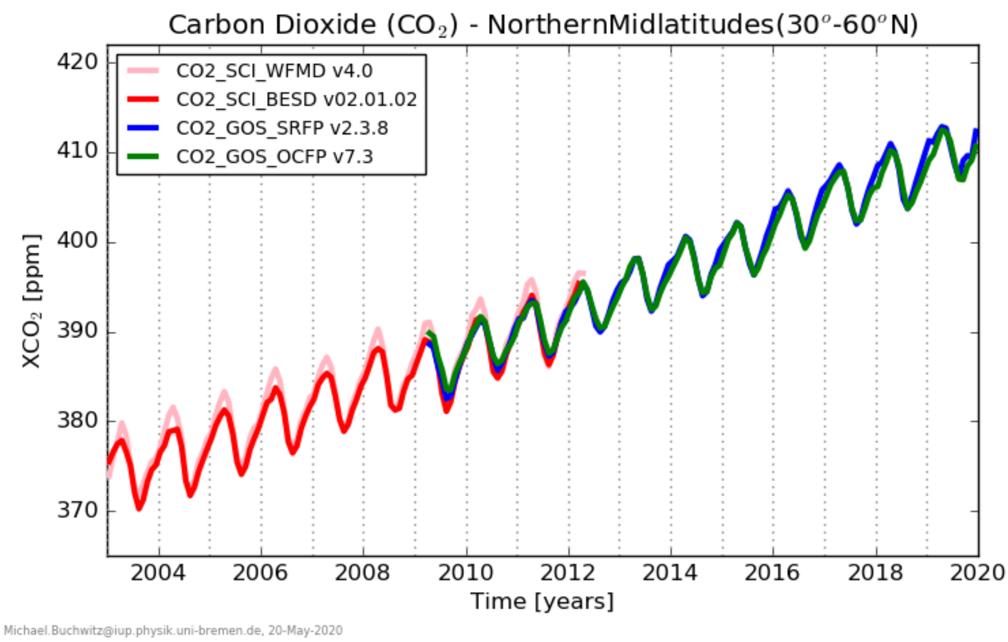

1.1.4 XCH_4

As explained, XCH_4 is the column-averaged dry-air mixing ratio (mole fraction) of atmospheric CH_4. A XCH_4 value of, for example, 1800 ppb at a given location means that 1800 CH_4 molecules are present in the atmosphere above that location per one billion air molecules excluding water molecules.

XCH_4 can be retrieved from instruments such as SCIAMACHY/ENVISAT and TANSO-FTS/GOSAT using Optimal Estimation (*Rodgers, 2000*) or DOAS (*Buchwitz et al., 2000*) retrieval algorithms as shown in various publications (e.g., *Buchwitz et al., 2005; Butz et al., 2011; Frankenberg et al., 2011; Schneising et al., 2011; Parker et al., 2011; Scheper et al., 2012; Yoshida et al., 2013*). These products have been validated using Total Carbon Column Observing Network (TCCON) (*Wunch et al., 2010, 2011, 2015*) XCH_4 ground based observations (e.g., *Dils et al., 2014*). In this document, the latest versions of these data products are described.

As an example, Figure 6 shows time series of satellite-derived XCH_4. As can be seen, XCH_4 is increasing since 2007 by about 5-8 ppb/year. The reason for this is not entirely clear (several potential reasons are discussed in the scientific literature).

Figure 6 – Satellite-derived northern mid-latitudes XCH_4 time series. Shown are six time series, each corresponding to one of the six individual satellite sensor Level 2 XCH_4 products, which are described in this document.

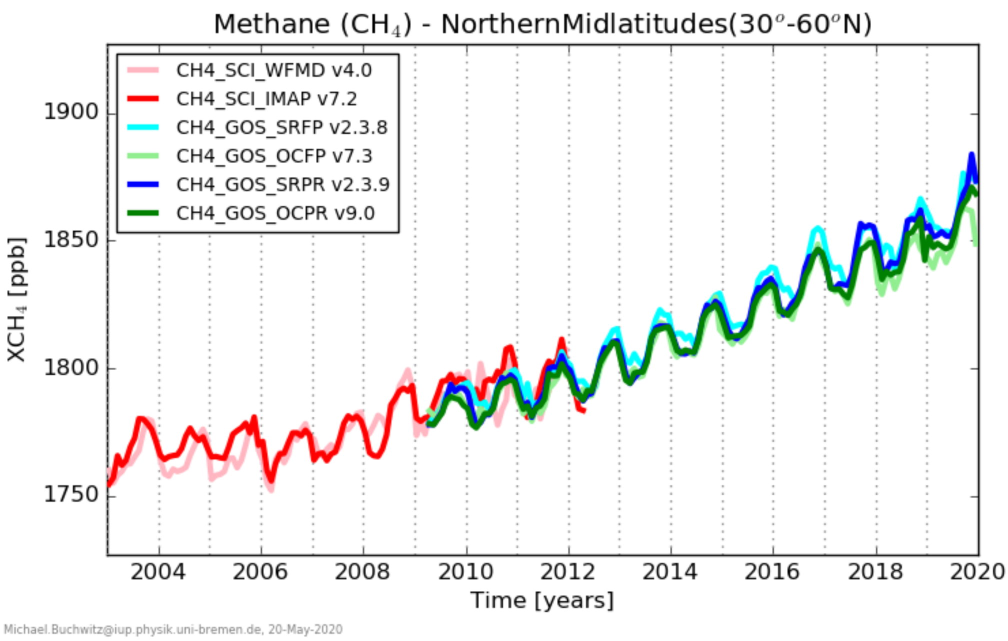

1.1.5 List of XCO_2 and XCH_4 data products

Table 4 and Table 5 list the XCO_2 and XCH_4 data products, respectively.

As can be seen from Table 4, for each individual sensor Level 2 XCO_2 product two products have been generated using two different retrieval algorithms (OCFP is University of Leicester's Full Physics (FP) algorithm and SRFP is SRON's retrieval algorithm, also known as RemoTeC).

Products with comment «Existing GHG-CCI product» are the latest versions of Level 2 products, which have been generated in the framework of the GHG-CCI project. They are available via the C3S CDS but are also available from the GHG-CCI website including documentation. They have been used within this project to generate the merged Level 2 and Level 3 EMMA and OBS4MIPS products but the individual sensor L2 products have not been regenerated. They have been provided for C3S «as is» and are available via the C3S CDS.

Table 4 - Overview XCO_2 data products.

Product ID	Level	Sensor(s)	(Planned) Availability	Comments
CO2_GOS_OCFP	2	GOSAT	Oct. 2017: 2009-2016 Oct. 2018: 2009-2017 Dec. 2019: 2009-2018 Dec. 2020: 2009-2019	
CO2_GOS_SRFP	2	GOSAT	Oct. 2017: 2009-2016 Oct. 2018: 2009-2017 Dec. 2019: 2009-2018 Dec. 2020: 2009-2019	
CO2_SCI_BESD	2	SCIAMACHY	Oct. 2017: 2003-2012	Existing GHG-CCI product
CO2_SCI_WFMD	2	SCIAMACHY	Oct. 2017: 2002-2012	Existing GHG-CCI product
XCO2_EMMA	2	Merged SCIAMACHY, GOSAT, OCO-2	Oct. 2017: 2003-2016 Oct. 2018: 2003-2017 Dec. 2019: 2003-2018 Dec. 2020: 2003-2019	
XCO2_OBS4MIPS	3	Merged SCIAMACHY, GOSAT, OCO-2	Oct. 2017: 2003-2016 Oct. 2018: 2003-2017 Dec. 2019: 2003-2018 Dec. 2020: 2003-2019	

As can be seen from Table 5, for each individual sensor Level 2 XCH_4 product four products will be generated from GOSAT using four different retrieval algorithms using two «Full Physics» (FP) and two «Proxy» (PR) algorithms. For a discussion of FP versus PR algorithms see also, for example, *Schepers et al., 2012*. Each type of algorithm has different advantages and disadvantages. Typically, the PR products contain more data and therefore somewhat better spatio-temporal coverage (as quality filtering can be less strict) but the PR algorithms rely on a CO_2 model to correct for XCO_2 variations. FP products contain less data points but the advantage of this product is that it is independent of a CO_2 model.

Table 5 - Overview XCH_4 data products.

Product ID	Level	Sensor(s)	(Planned) Availability	Comments
CH4_GOS_OCPR	2	GOSAT	Oct. 2017: 2009-2016 Oct. 2018: 2009-2017 Dec. 2019: 2009-2018 Dec. 2020: 2009-2019	
CH4_GOS_SRPR	2	GOSAT	Oct. 2017: 2009-2016 Oct. 2018: 2009-2017 Dec. 2019: 2009-2018 Dec. 2020: 2009-2019	
CH4_GOS_OCFP	2	GOSAT	Oct. 2017: 2009-2016 Oct. 2018: 2009-2017 Dec. 2019: 2009-2018 Dec. 2020: 2009-2019	
CH4_GOS_SRFP	2	GOSAT	Oct. 2017: 2009-2016 Oct. 2018: 2009-2017 Dec. 2019: 2009-2018 Dec. 2020: 2009-2019	
CH4_SCI_WFMD	2	SCIAMACHY	Oct. 2017: 2002-2011	Existing GHG-CCI product
CH4_SCI_IMAP	2	SCIAMACHY	Oct. 2017: 2003-2012	Existing GHG-CCI product
XCH4_EMMA	2	Merged SCIAMACHY & GOSAT	Oct. 2017: 2003-2016 Oct. 2018: 2003-2017 Dec. 2019: 2003-2018 Dec. 2020: 2002-2019	
XCH4_OBS4MIPS	3	Merged SCIAMACHY & GOSAT	Oct. 2017: 2003-2016 Oct. 2018: 2003-2017 Dec. 2019: 2003-2018 Dec. 2020: 2003-2019	

On the following pages maps of these products are shown so that users can see how a product «looks like».

Figure 7 shows product CO2_SCI_BESD for January to June 2003 (top) and July to December 2003 (bottom) gridded at 1°x1°. As can be seen, only data over land are available. Gaps over land are due to clouds and for other reasons (e.g., solar zenith angle to large or due to too high aerosol load).

Figure 8 shows the same maps but for product CO2_SCI_WFMD. As can be seen, the data coverage of this product is somewhat better compared to product CO2_SCI_BESD (but validation indicates that this product is of somewhat lower quality in terms of random and systematic errors).

Figure 9 shows product CO2_GOS_OCFP for January to June 2019 (top) and July to December 2019 (bottom) also gridded at 1°x1°. As can be seen – compared to the SCIAMACHY XCO_2 products - also data over ocean are available but the land coverage is sparser due to the GOSAT sampling pattern and its smaller ground pixel size.

Figure 10 shows the same maps but for product CO2_GOS_SRFP. As can be seen, this product is similar but not exactly identical compared to product CO2_GOS_OCFP.

Figure 11 shows product CH4_SCI_WFMD for January to June 2003 (top) and July to December 2003 (bottom) gridded at 1°x1°.

Figure 12 shows the same maps but for product CH4_SCI_IMAP. As can be seen, only data over land are available compared to product CH4_SCI_WFMD. Note however, that product CH4_SCI_WFMD is also only available over land for year 2006 and later years (due to SCIAMACHY detector degradation issues).

Figure 13 shows product CH4_GOS_OCPR for January to June 2019 (top) and July to December 2019 (bottom) gridded at 1°x1°.

Figure 14 shows the same maps but for product CH4_GOS_SRFP. As can be seen, the two "proxy" (PR) products are similar but not exactly identical.

Figure 15 shows the same maps but for product CH4_GOS_OCFP. This « full physics » (FP) product is sparser compared to the corresponding « proxy » (PR) product CH4_GOS_OCPR.

Figure 16 shows the same maps but for product CH4_GOS_SRFP. This «full physics» (FP) product is also sparser compared to the corresponding «proxy» (PR) product CH4_GOS_SRPR.

Figure 7 - XCO_2 product CO2_SCI_BESD. Top: January to June 2003. Bottom: July – December 2003.

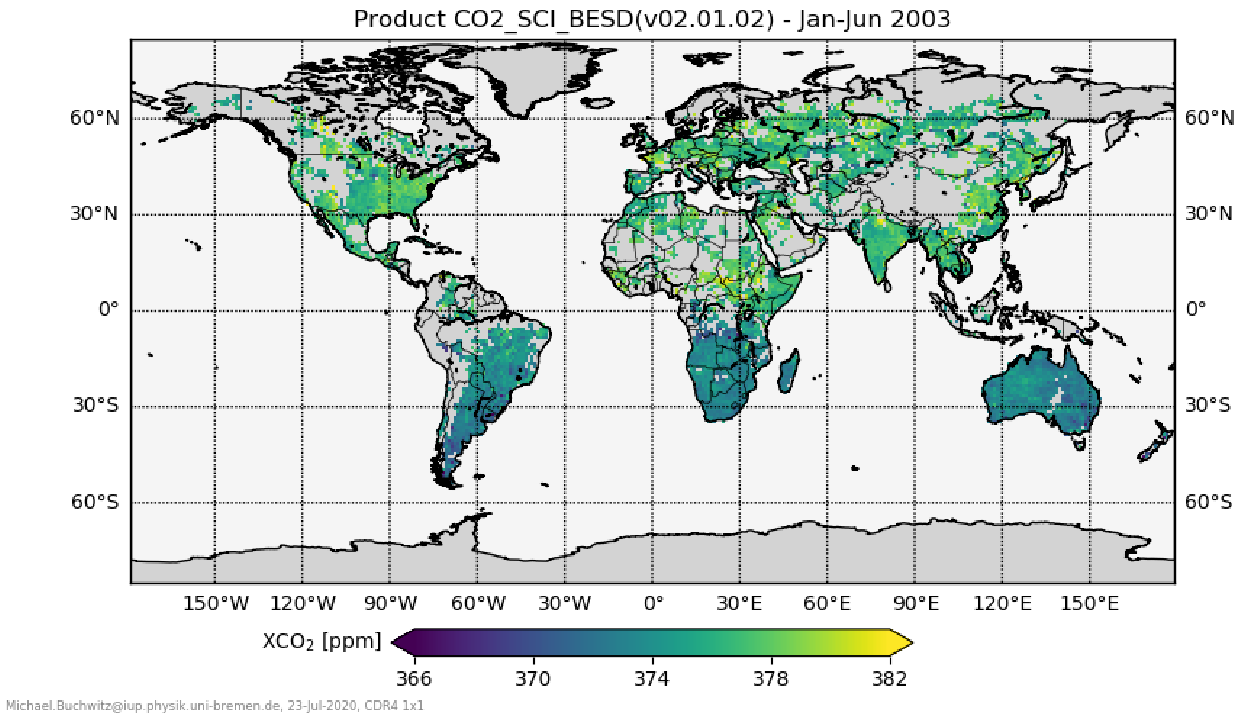

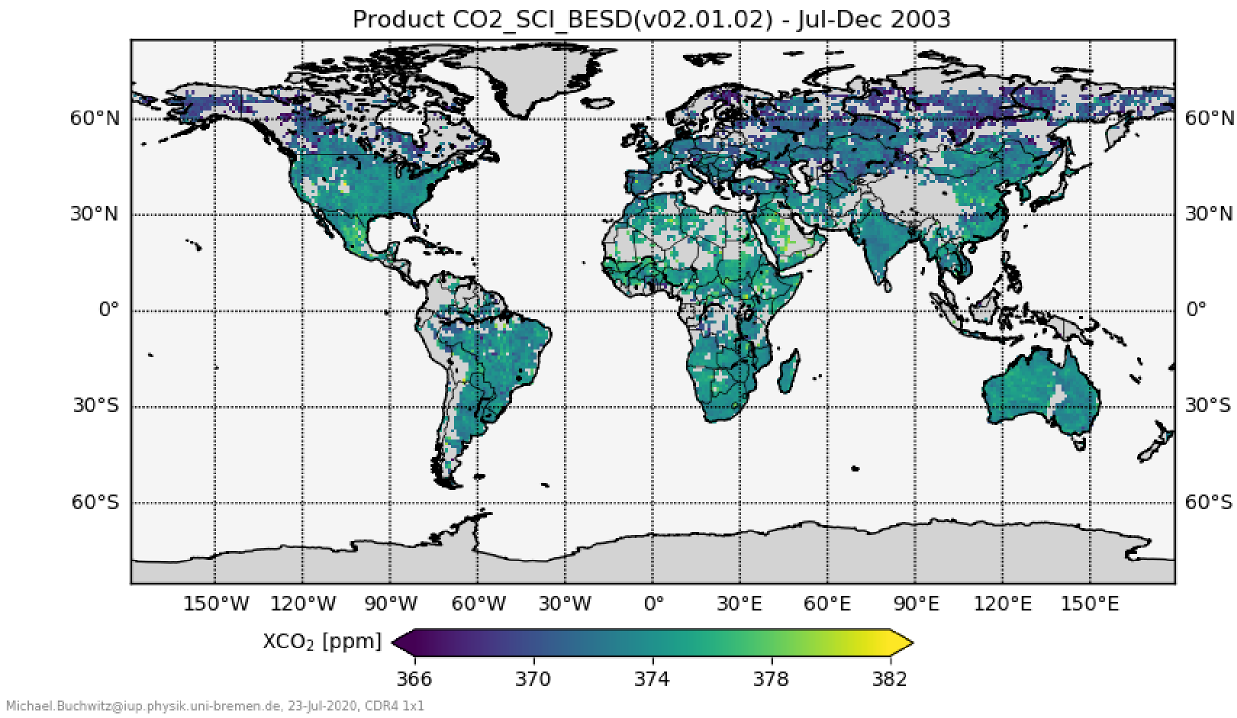

Figure 8 - XCO_2 product CO2_SCI_WFMD. Top: January to June 2003. Bottom: July – December 2003.

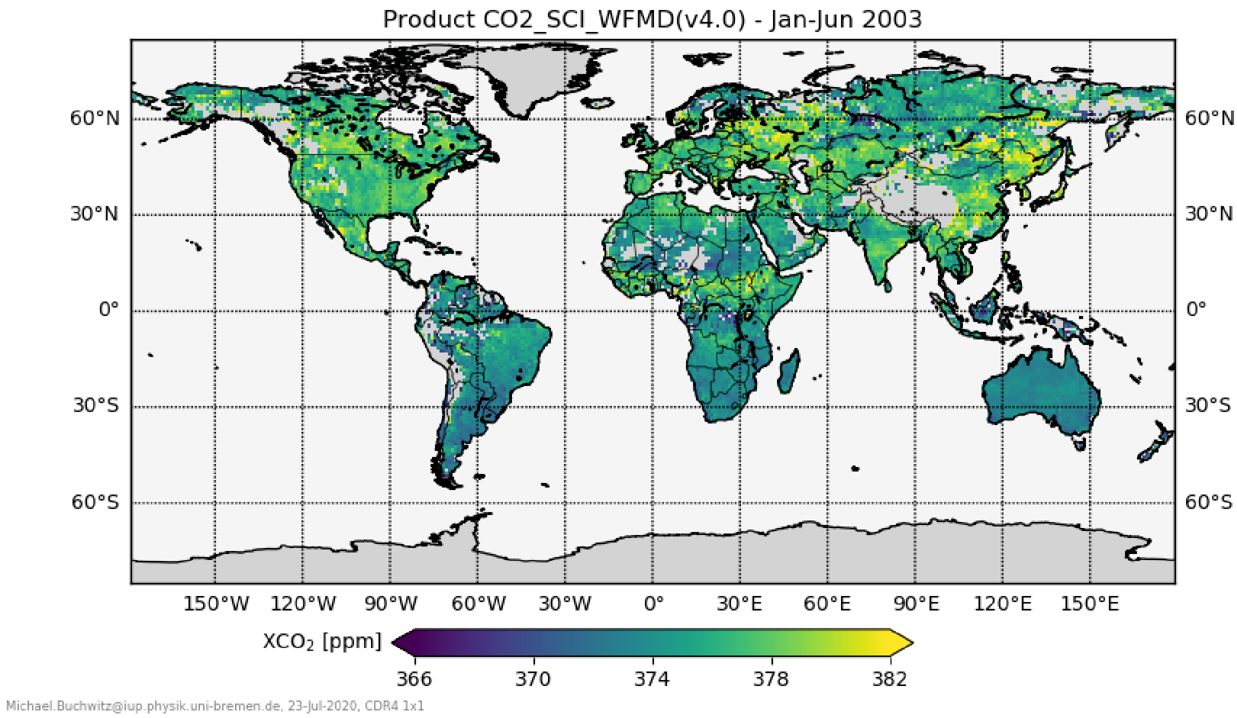

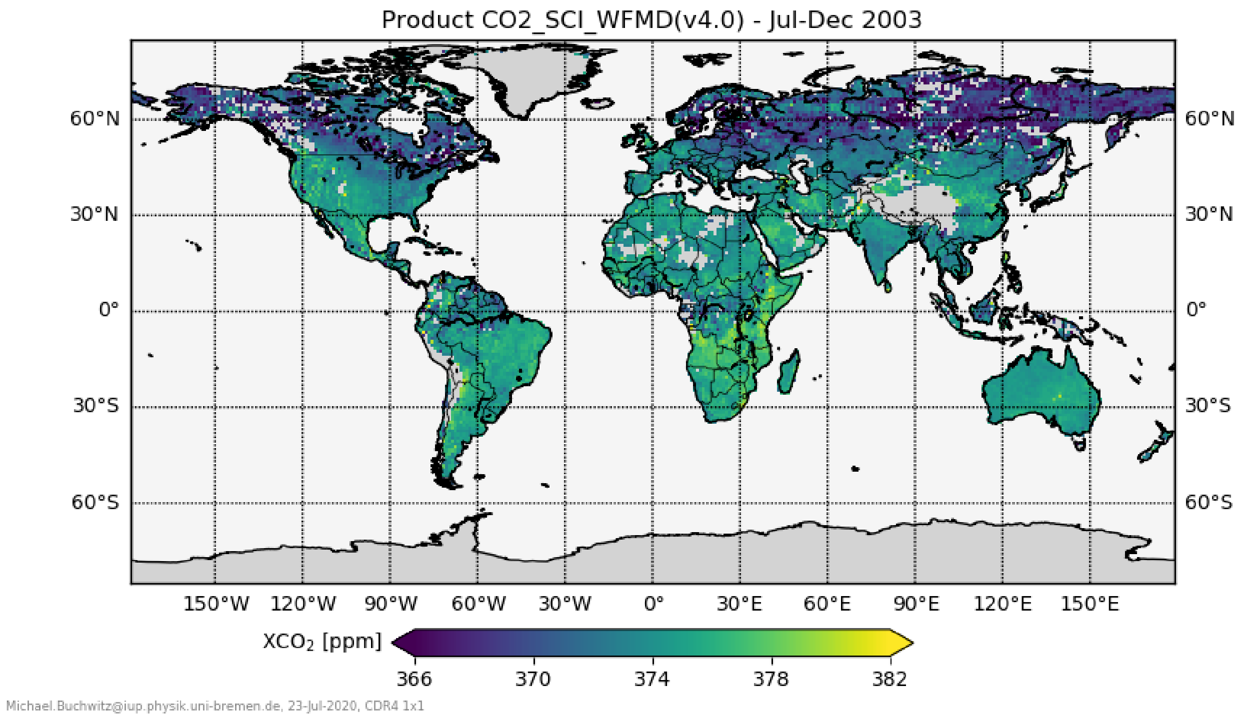

Figure 9 - XCO_2 product CO2_GOS_OCFP. Top: January to June 2019. Bottom: July – December 2019.

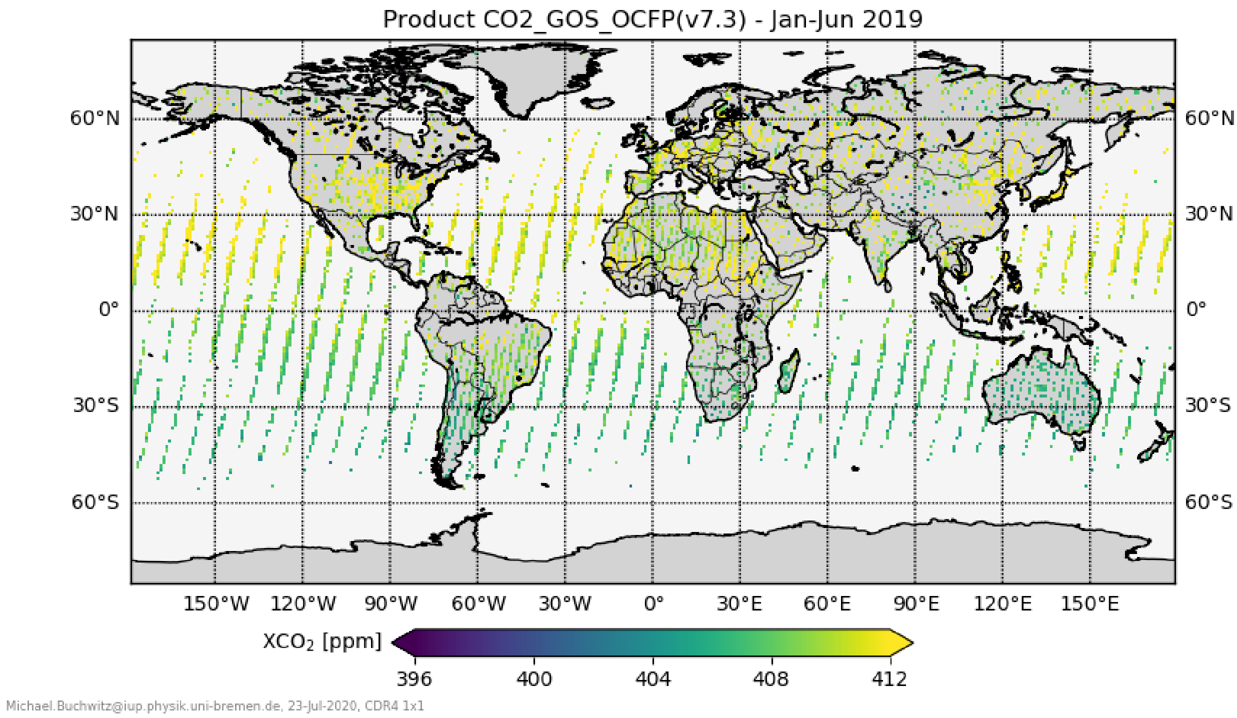

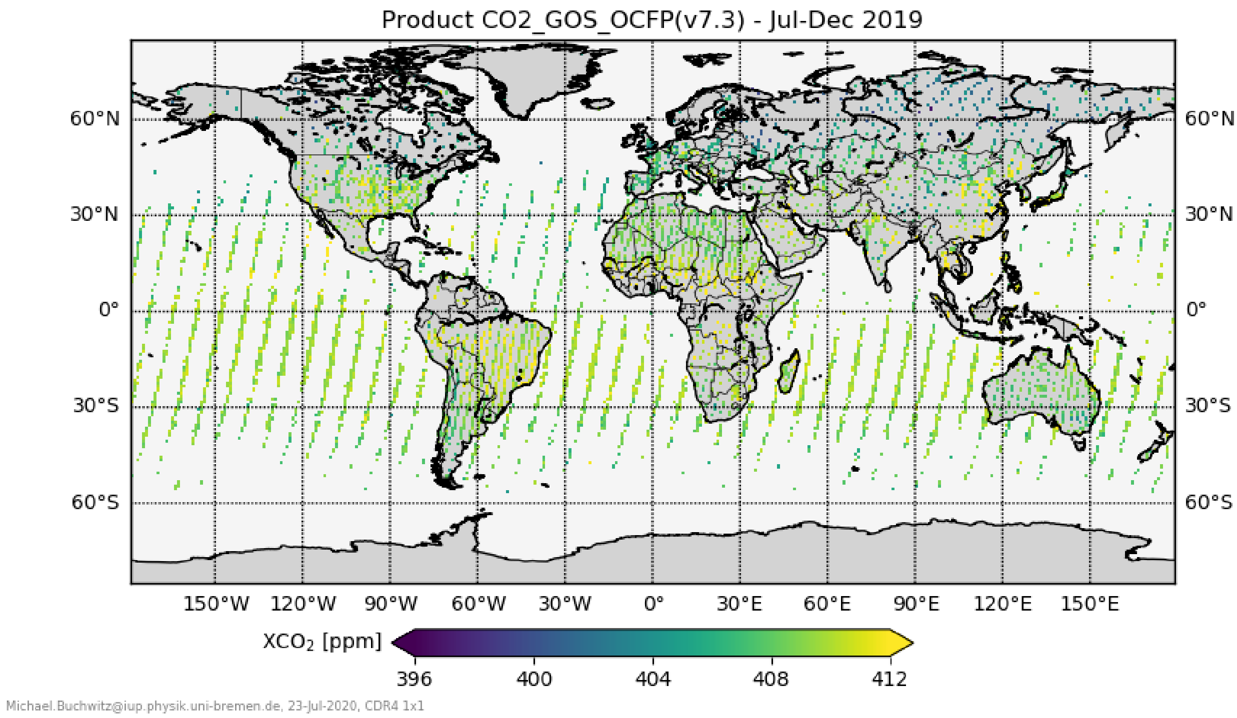

Figure 10 - XCO_2 product CO2_GOS_SRFP. Top: January to June 2019. Bottom: July – December 2019.

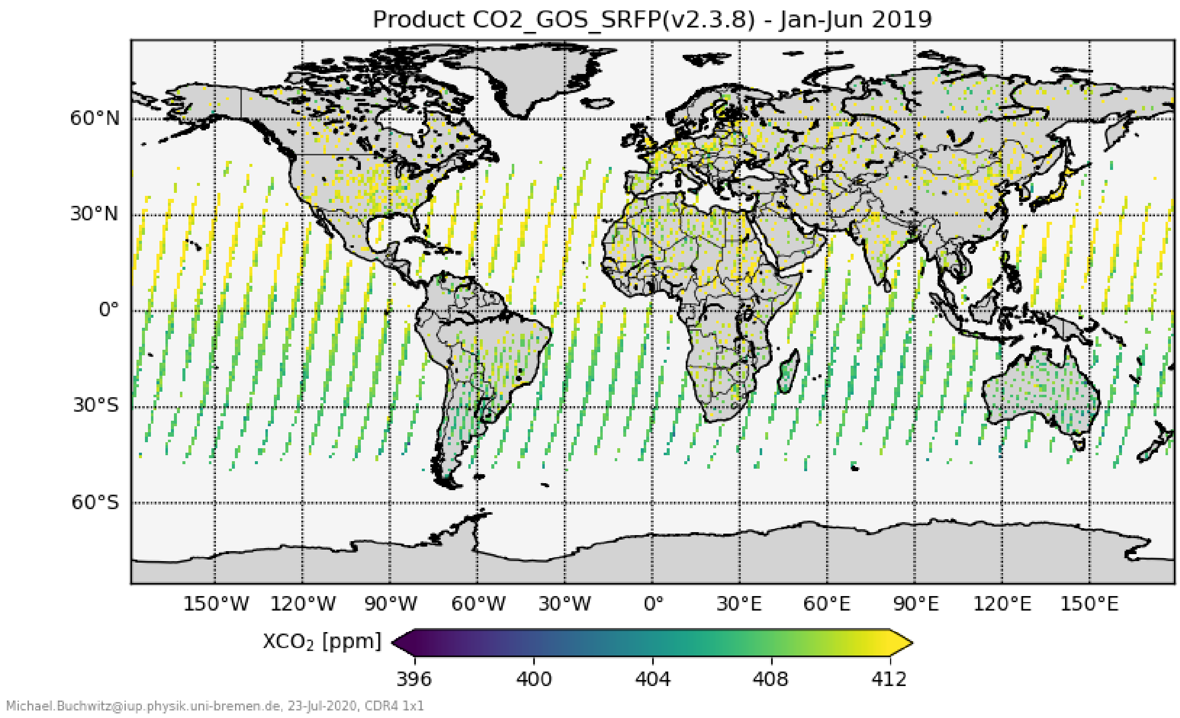

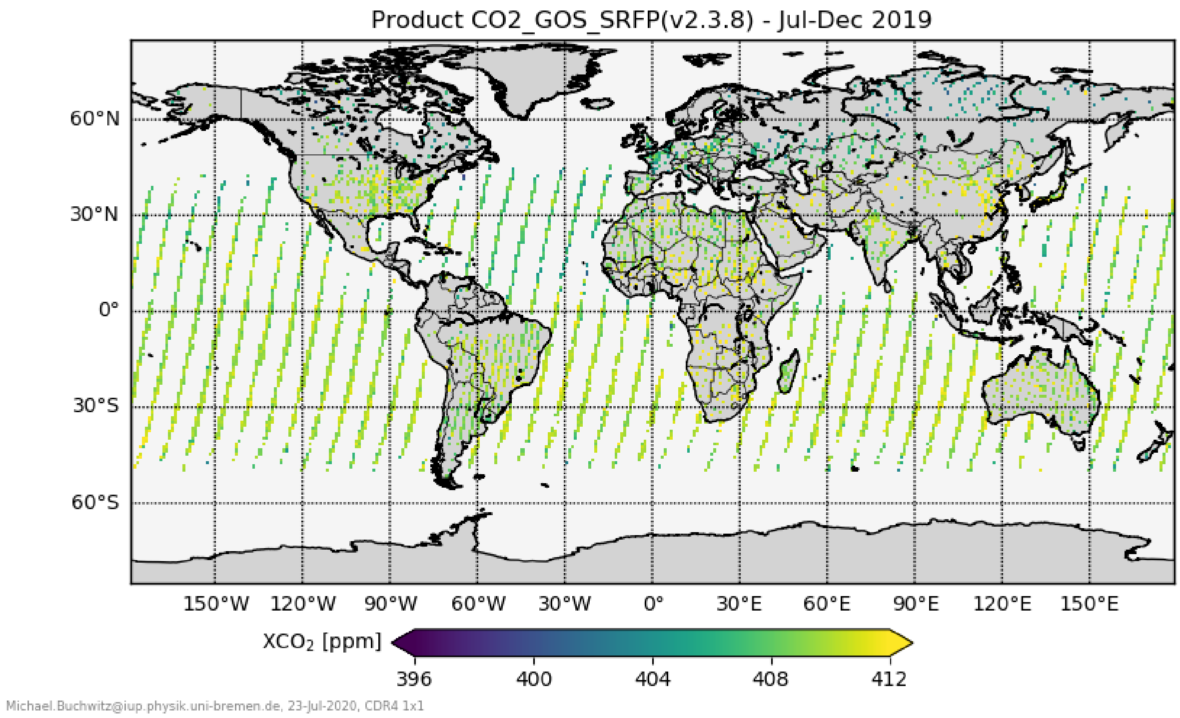

Figure 11 - XCH_4 product CH4_SCI_WFMD. Top: January to June 2003. Bottom: July – December 2003.

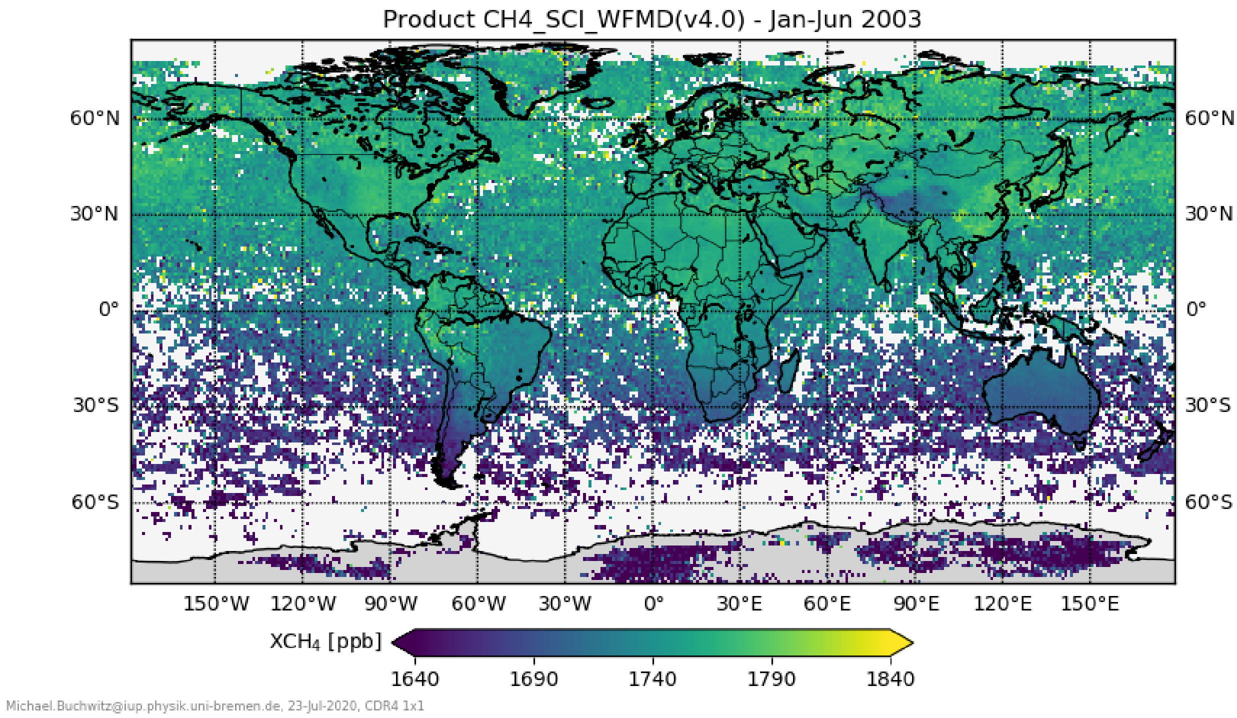

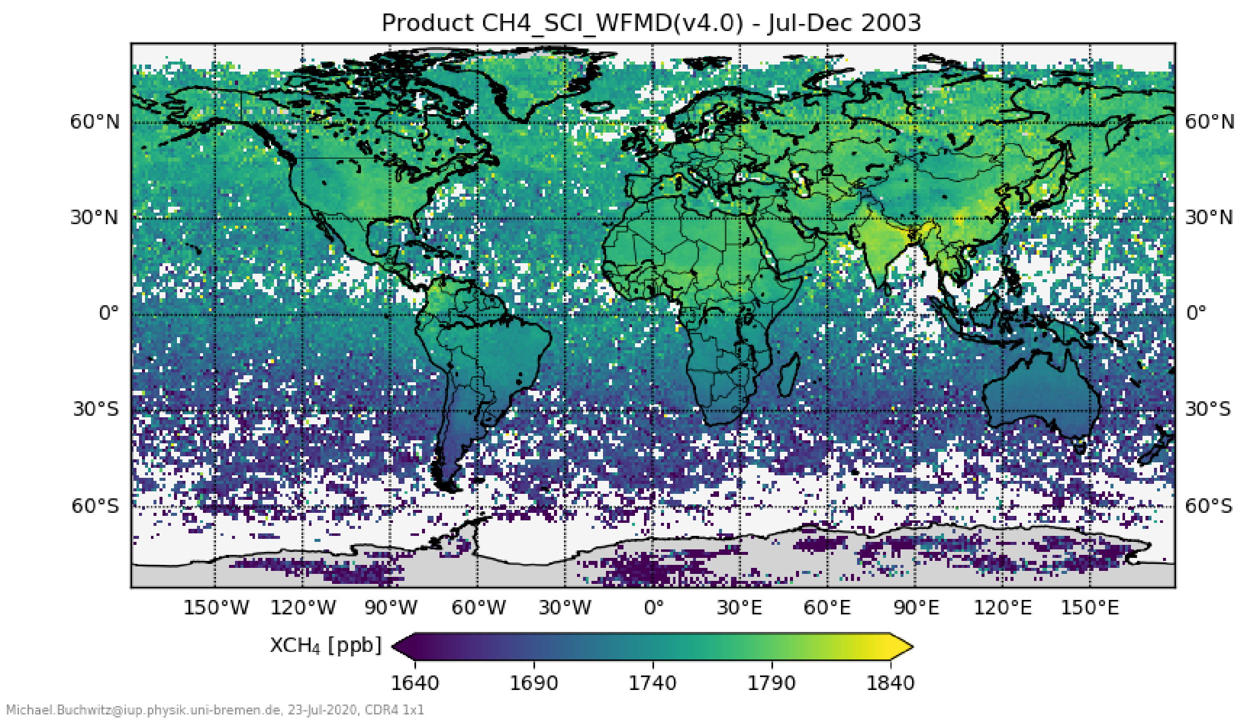

Figure 12 - XCH_4 product CH4_SCI_IMAP. Top: January to June 2003. Bottom: July – December 2003.

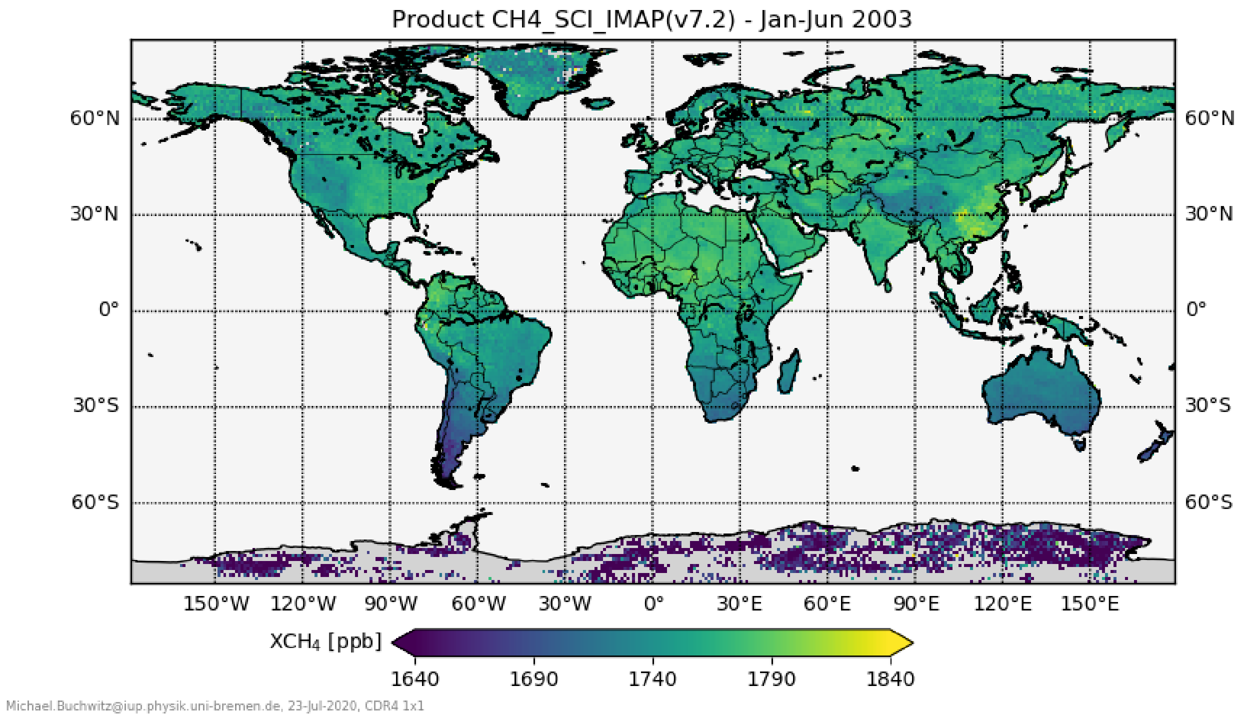

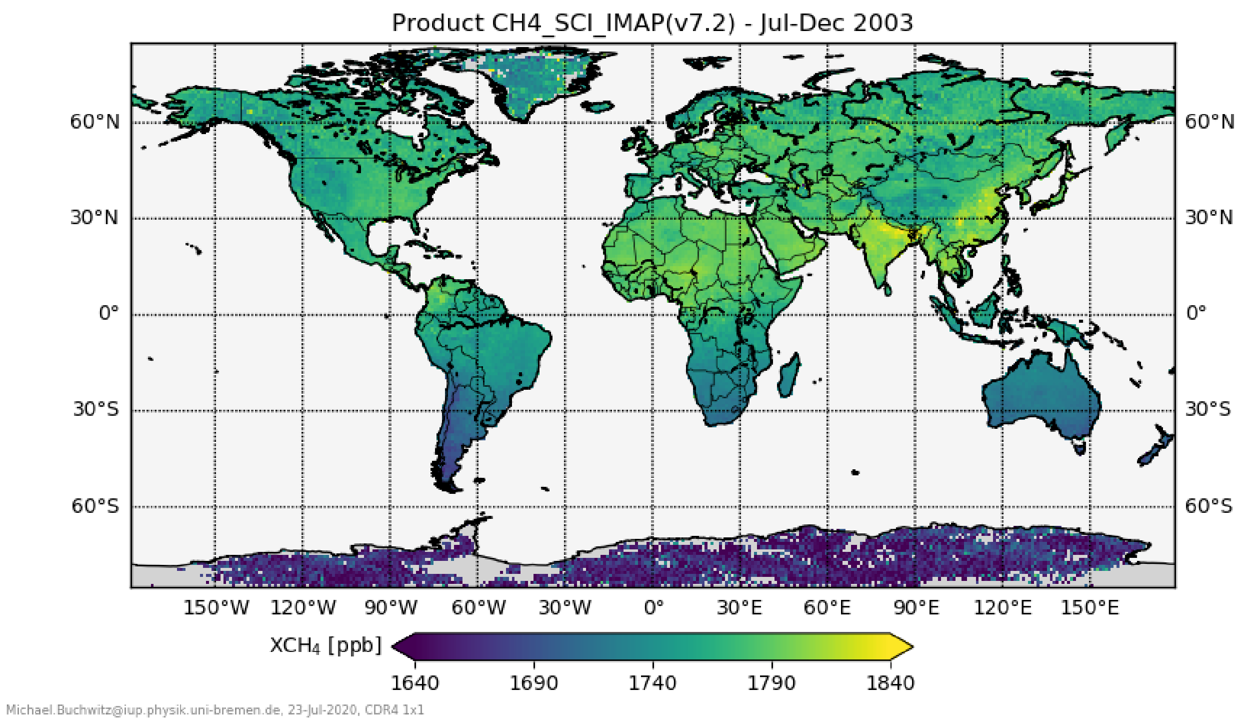

Figure 13 - XCH_4 product CH4_GOS_OCPR. Top: January to June 2019. Bottom: July – December 2019.

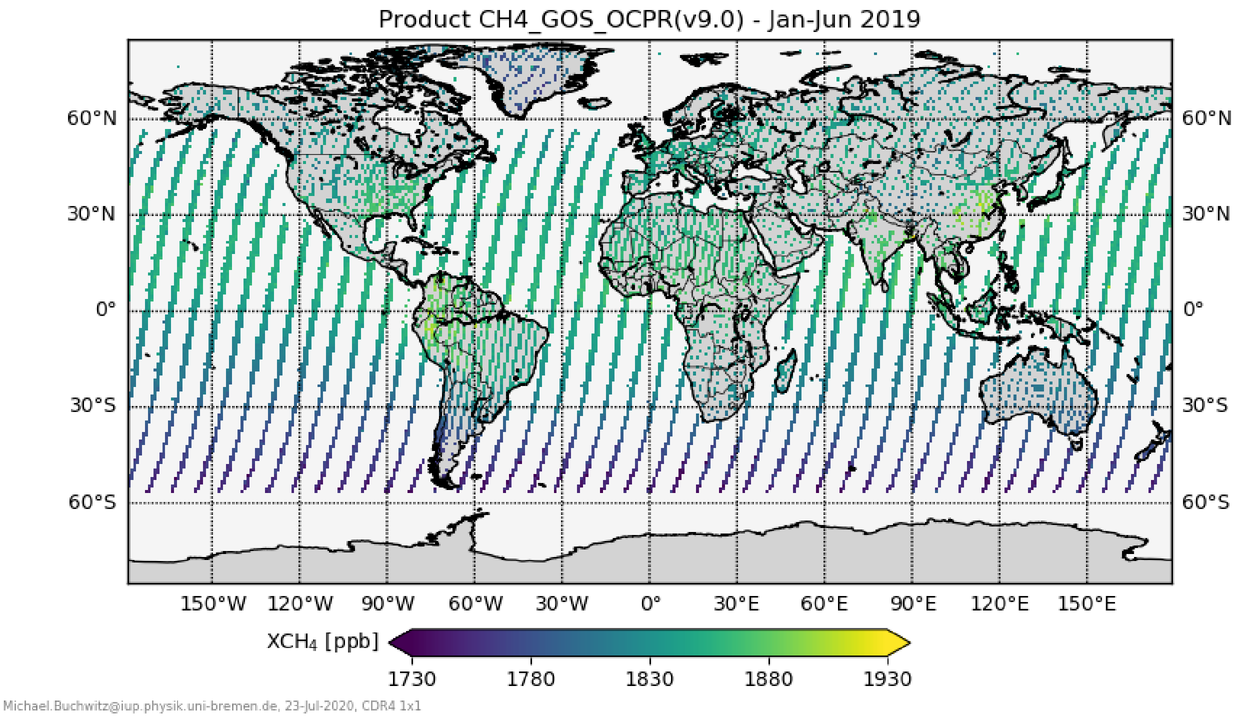

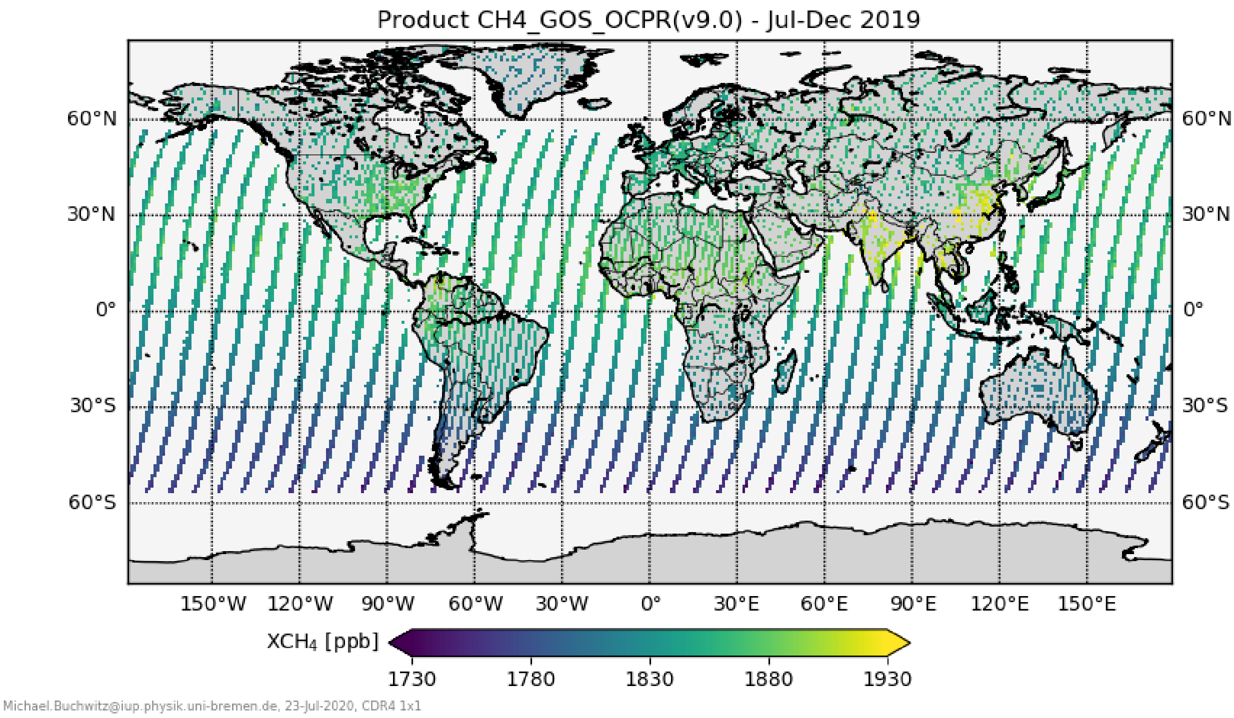

Figure 14 - XCH_4 product CH4_GOS_SRPR. Top: January to June 2019. Bottom: July – December 2019.

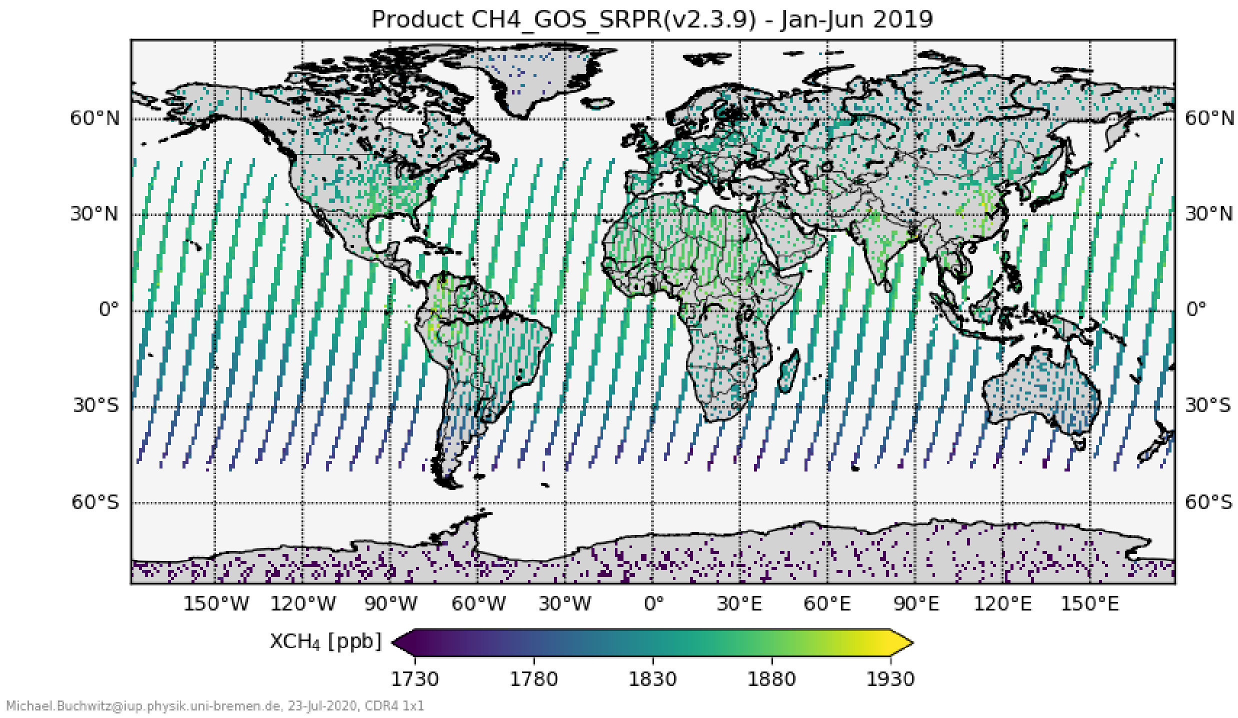

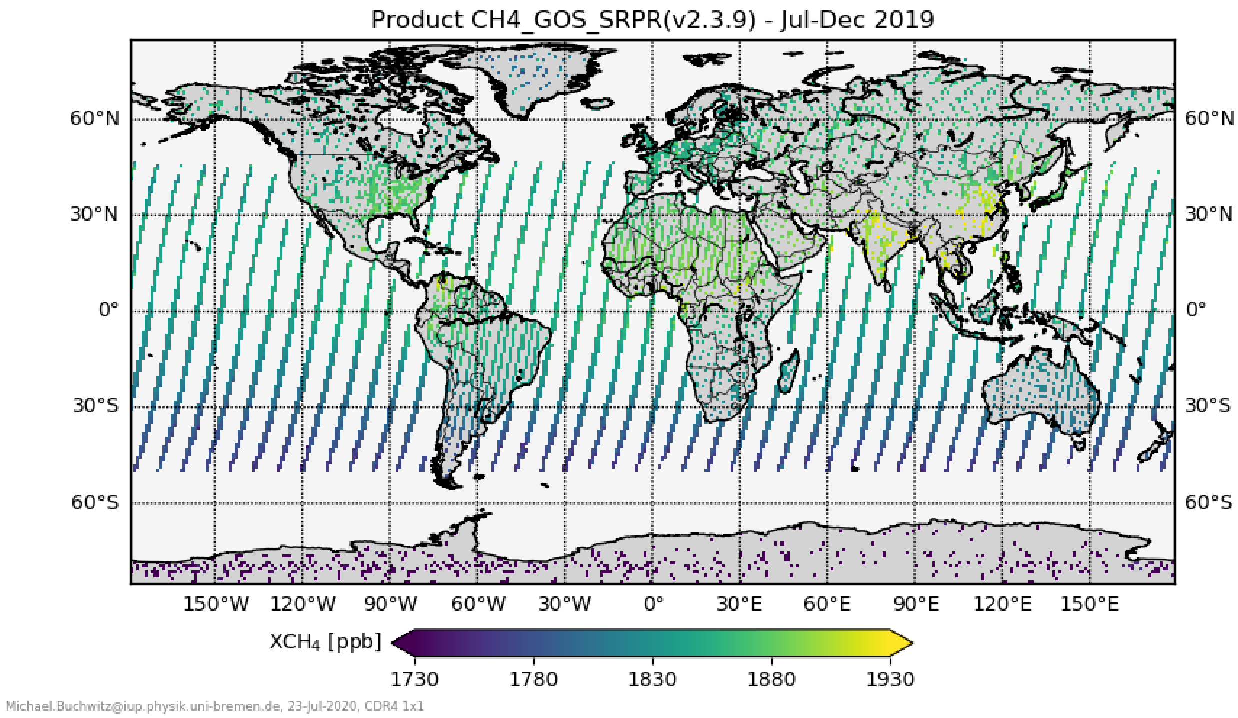

Figure 15 - XCH_4 product CH4_GOS_OCFP. Top: January to June 2019. Bottom: July – December 2019.

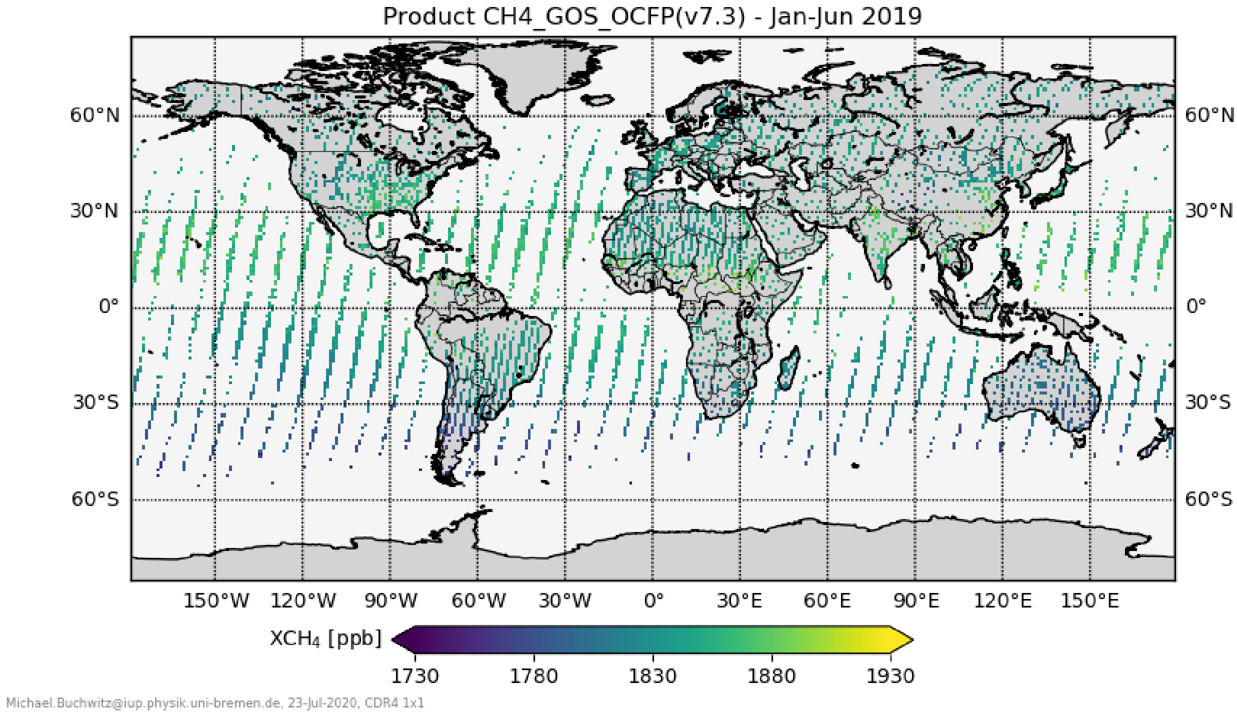

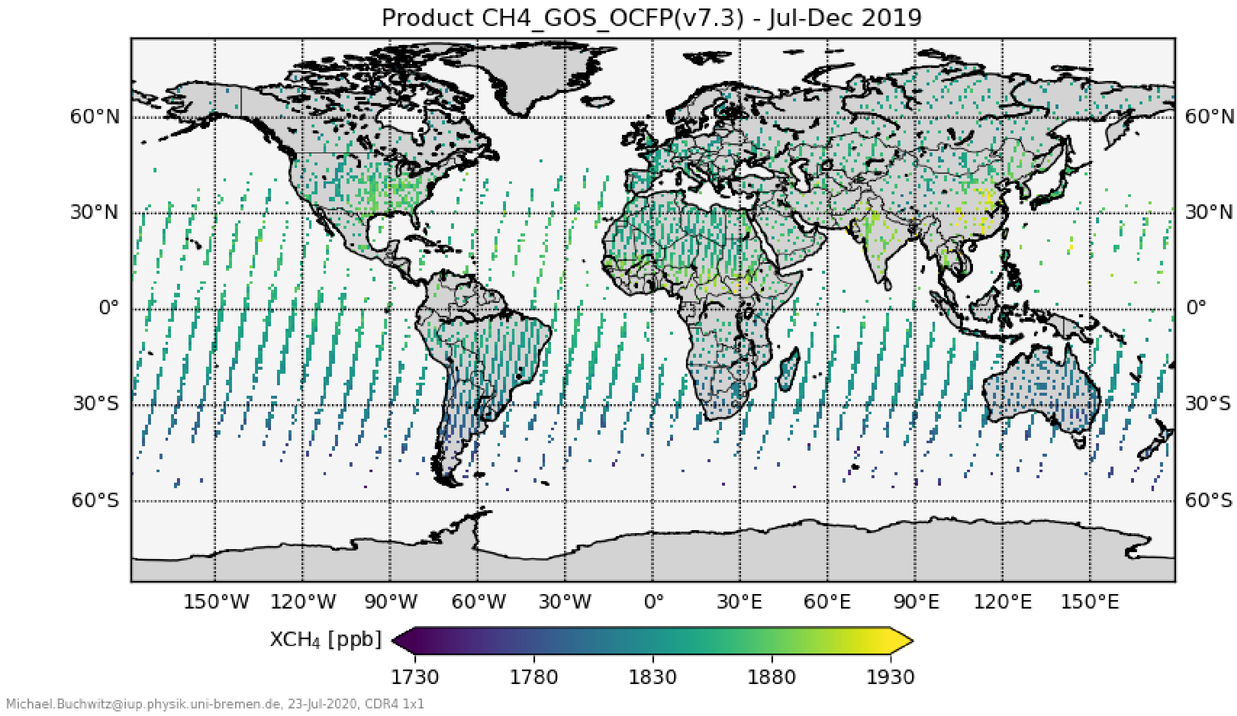

Figure 16 - XCH_4 product CH4_GOS_SRFP. Top: January to June 2019. Bottom: July – December 2019.

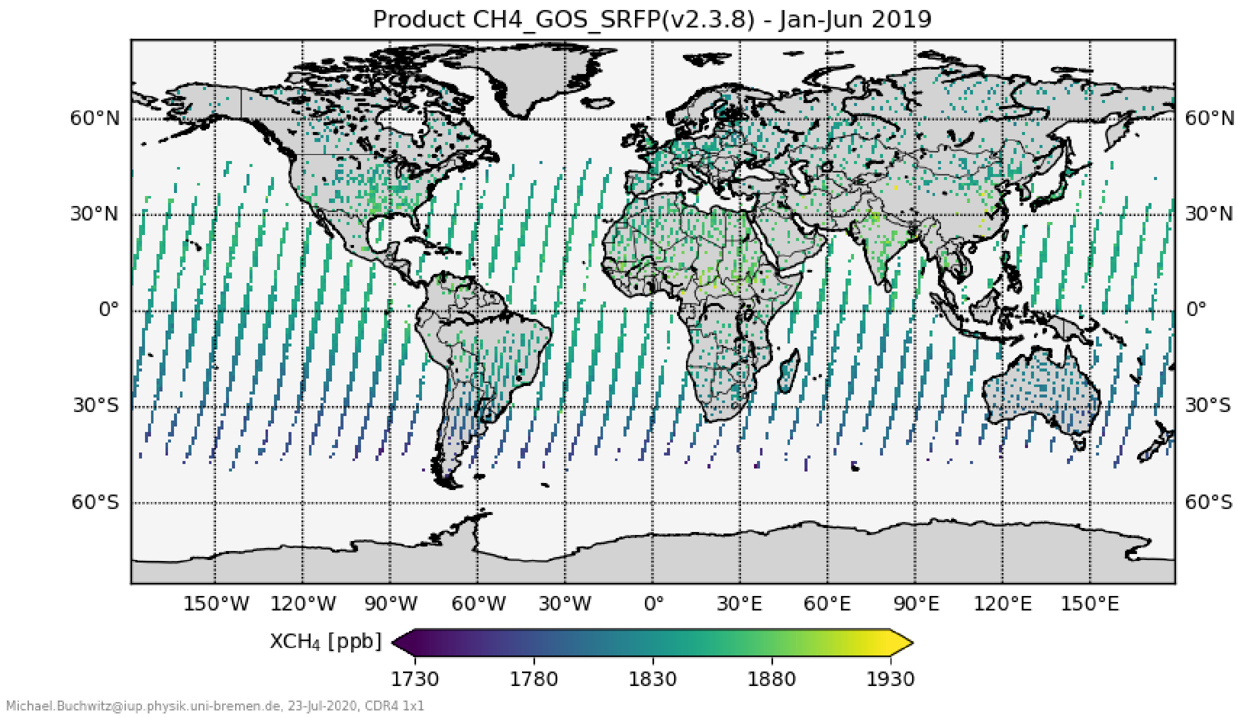

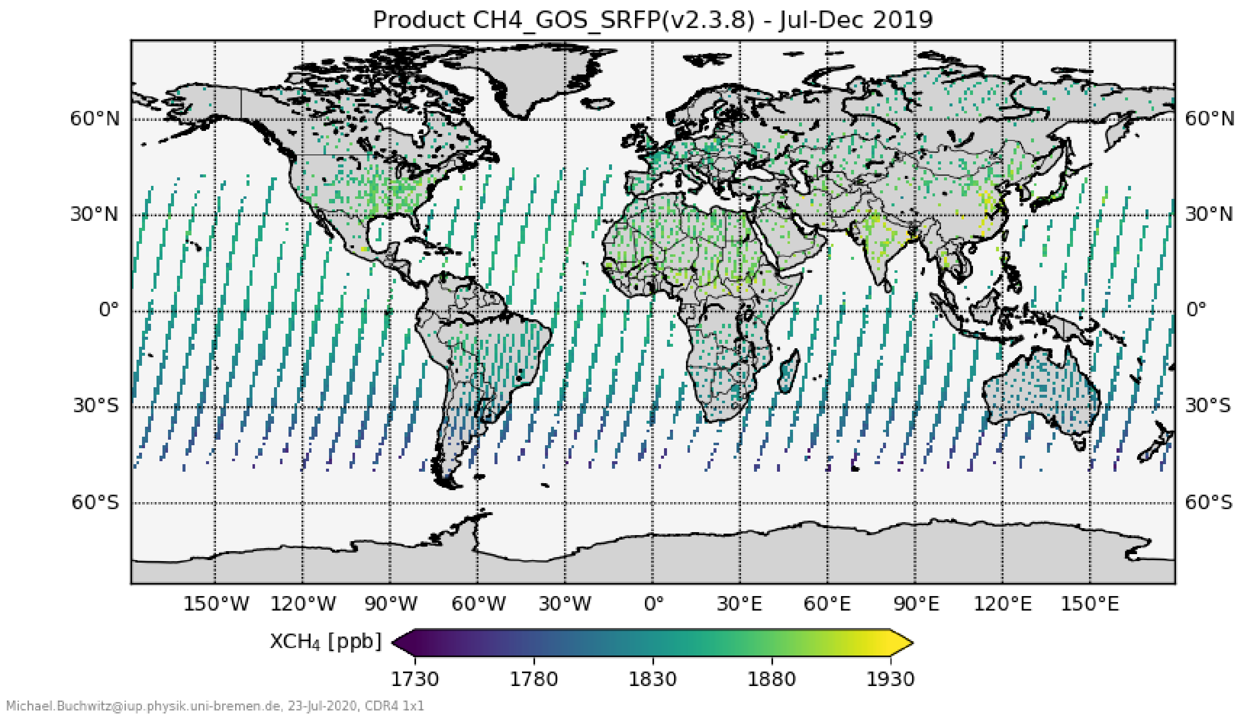

Latitude-time plots of products XCO2_EMMA (Figure 17) and XCH4_EMMA (Figure 18) are shown in the figures below. Discontinuities for «Uncertainty» and number of observations («Nobs») are due to the use of different satellites, which have - for example - different noise characteristics.

Figure 17 – Latitude – time plot of XCO_2 product XCO2_EMMA.

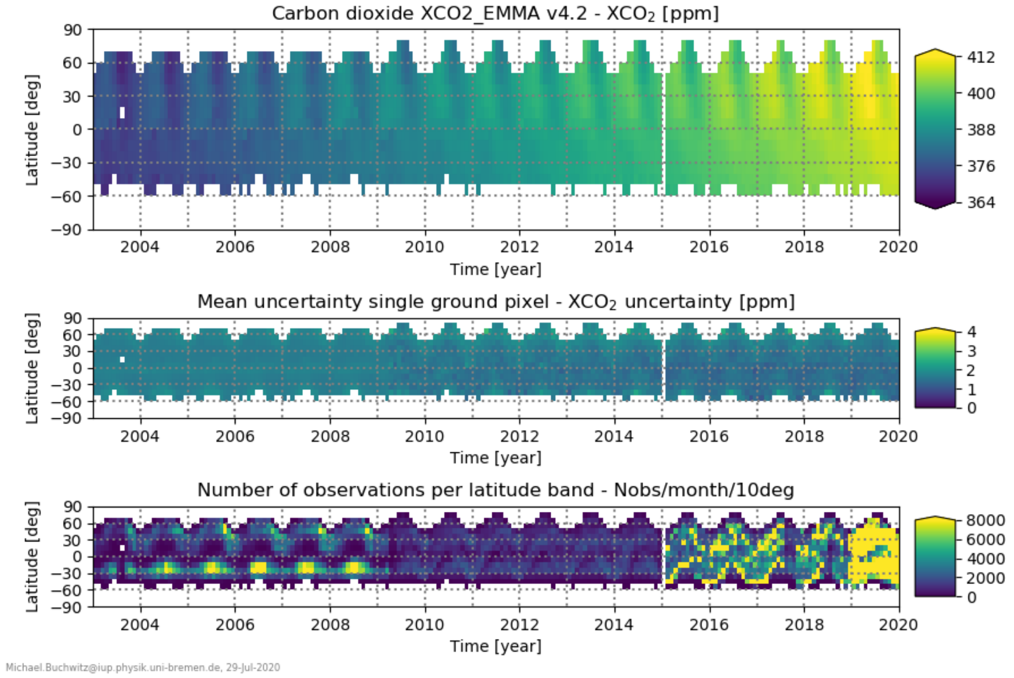

Figure 18 – Latitude – time plot of XCH_4 product XCH4_EMMA.

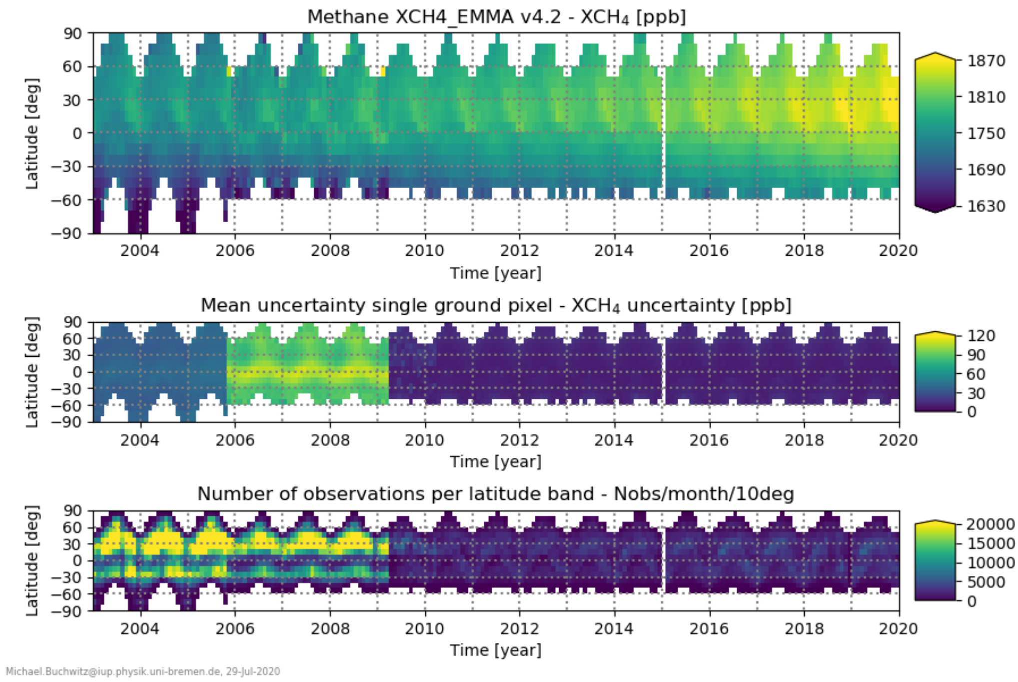

1.2 Mid-tropospheric mixing ratios of CO_2 and CH_4

1.2.1 Overview

Satellite radiance observations in the thermal infrared (TIR) spectral region in nadir (down looking) observation viewing mode are sensitive to atmospheric CO_2 and CH_4 mixing ratio changes in the mid and upper tropospheric region. They can thus be interpreted in terms of integrated mid-tropospheric columns, with typical sensitivity between 5 and 12 km.

In the following, the 2 hyperspectral infrared sounders AIRS and IASI are shortly described.

1.2.2 Instruments

1.2.2.1 AIRS

The Atmospheric Infrared Sounder (AIRS) is a polar orbiting nadir-viewing high-resolution infrared sounder operating in a cross-track-scanning mode. It was launched onboard the EOS Aqua satellite in May 2002, with two operational microwave sounders, AMSU and HSB, and is operational since September 2002. It is a high-spectral resolution, grating multispectral infrared sounder with 2378 channels. Its spectral domain ranges from 650 cm^{-1} to 2665 cm^{-1} (15.4 µm and 3.8 µm), with a spectral resolving power of 1200 (i.e., a spectral resolution ranging from 0.5 cm^{-1} to 2 cm^{-1}). This domain is divided into three spectral bands, from 650 to 1135 cm^{-1}, from 1215 to 1615 cm^{-1} and from 2180 to 2665 cm^{-1}. AIRS cross-track scanning is 1650 km and covers 70% of the earth every day. The instantaneous field of view (IFOV) is sampled by 3×3 circular pixels whose ground resolution is 13 km at nadir. Measurements from the three instruments are analyzed jointly to filter out the effects of clouds from the IR data in order to derive clear-column air-temperature profiles and surface temperatures with high vertical resolution and accuracy (1 K per 1 km layer in the troposphere).

1.2.2.2 IASI

The Infrared Atmospheric Sounding Interferometer (IASI) is a high resolution Fourier Transform Spectrometer based on a Michelson Interferometer coupled to an integrated imaging system that measures infrared radiation emitted from the Earth. Developed by the Center National d'Etudes Spatiales (CNES) in collaboration with the European Organisation for the Exploitation of Meteorological Satellites (EUMETSAT), IASI was launched in October 2006 onboard the polar orbiting Meteorological Operational Platform (Metop-A), in September 2012 onboard Metop-B, and in November 2018 onboard Metop-C. IASI provides 8461 spectral samples, ranging from 645 cm^{-1} to 2760 cm^{-1} (15.5 µm and 3.6 µm), with a spectral sampling of 0.25 cm^{-1}, and a spectral resolution of 0.5 cm^{-1} after apodisation ('Level 1c' spectra). IASI is an across track scanning system, whose swath width is of 2200 km, allowing global coverage twice a day. The IFOV is sampled by 2×2 circular pixels whose ground resolution is 12 km at nadir. IASI has demonstrated the possibility to retrieve or detect several chemistry and climate variables from hyperspectral infrared observation: for instance, water vapour (H_2O), carbon dioxide (CO_2), carbon monoxide (CO), methane (CH_4), ozone (O_3), sulfur dioxide (SO_2), hydrogen sulfide (H_2S), ammonia (NH_3), nitric acid (HNO_3), volatile organic compounds (VOCs) and aerosols (*Hilton et al., 2012; Clarisse et al., 2011*) on regional and global scales. IASI enables the monitoring of key gases for climate and atmospheric chemistry in near real time and has also highlighted the benefit of high-performance infrared sounders for numerical weather prevision (NWP) applications.

1.2.3 CO_2

Mid-tropospheric columns of CO_2 can be retrieved from hyperspectral infrared sounders such as AIRS and IASI (*Chédin et al., 2003; Crevoisier et al., 2003*) using non-linear inference scheme (Crevoisier et al., 2009a).

Products have been validated using aircraft measurements, mostly from the Comprehensive Observation Network for TRace gases by AIrLiner (CONTRAIL) program (*Machida et al., 2008; Matsueda et al. 2008*).

As an example, Figure 19 shows time series of IASI/Metop-A derived mid-tropospheric CO_2 column as a function of time and latitude. The trend, seasonality and latitudinal gradient of CO_2 are well seen in the figure.

Figure 20 shows the same but for IASI/Metop-B.

Figure 21 and Figure 22 show spatial maps for the IASI/Metop-A and IASI/Metop-B products, respectively, to also illustrate the spatial coverage of the data for a typical month including number of observations an standard deviation.

Figure 19 – Monthly and latitudinal evolution of mid-tropospheric CO_2 (top) as seen by IASI/Metop-A and number of observations per 10 deg latitude band (bottom).

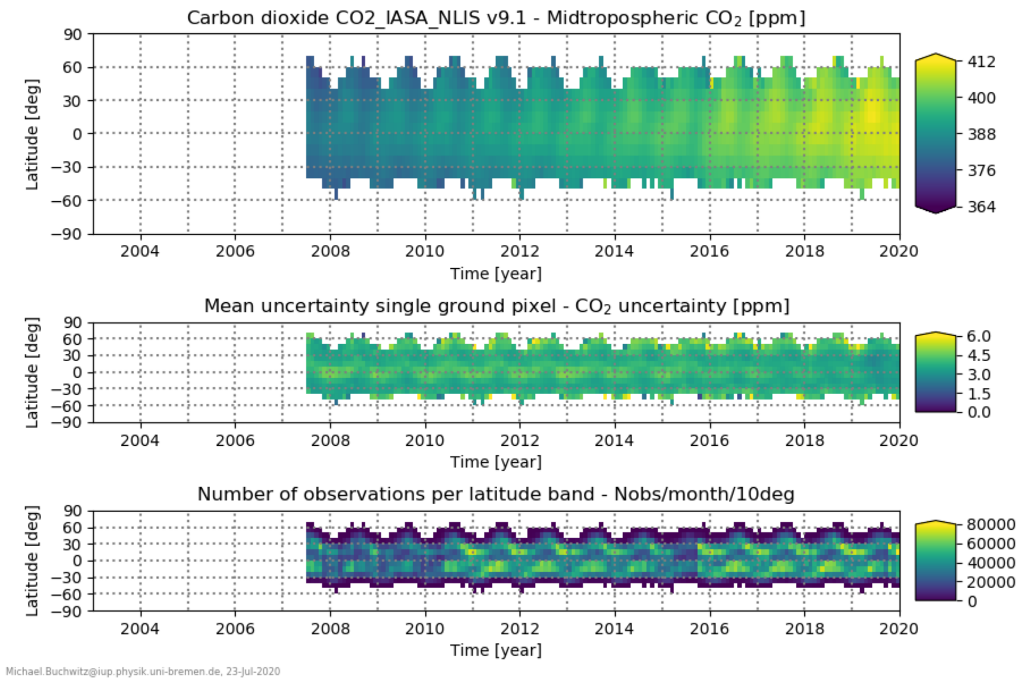

Figure 20 - Monthly and latitudinal evolution of mid-tropospheric CO_2 (top) as seen by IASI/Metop-B and number of observations per 10 deg latitude band (bottom).

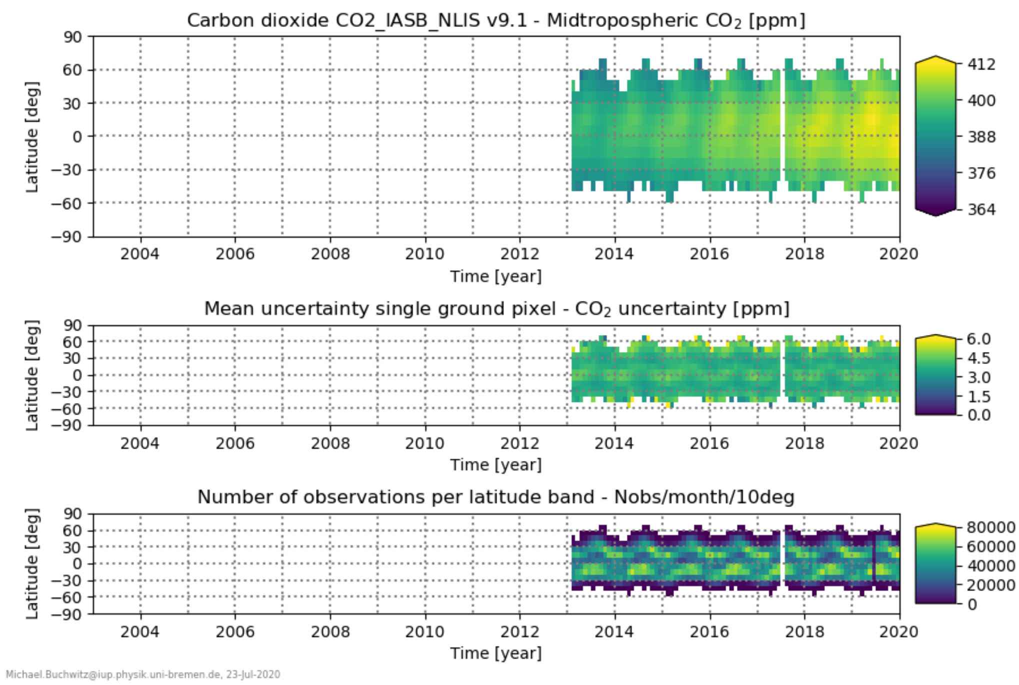

Figure 21 - Map of mid-tropospheric CO_2 from IASI/Metop-A for August 2019 (top left). Mean value of the reported uncertainty (top right), number of observations per 5°x5° grid size (bottom left) and standard deviation (bottom right).

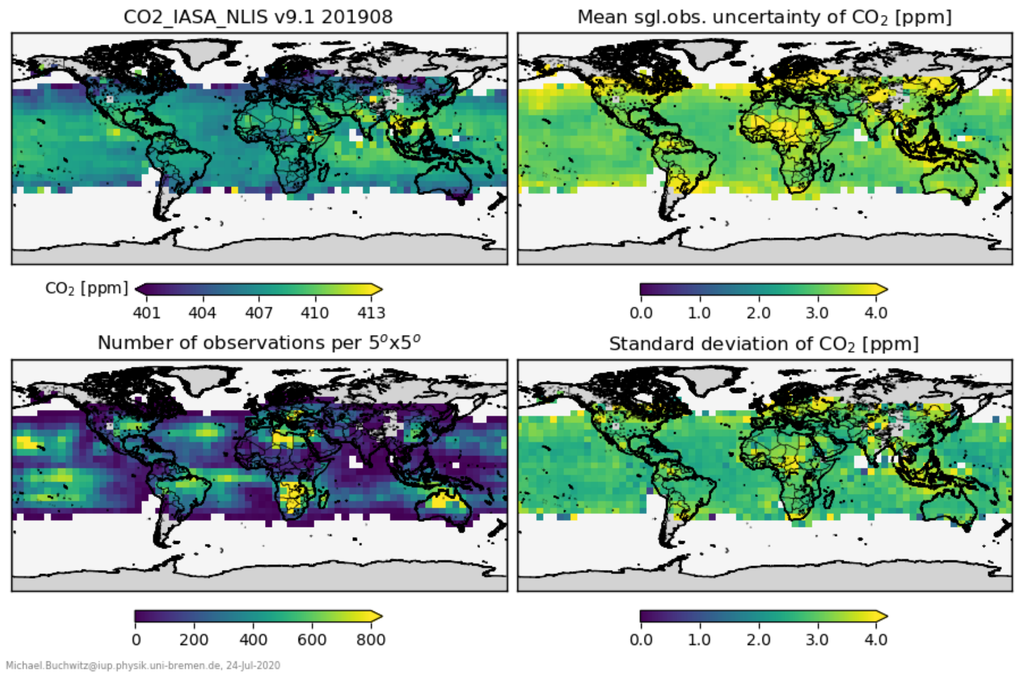

Figure 22 - Map of mid-tropospheric CO_2 from IASI/Metop-B for August 2019 (top left). Mean value of the reported uncertainty (top right), number of observations per 5°x5° grid size (bottom left) and standard deviation (bottom right).

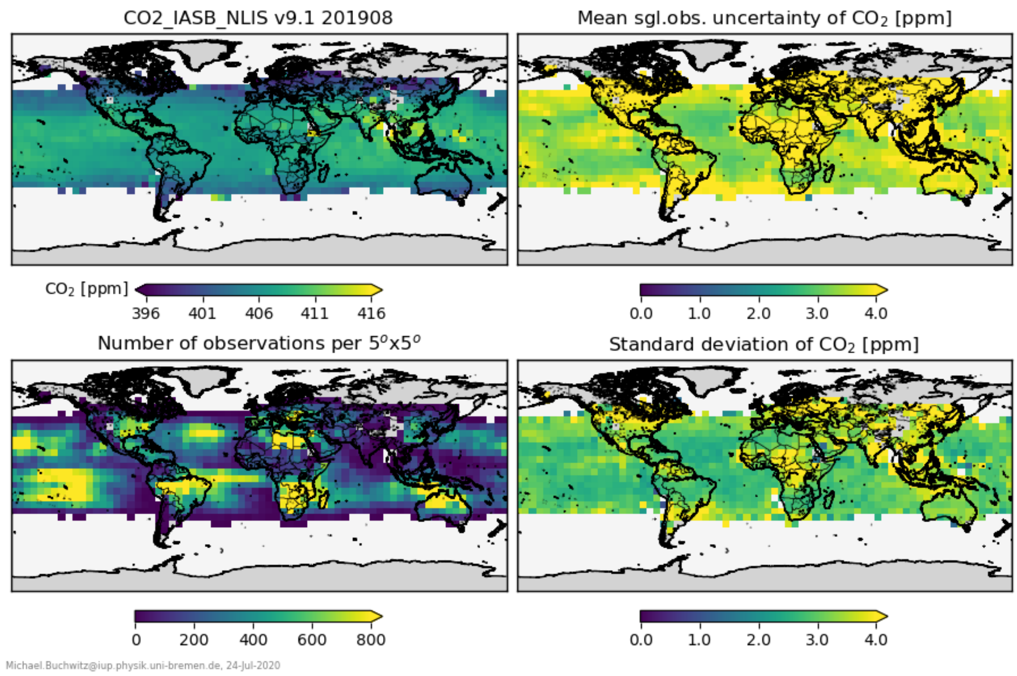

1.2.4 CH_4

Mid-tropospheric columns of CH_4 can be retrieved from the hyperspectral infrared sounder IASI (Crevoisier et al., 2003, 2013) using non-linear inference scheme (*Crevoisier et al., 2009b*).

Products have been validated using aircraft measurements, from the Comprehensive Observation Network for TRace gases by AIrLiner (CONTRAIL) program (*Machida et al., 2008; Matsueda et al. 2008*) and the HIAPER Pole-to-Pole Observations (HIPPO) project (Wofsy et al., 2012), as well as from balloon measurements from AirCores (*Membrive et al., 2016*).

As an example, Figure 23 shows time series of IASI/Metop-A derived mid-tropospheric CO_2 column as a function of time and latitude. The trend, seasonality and latitudinal gradient of CO_2 are well seen in the figure.

Figure 24 shows the same but for IASI/Metop-B.

Figure 25 and Figure 26 show spatial maps for the IASI/Metop-A and IASI/Metop-B products, respectively, to also illustrate the spatial coverage of the data for a typical month including number of observations and standard deviation.

Figure 23 – Monthly and latitudinal evolution of mid-tropospheric CH_4 (top) as seen by IASI/Metop-A and number of observations per 10 deg latitude band (bottom).

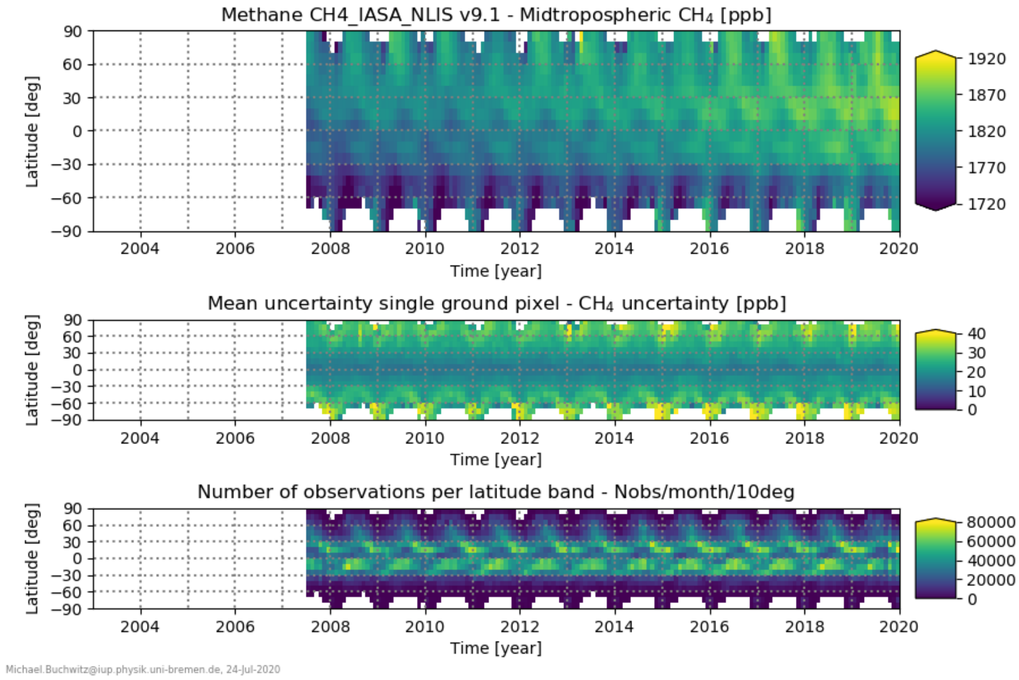

Figure 24 - Monthly and latitudinal evolution of mid-tropospheric CH_4 (top) as seen by IASI/Metop-B and number of observations per 10 deg latitude band (bottom).

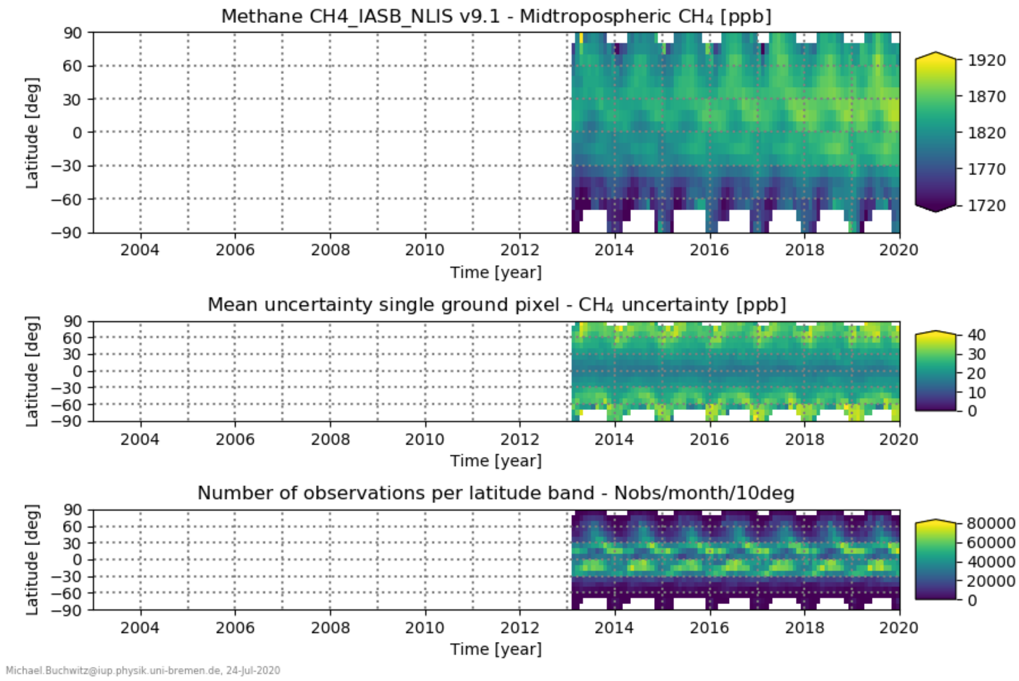

Figure 25 - Map of mid-tropospheric CH_4 from IASI/Metop-A for August 2019 (top left). Mean value of the reported uncertainty (top right), number of observations per 5°x5° grid size (bottom left) and standard deviation (bottom right).

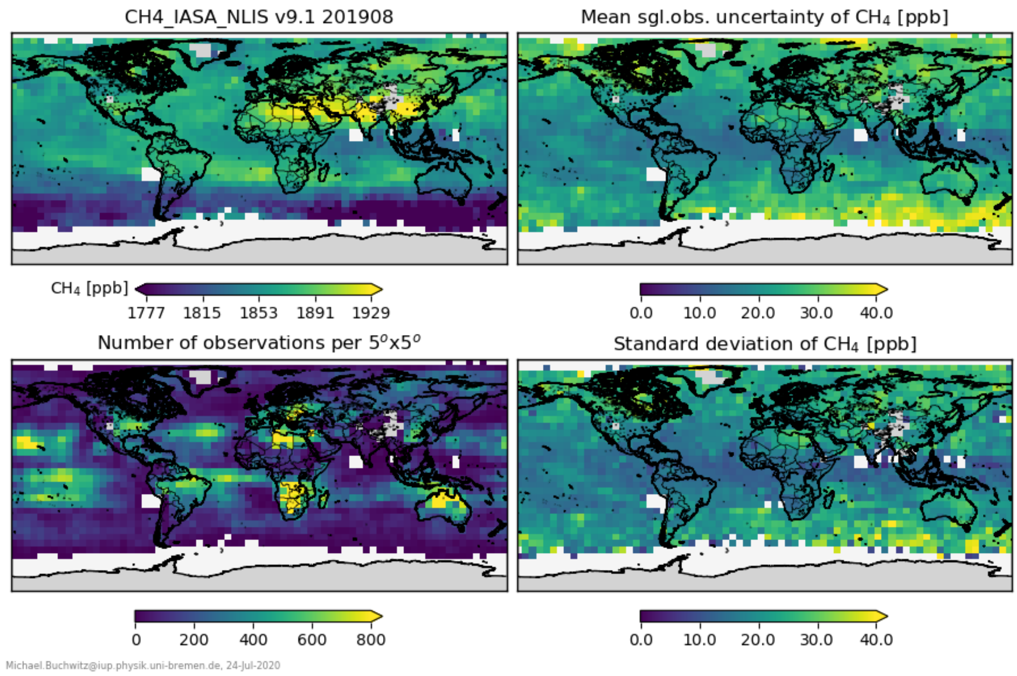

Figure 26 - Map of mid-tropospheric CH_4 from IASI/Metop-B for August 2019 (top left). Mean value of the reported uncertainty (top right), number of observations per 5°x5° grid size (bottom left) and standard deviation (bottom right).

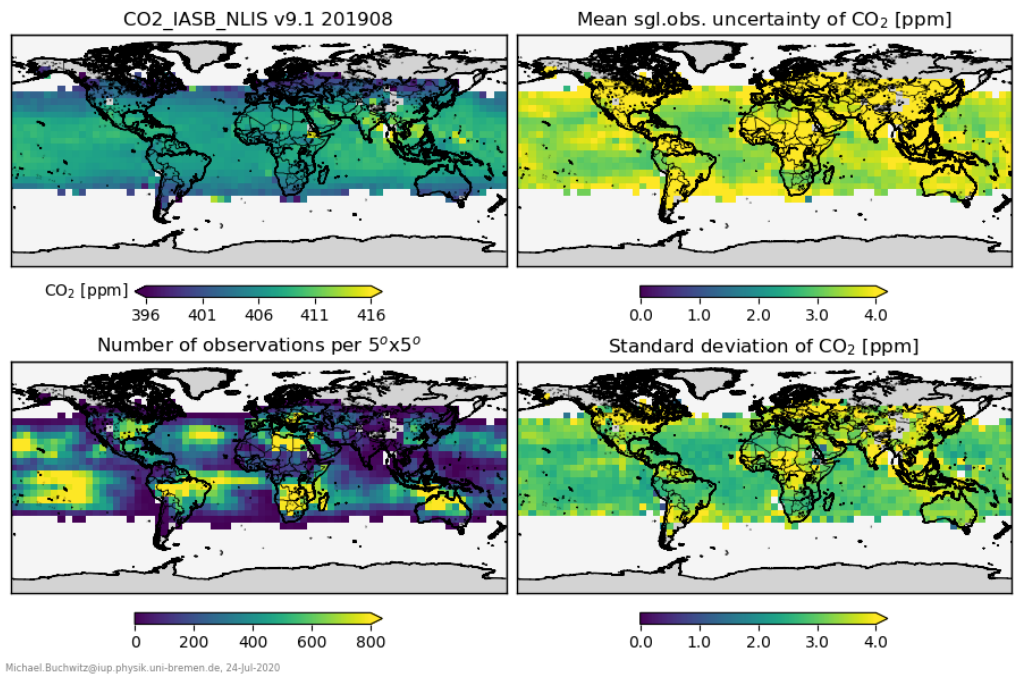

1.2.5 List of mid-tropospheric CO_2 and CH_4 data products

Table 6 lists the CO_2 and CH_4 mid/upper troposphere data products.

The product with comment «Existing GHG-CCI product» is the latest versions of AIRS CO_2 Level 2 products, which had been generated in the framework of the ESA GHG-CCI project.

Table 6 - Overview mid/upper troposphere CO_2 and CH_4 data products.

Product ID	Level	Sensor(s)	(Planned) Availability	Comments
CO2_IASA_NLIS	2	IASI / Metop-A	Oct. 2017: 2007-2015 Dec. 2020: 2007-2019	
CH4_IASA_NLIS	2	IASI / Metop-A	Oct. 2017: 2007-2015 Dec. 2020: 2007-2019	
CO2_IASB_NLIS	2	IASI / Metop-B	Oct. 2017: 2013-2016 Oct. 2018: 2013-2017 Dec. 2019: 2013-2018 Dec. 2020: 2013-2019	
CH4_IASB_NLIS	2	IASI / Metop-B	Oct. 2017: 2013-2016 Oct. 2018: 2013-2017 Dec. 2019: 2013-2018 Dec. 2020: 2013-2019	
CO2_AIR_NLIS	2	AIRS	Feb. 2017: 2003-2007	Existing GHG-CCI product

2. Level 2 XCO_2 and XCH_4 data products

2.1 Product description

The format of these data products is described in and compliant with the specification of the corresponding pre-cursor products as given in the GHG-CCI project Product Specification Document (PSD), version 3 (*Buchwitz et al., 2014*):

- Buchwitz, M., et al., ESA Climate Change Initiative (CCI) Product Specification Document (PSD) for the Essential Climate Variable (ECV) Greenhouse Gases (GHG), 6-June-2014, Version 3, 2014.

These products are in NetCDF-4 (classic) format and are in-line with CF (Climate and Forecasting) convention 3. The products are essentially self-explaining in particular due to the metadata contained in each data product.

The file names consist of ESACCI-GHG (to be consistent with the pre-cursor products), processing level (L2), product type (CO_2 or CH_4), sensor (e.g., SCIAMACHY, GOSAT), algorithm (e.g., BESD or SRFP), date (YYYYMMDD), file version (fv#) and file name extension (.nc), separated by hyphens ("-").
Examples:
ESACCI-GHG-L2-CO2-SCIAMACHY-BESD-20021216-fv1.nc
ESACCI-GHG-L2-CH4-GOSAT-SRFP-20120909-fv1.nc

Each *.nc product file corresponds to one day of satellite observations.

In *Buchwitz et al., 2014* the so-called Common Parameters of these products are described. These are those parameters which are relevant for all users. In addition, each product may contain additional (algorithm specific) parameters, which are described in separate Product User Guides (PUGs).

For the C3S products a similar approach is used. In the following the common parameters are described and the additional (algorithm specific) parameters are described in specific ANNEXes (see Sect. 9).

The description given in the following is applicable to the following C3S data products:

- CO2_GOS_OCFP
- CO2_GOS_SRFP
- CH4_GOS_OCFP
- CH4_GOS_SRFP
- CH4_GOS_OCPR
- CH4_GOS_SRPR
- XCO2_EMMA
- XCH4_EMMA

The description is also applicable to the following existing GHG-CCI SCIAMACHY data products:

- CO2_SCI_BESD
- CO2_SCI_WFMD
- CH4_SCI_WFMD
- CH4_SCI_IMAP

2.1.1 Common parameters

In this section the common parameters of the XCO_2 and XCH_4 Level data products are described.

In order to use these products as easily as possible it has been aimed at harmonizing these various products. The goal was to make sure that users can easily switch from one product to another. This has been achieved for all products and parameters with the **exception** of the averaging kernels and related parameters. These parameters are closely related to retrieval algorithm specific characteristics and require special consideration by the users of these products as is explained in detail in Sect. 2.1.2.

Dimensions in Table 5 and Table 6 are defined as follows:

- ***n*****:** number of satellite observations (ground pixels) (per file, i.e., for the given day of observations)
- For Averaging Kernel (AK) and related parameters:
  - As explained in Sect. 2.1.2, the AK and related parameters are provided for “layer-based AKs” and “level-based AKs”
    - For layer-based AK ***m*** is the number of layers which are defined by ***k = m+1*** pressure levels.
    - For level-based AK only levels are used. Here all parameters have the same number of elements, namely ***m*** levels. Here the number of pressure levels is also ***m*** (i.e., ***k = m***).

Table 7 and Table 8 present an overview about all common parameters including a short description of each parameter. A detailed description is given afterwards.

Table 7: Description of Common Parameters of the XCO_2 and XCH_4 Level 2 data products.

Name	Type	Dimensions	Units	Short Description
Common parameters for XCO_2 products:				
xco2	Float	n	micromol per mol, abbreviated ppm, i.e., 10^{-6}	Retrieved column-averaged dry-air mole fraction of atmospheric carbon dioxide (XCO_2) in ppm.
xco2_uncertainty	Float	n	micromol per mol, abbreviated ppm, i.e., 10^{-6}	Statistical uncertainty of XCO_2 in ppm (1-sigma).
xco2_averaging_kernel	Float	n x m	[-]	XCO_2 averaging kernel (a profile = vector for each single observation). Quantifies the altitude sensitivity of the XCO_2 retrieval.
co2_profile_apriori	Float	n x m	micromol per mol, abbreviated ppm, i.e., 10^{-6}	A priori mole fraction profile of atmospheric CO_2 in ppm.
xco2_quality_flag	Byte	n	[-]	Quality flag for XCO_2 retrieval. 0=good.
Common parameters for XCH_4 products:				
xch4	Float	n	nanomol per mol, abbreviated ppb, i.e., 10^{-9}	Retrieved column-averaged dry-air mole fraction of atmospheric methane (XCH_4) in ppb.
xch4_uncertainty	Float	n	nanomol per mol, abbreviated ppb, i.e., 10^{-9}	Statistical uncertainty of XCH_4 in ppb (1-sigma)
xch4_averaging_kernel	Float	n x m	[-]	XCH_4 averaging kernel (a profile = vector for each single observation). Quantifies the altitude sensitivity of the XCH_4 retrieval.
ch4_profile_apriori	Float	n x m	nanomol per mol, abbreviated ppb, i.e., 10^{-9}	A priori mole fraction profile of atmospheric CH_4 in ppb.
xch4_quality_flag	Byte	n	[-]	Quality flag for XCH_4 retrieval, 0 = good.
Continued in Table 8				

Table 8: Continuation of Table 7.

Name	Type	Dimensions	Units	Short Description
Common parameters for XCO_2 and XCH_4 products:				
solar_zenith_angle	Float	n	Degrees	Solar zenith angle
sensor_zenith_angle	Float	n	Degrees	Sensor zenith angle
time	Double	n	Seconds	Measurement time
longitude	Float	n	Degrees	Center longitude of the measurement
latitude	Float	n	Degrees	Center latitude of the measurement
pressure_levels	Float	n x k (note: k = m or k = m+1)	hPa	Vertical altitude coordinate in pressure units as used for averaging kernels
pressure_weight	Float	n x m	[-]	Pressure weights as used for averaging kernels

Description of each parameter:

xco2

Main XCO_2 parameter. Retrieved column-average dry-air mole fraction of atmospheric carbon dioxide (XCO_2) in ppm.

xco2_uncertainty

Statistical uncertainty of main XCO_2 parameter: 1-sigma uncertainty of the retrieved XCO_2 in ppm.

xco2_averaging_kernel

XCO_2 averaging kernel (for each observation: vertical profile = vector of dimension *m*).

Represents the sensitivity of the retrieved XCO_2 to atmospheric carbon dioxide mole fraction perturbations depending on pressure (height).

For details see Sect. 2.1.2.

co2_profile_apriori

A priori mole fraction profile of atmospheric carbon dioxide in ppm needed to apply the XCO_2 averaging kernels.

For details see Sect. 2.1.2.

xco2_quality_flag

Quality flag for XCO_2 retrieval. 0 = good. 1 = bad.

xch4

Main XCH_4 parameter. Retrieved column-average dry-air mole fraction of atmospheric methane (XCH_4) in ppb

xch4_uncertainty

Statistical uncertainty of main XCH_4 parameter: 1-sigma uncertainty of the retrieved XCH_4 in ppb.

xch4_averaging_kernel

XCH_4 averaging kernel (for each observation: vertical profile = vector of dimension *m*).

Represents the sensitivity of the retrieved XCH_4 to atmospheric methane mole fraction perturbations depending on pressure (height).

For details see Sect. 2.1.2.

ch4_profile_apriori

A priori mole fraction profile of atmospheric methane in ppb needed to apply the XCH_4 averaging kernels.

For details see Sect. 2.1.2.

xch4_quality_flag

Quality flag for XCH_4 retrieval. 0 = good. 1 = bad.

solar_zenith_angle

Solar zenith angle (SZA). Angle between the line of sight to the sun and the local vertical. SZA is a positive number (i.e., larger or equal to 0 deg).

sensor_zenith_angle

Sensor zenith angle is the angle between the line of sight from the observed ground pixel to the sensor and the local vertical. The sensor zenith angle is a positive number (i.e., larger or equal to 0 deg; 0 deg for exact nadir (downlooking) observation).

time

Measurement time in seconds since 01.01.1970 00:00:00.

longitude

Center longitude of the measurement. A number in the range -180 deg to +180 deg.
0 deg passes through Greenwich.

latitude

Center latitude of the measurement. A number in the range -90 deg (south pole) to +90 deg (north pole). 0 deg = equator.

pressure_levels

Pressure levels as used for the averaging kernels. Ordered from the bottom of the atmosphere to the top of the atmosphere (i.e., by decreasing pressure).

For details see Sect. 2.1.2.

pressure_weight

Layer / level dependent weights needed to apply the averaging kernels.

For details see Sect. 2.1.2.

2.1.2 How to use the averaging kernels (AK) ?

2.1.2.1 Introduction

In order to compare the satellite-retrieved XCO_2 and XCH_4 data products with model simulations and for inverse modelling of surface fluxes (see, e.g., *Bergamaschi el al., 2007*) the altitude sensitivity of the satellite retrievals has to be taken into account. Information on the altitude sensitivity is provided by the satellite XCO_2 and XCH_4 averaging kernels and corresponding CO_2 and CH_4 *a priori* vertical profiles.

Also for validation purposes the averaging kernels have to be considered, see, e.g., *Wunch et al., 2010, 2011, Dils et al., 2013*.

All common variables described in the previous section (e.g., xco2, xco2_uncertainty, time, longitude, etc.) can be used identically for all GHG-CCI ECA products with the **exception** of the averaging kernels and related parameters, as these parameters are closely related to the retrieval algorithm used.

In this section it is explained how the averaging kernels and related parameters can be used.

How these parameters have been defined depends on the retrieval algorithm used to generate a certain product and it was not possible to fully harmonize their use, i.e., their use depends on the product.

The purpose of this section is to explain how to use the averaging kernels and their related parameters and for which data product which method is recommended.

There are two different averaging kernel (AK) categories:
Depending on product, the AKs are

- "layer-based" (IUP, Univ. Bremen, and SRON products)

or

- "level-based" (Univ. Leicester products).

In the following sub-sections more information on this is given including the information for which product which category is valid.

Note that user can also determine "automatically" or via inspection of the product files which category a given product belongs to:

- For "layer-based" products the vertical dimension of parameter **pressure_levels** is *m+1*, i.e., there is one entry more than for parameter **pressure_weight** (or any of the other parameters with a vertical dimension), which has *m* vertical entries, i.e., one entry less than parameter **pressure_levels**.
- For "level-based" products all parameters have *m* entries.

In the following sub-sections the relevant parameters are listed and shortly explained followed by detailed explanations of how these parameters can be used for the layer-based AK products and for the level-based AK products.

Important note:
The AK related parameters and how they can be used as described in this document is most interesting for users who want to use different products and prefer to easily switch from one product to another. The main purpose of the common parameters and methods described in this document is to provide the users with the parameters and formulas to do this. However, all products also contain additional parameters, not described in this document, but in the PUGS of the individual products (please see also the Algorithm Theoretical Basis Documents (ATBDs) of the individual algorithms used to generate the individual products). Using these additional parameters (and corresponding formulas) users may be able to obtain somewhat more accurate results (although the differences are expected to be very small).

2.1.2.2 Averaging kernel related parameters

For each single observation (ground pixel) several averaging kernel related parameters are contained in the satellite product files. These parameters are listed in **Table 9**.

For additional information and how to use these parameters please see the following two sub-sections.

Table 9: Overview of averaging kernel (AK) and related parameters. (*) The ground pixel dimension (*n*, see previous sections) is not listed below. Here each array is 1-dimensional (a vector of dimension *k* or *m*). Each element corresponds to one atmospheric level or layer as explained in the following sections.

Parameter Name	Mathematical symbol	Dimension (*)	Unit	Explanation
pressure_levels	*p*	*k*	[hPa]	Pressure levels; note: *k = m +1* (for layer-based approach) or *k = m* (for level-based approach)
pressure_weight	*pw*	*m*	[-]	Pressure weights for all layers / levels
xco2_averaging_kernel	*AK*	*m*	[-]	XCO_2 averaging kernel
co2_profile_apriori	*VMR*	*m*	µmol/mol, abbreviated ppm (10^{-6})	CO_2 *a priori* profile
xch4_averaging_kernel	*AK*	*m*	[-]	XCH_4 averaging kernel
ch4_profile_apriori	*VMR*	*m*	nanomol/mol, abbreviated ppb (10^{-9})	CH_4 *a priori* profile

2.1.2.3 How to use layer-based AKs?

In this section it is described how the common parameters related to averaging kernels (AKs) can be used to apply the satellite's AKs to model profiles in order to take the altitude sensitivity of the satellite's XCO_2 and XCH_4 retrievals into account.

As explained, each product may (or may not) contain additional parameters and corresponding formulas, not described in this document (but in the corresponding PUG), which can be used to obtain somewhat more accurate results for a specific product (although the differences compared to the method described in this section are expected to be small).

For the layer-based approach the AKs and corresponding *a priori* CO_2 and CH_4 profiles are defined for layers and they correspond to layer averages. There are ***m*** layers, which are defined by ***k = m+1*** pressure levels.

The "AK layer-based approach", which is explained in this sub-section, needs to be applied for the following products (all IUP, Univ. Bremen, and SRON products):

- CO2_SCI_BESD
- CO2_GOS_SRFP
- XCO2_EMMA
- CH4_SCI_WFMD
- CH4_SCI_IMAP
- CH4_GOS_SRFP
- CH4_GOS_SRPR
- XCH4_EMMA

As already described above:
Note that user can also determine "automatically" or via inspection of the product files which category a given product belongs to:

- For "layer-based" products the vertical dimension of parameter **pressure_levels** is *m+1*, i.e., there is one entry more than for parameter **pressure_weight** (or any of the other parameters with a vertical dimension), which has *m* vertical entries, i.e., one entry less than parameter **pressure_levels**.
- For "level-based" products all parameters have *m* entries.

The layer-based approach is also described and used in *Bergamaschi et al., 2007*. Here a slightly modified version of their Eq. 2 is shown (here GHG = CO_2 or CH_4):

$$XGHG^{mod} = \sum_{i=1}^{m} \left[VMR_i^{apri} + AK_i (VMR_i^{mod} - VMR_i^{apri}) \right] pw_i \qquad \textbf{Eq. (1)}$$

- Here $XGHG^{mod}$ is the desired modelled XCO_2 or XCH_4 value, which corresponds to the satellite XCO_2 or XCH_4 retrievals.
- The sum is over the *m* atmospheric layers (located between pressure levels p_i and p_{i+1} with $i = 1...m$). Here pressure is the “normal” or “total” or “wet” pressure (not the “dry pressure”, see below). Here $i = 1$ corresponds to the bottom of the atmosphere and $i = k = m+1$ corresponds to the top of the atmosphere.
- pw_i is a layer-dependent weight (depending on algorithm/product this corresponds to $\Delta p_i/p_{surf}$ of *Bergamaschi et al., 2007,* times a conversion factor for the conversion of wet to dry pressure).
- VMR_i^{apri} is the satellite *a priori* layer-averaged CO_2 or CH_4 volume mixing ratio (VMR) or, more precisely, Dry Mole Fraction (DMF), between pressure levels $p_i$and p_{i+1}(note: $p_i > p_{i+1}$).
- VMR_i^{mod} is the corresponding value of the model (CO_2 of CH_4) VMR (DMF) between pressure levels p_i and p_{i+1}.
- AK_i is the satellite XCO_2 or XCH_4 averaging kernel for layer *i*.

Note that in this equation all parameters are coming from the satellite product with the exception of VMR_i^{mod}.

Note that the described approach permits to use all satellite data as they are without the need to manipulate them, e.g., by interpolation. Only the model quantity VMR_i^{mod} needs to be computed.

For illustration and a short overview please see Figure 27.

For a modeler the receipt to compute $XGHG^{mod}$ is the following:

- For each satellite observation:
  - Interpolate the model profiles to the location and time of the satellite observation.
  - Compute for each satellite layer *i*, as defined by pressure levels p_i and p_{i+1}:
    - The layer-averaged model (CO_2 or CH_4) VMR (DMF), i.e., VMR_i^{mod}
  - Apply the formula given above to compute the desired quantity $XGHG^{mod}$ (see also Figure 27 and Figure 28).

Figure 27 and Figure 28 explain how the parameters as provided via the satellite product files (Table 7) have to be used in order to apply Eq. (1).

Figure 27 - Overview how to compute XCO_2 or XCH_4 (= XGHG) using the „layer-based“ AK method. Additional explanations are given in Figure 28.

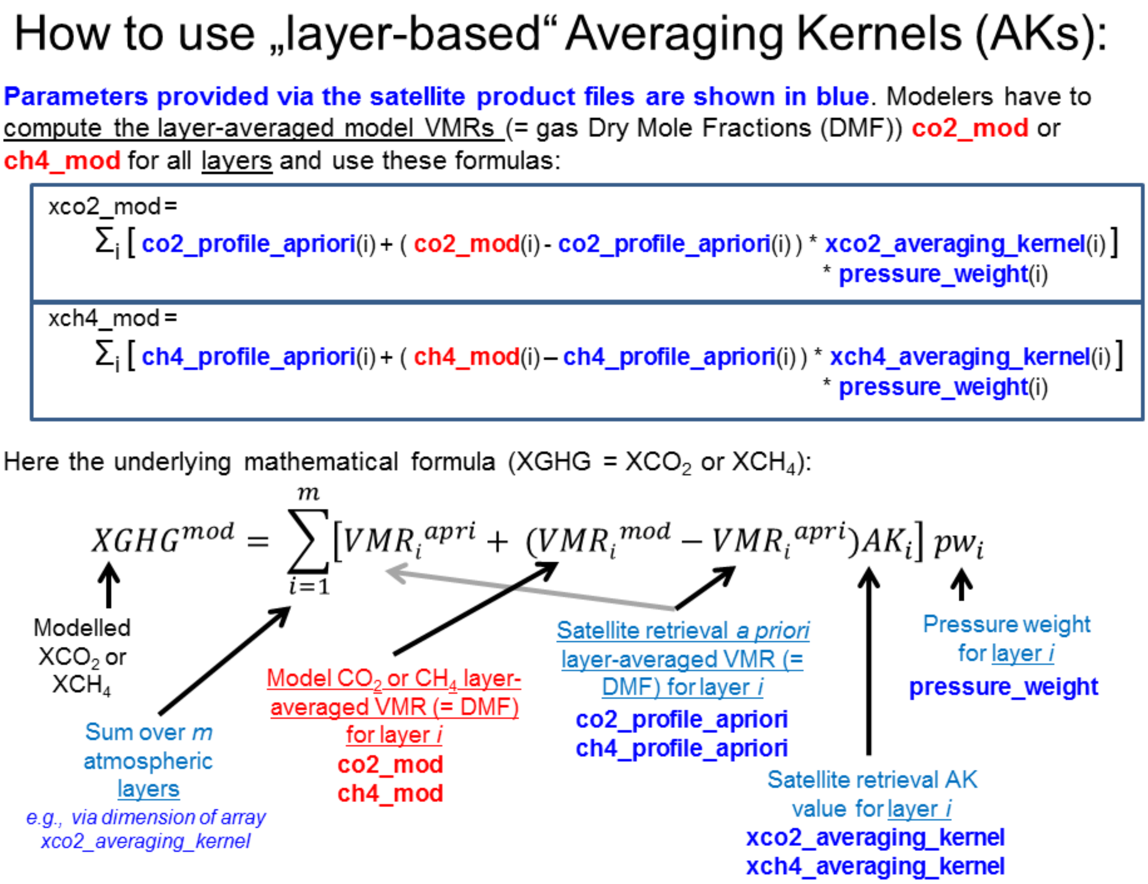

Figure 28 - Additional explanations related to the parameters needed to use the "layer-based AK approach".

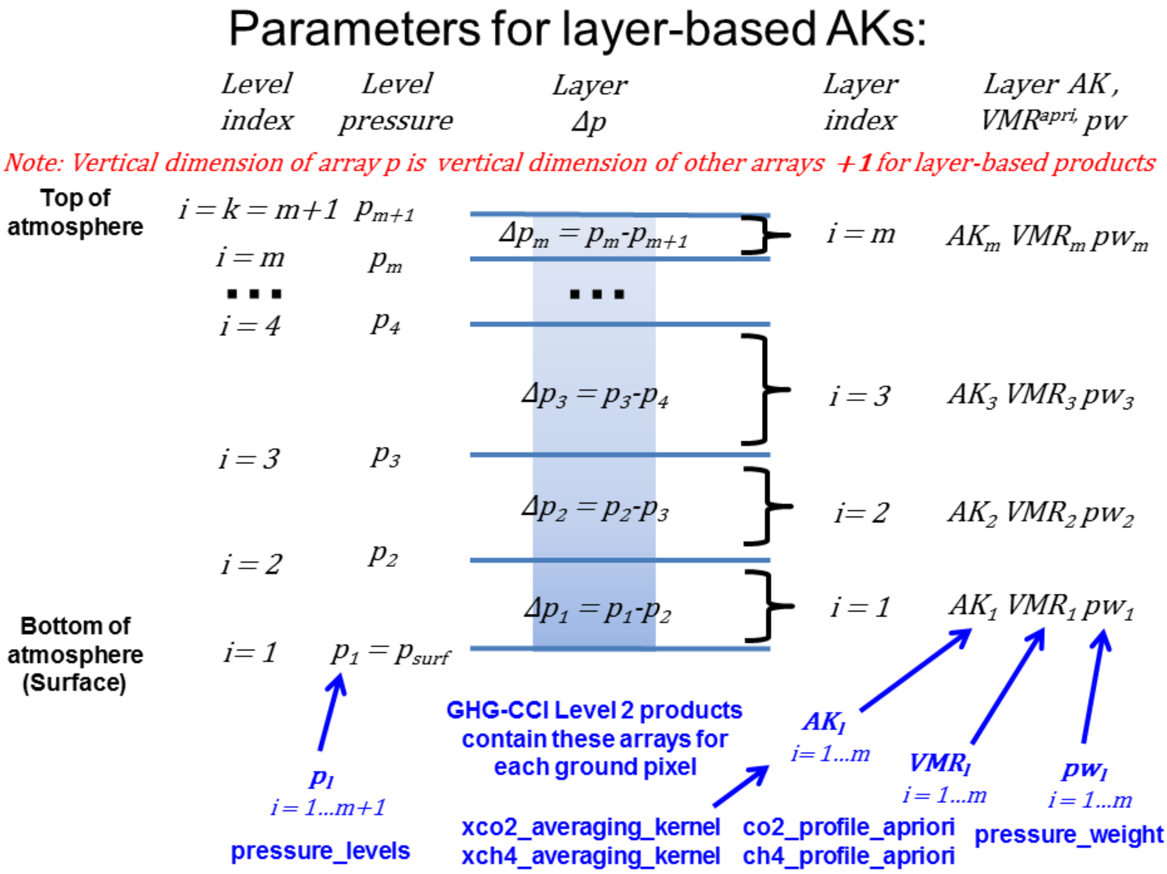

2.1.2.4 How to use level-based AKs ?

For the level-based approach the AKs and corresponding a priori VMR (= DMF) profiles are defined on levels (not on layers).

The same parameters (variable names etc.) as provided via the satellite products files are used as for the layer-based approach described in the previous section but with a slightly different implementation to apply these parameters to compute the modelled XCO_2 or XCH_4.

For the level-based approach all AK related arrays are given for *m* levels.

The "AK level-based approach", which is explained in this sub-section, needs to be applied for the following GHG-CCI ECA products (all UoL products, i.e., all "OC" products):

- CO2_GOS_OCFP
- CH4_GOS_OCPR
- CH4_GOS_OCFP

As already described above:
Note that user can also determine "automatically" or via inspection of the product files which category a given product belongs to:

- For "layer-based" products the vertical dimension of parameter **pressure_levels** is *m+1*, i.e., there is one entry more than for parameter **pressure_weight** (or any of the other parameters with a vertical dimension), which has *m* vertical entries, i.e., one entry less than parameter **pressure_levels**.
- For "level-based" products all parameters have *m* entries.

For model comparisons and inverse modelling the following method is recommended in order to compute the modelled XCO_2 or XCH_4.

The equation to apply the level-based averaging kernels to the model data is the same as for the layer-based approach (**Eq. 1**) but with the variables now all on levels, rather than layers. The key point is that the model data (co2_mod or ch4_mod in Figure 29) must be interpolated onto the retrieval pressure levels (p_i). This interpolation should be done with care so as to conserve the total column amounts of *XGHG*.

For illustration and a short overview please see Figure 29.

For a modeller, the recipe to compute $XGHG^{mod}$ is the following:

- For each satellite observation:
  - Interpolate the model profiles to the location and time of the satellite observation.
  - Compute for model data at each satellite retrieval pressure level *i* the model VMR, i.e., VMR_i^{mod}
  - Apply the formula given above (**Eq. (1)**) to compute the desired quantity $XGHG^{mod}$ (see also Figure 29and Figure 30).

Figure 29 and Figure 30 explain how the parameters as provided via the satellite product files (Table 7) have to be used in order to apply **Eq. (1)**.

Figure 29 - Overview how to compute XCO_2 or XCH_4 (= XGHG) using the „level-based" AK method. Additional explanations are given in Figure 30.

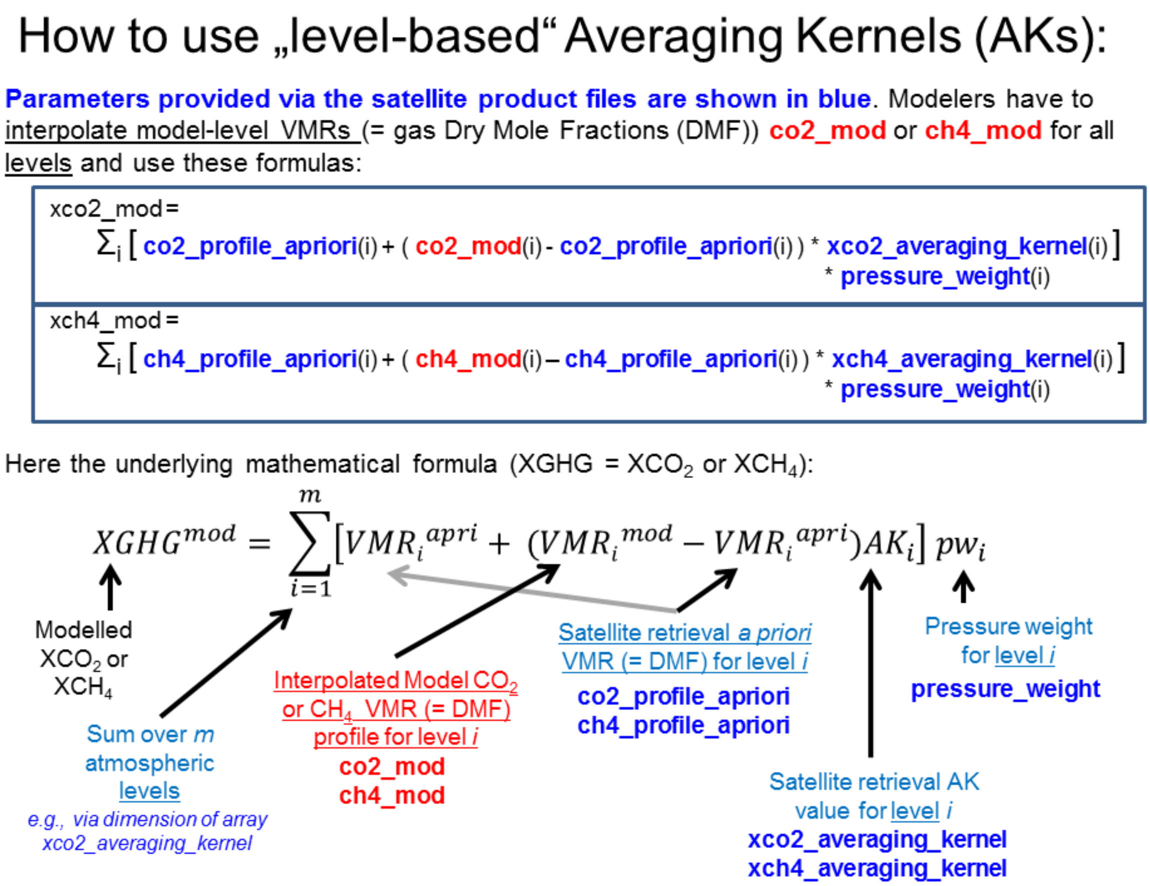

Figure 30 - Additional explanations related to the parameters needed to use the "level-based AK approach".

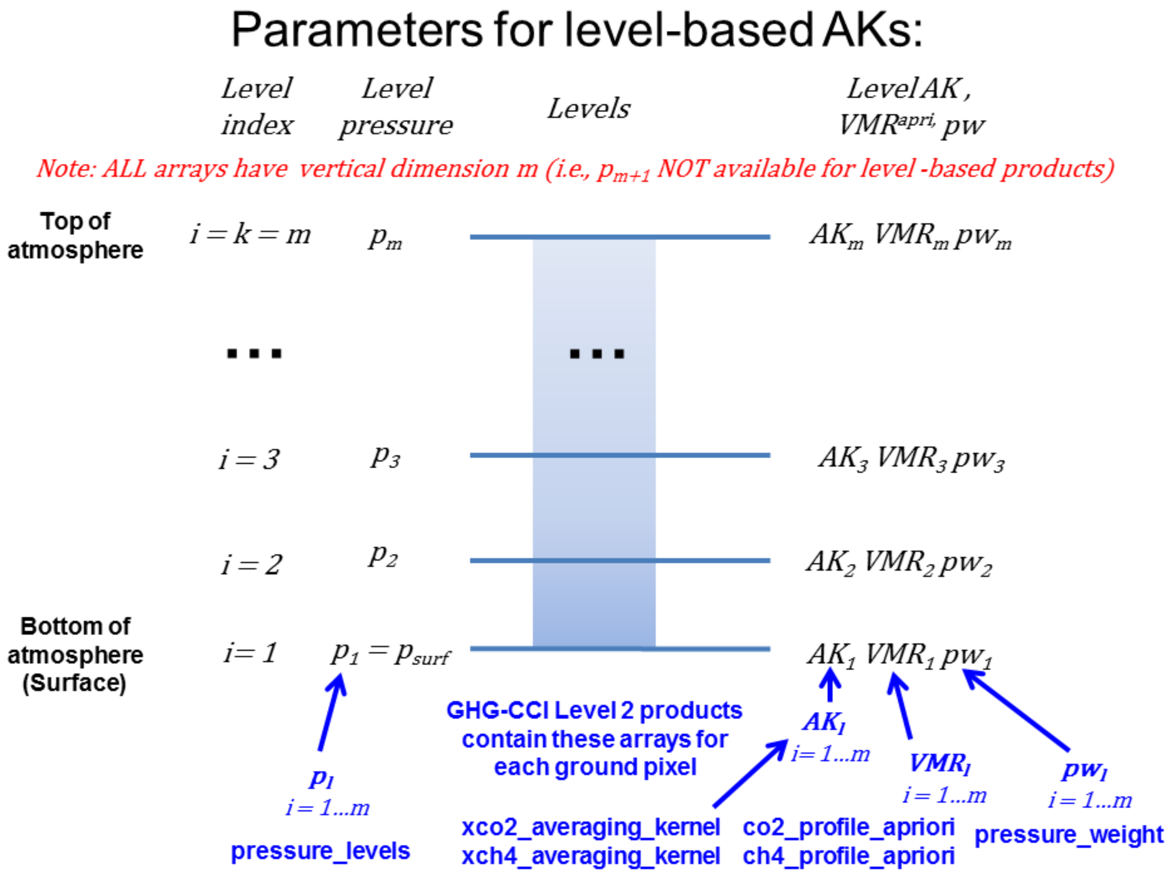

2.1.3 Algorithm specific parameters

Each product may contain additional parameters, see the product specific ANNEXes listed in Sect. 9.

2.2 Target requirements

The target requirements for these products are described in the Target Requirement Document (TRD) (*D4*).

2.3 Data usage information

The use of the data products is not trivial and typically the interpretation of these products requires appropriate modelling. The main reason for this is the long lifetime of CO_2 and CH_4 in the atmosphere combined with atmospheric transport (and for CH_4 also atmospheric chemistry needs to be considered). As a consequence of this atmospheric concentrations may be locally or regionally higher (or lower) compared to background concentration far away from the source (or sink) region. A further complication arises due to the sparseness of the data due to the spatial coverage of the satellite data, because measurements can only be made on parts of the dayside (the solar zenith angle must be smaller than about 75^o) but also because of cloud contamination and other reasons.

The described data products can be used in combination with appropriate modelling to obtain information on the various natural and anthropogenic surface and sinks of CO_2 and CH_4 as shown in a number of scientific publications such as *Alexe et al., 2015; Bergamaschi et al., 2009, 2013; Detmers et al., 2015; Guerlet et al., 2013; Houweling et al., 2004, 2015; Pandey et al., 2016; Reuter et al., 2014a, 2014b, 2017; Ross et al., 2013; Schneising et al., 2014a, 2014b; Turner et al., 2015, 2016*.

They can also be used for comparisons with models (e.g., carbon models or global chemistry-climate models) as also shown in a number of publications such as *Buchwitz et al., 2005, 2013; Cogan et al., 2011; Hayman et al., 2014; Parker et al., 2011; Shindell et al., 2013*.

They can also be used to study atmospheric trends and variability as shown in *Buchwitz et al., 2007; Frankenberg et al., 2011; Schneising et al., 2011*.

3. Level 3 XCO_2 and XCH_4 data products

3.1 Product description

These data products are in Obs3MIPs format, which is described on the Obs4MIPs website: https://www.earthsystemcog.org/projects/obs4mips/.

Obs4MIPs (Observations for Model Intercomparisons Project) is an activity to make observational products more accessible especially for climate model intercomparisons.

The XCO_2 and XCH_4 data products in Obs4MIPs format are gridded data products with a spatial resolution of 5^ox5^o and monthly time resolution.

These products have been generated using as input the Level 2 EMMA products described in Sect. 2.

Figure 31 to Figure 34 show how these products “looks like”.

In the following sub-sections the Obs4MIPs product format is described.

Figure 31 –OBS4MIPS XCO_2 (left) and corresponding uncertainty (right) for August 2003.

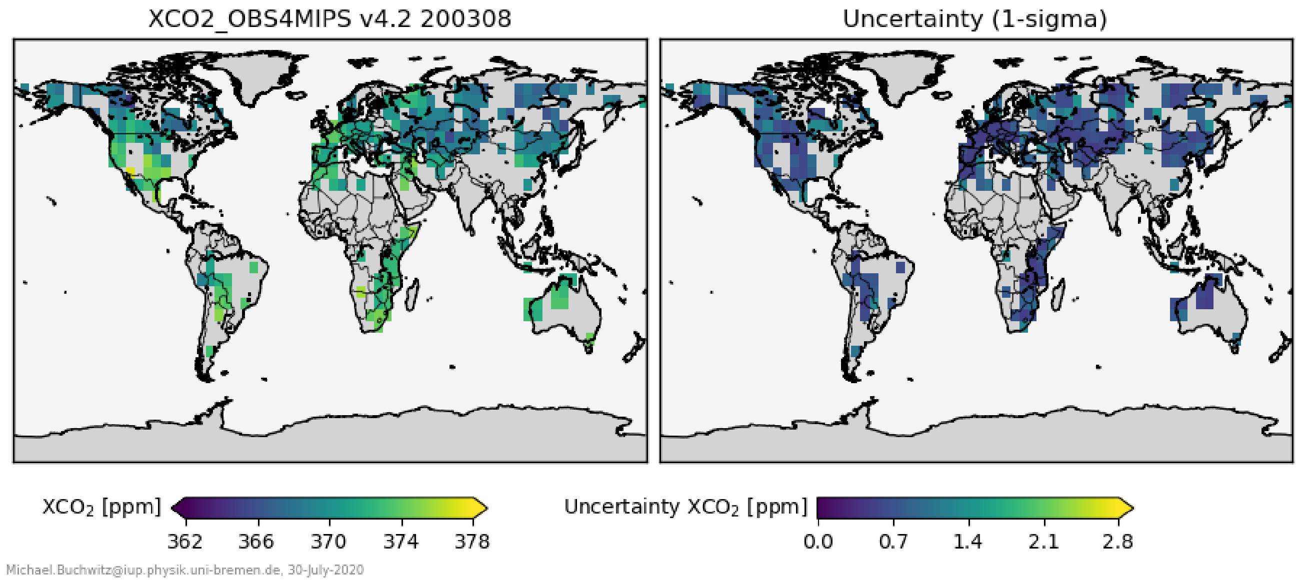

Figure 32 – OBS4MIPS XCO_2 (left) and corresponding uncertainty (right) for August 2019.

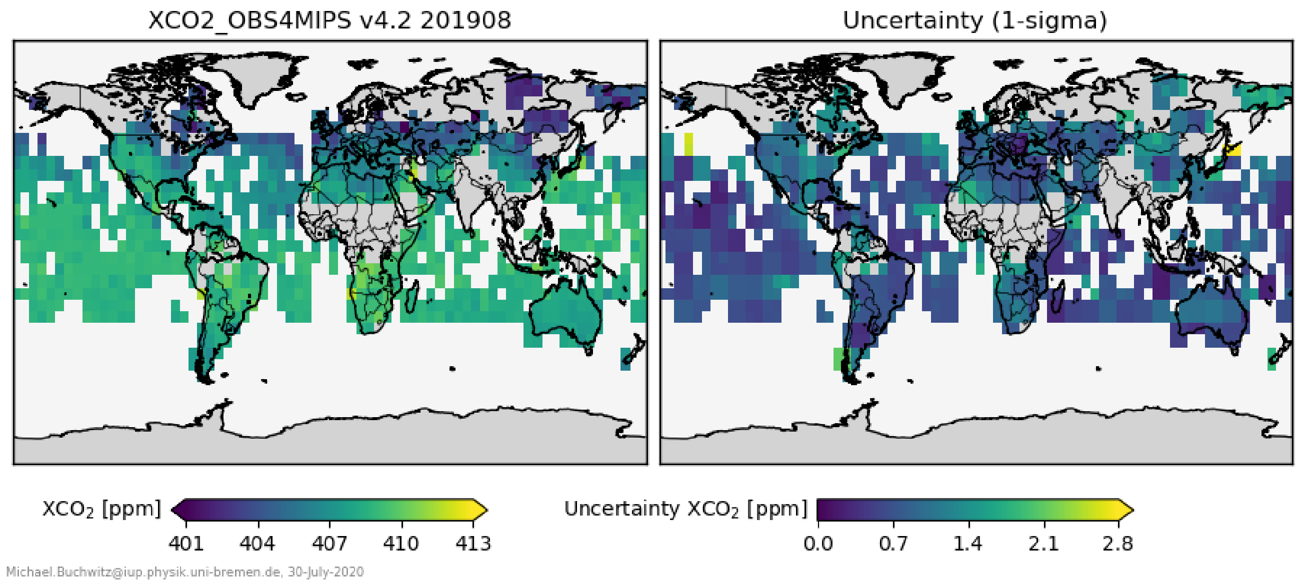

Figure 33 –OBS4MIPS XCH_4 (left) and corresponding uncertainty (right) for August 2003.

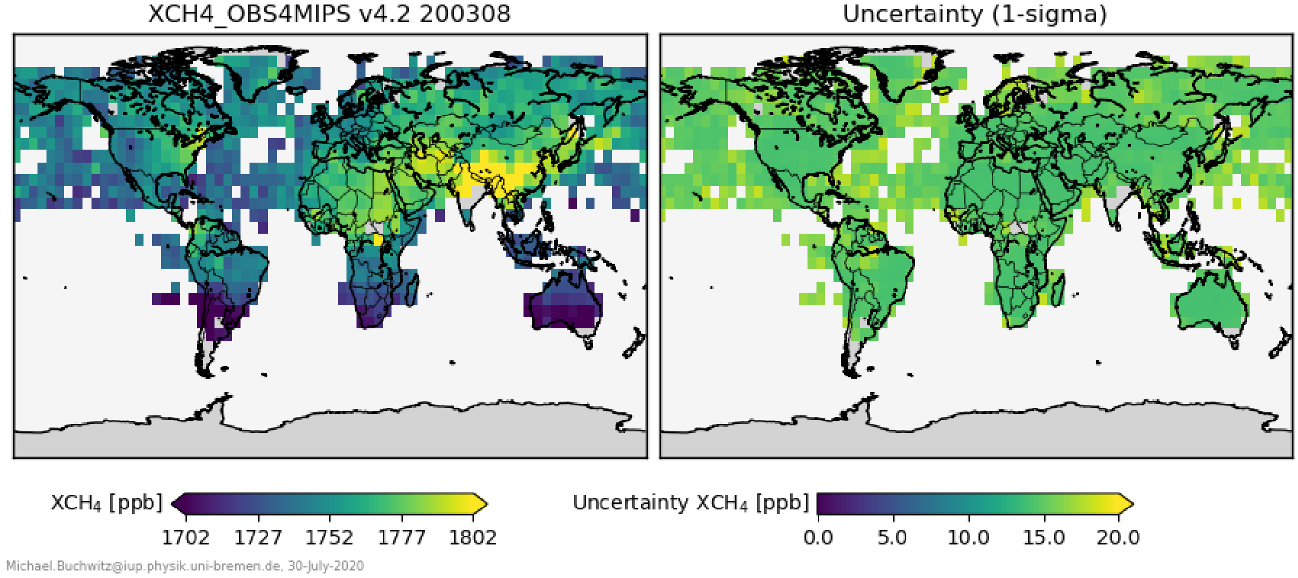

Figure 34 – OBS4MIPS XCH_4 (left) and corresponding uncertainty (right) for August 2019.

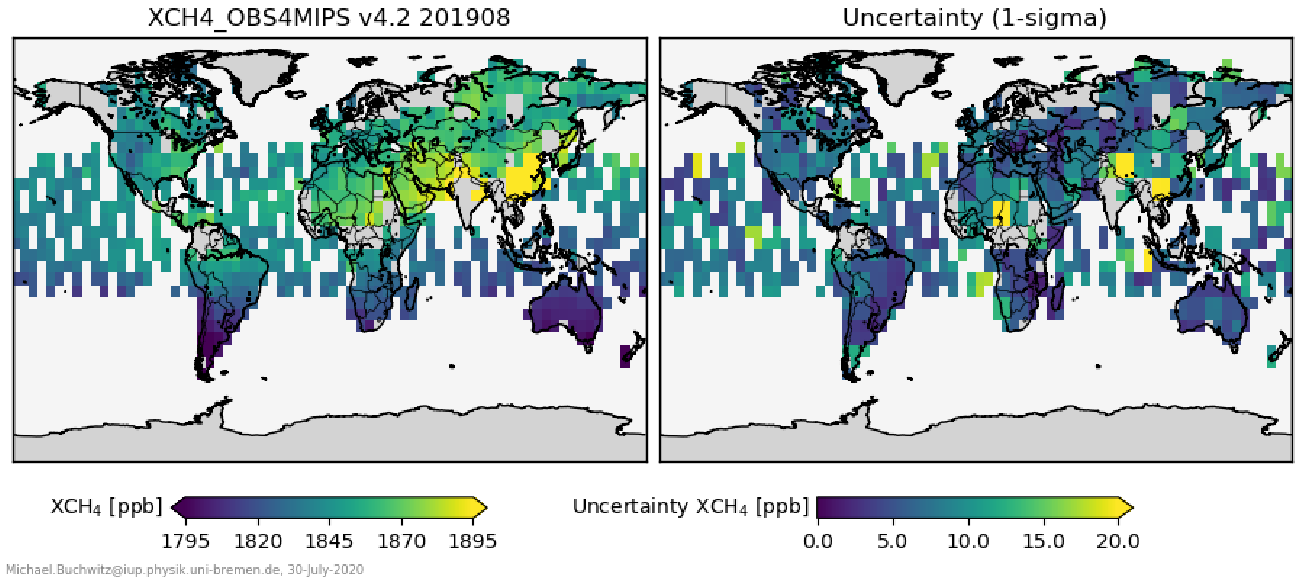

3.1.1 Obs4MIPS XCO_2 product format

The initial version of this product has been generated based on the GHG-CCI CRDP3 data set.

The product described in this document has the same format but is updated in terms of input Level 2 products and extension in time, i.e., it covers a longer time period.

The entire product is contained in a single file using this file name convention:

xco2_c3s_l3_v42_200301_201912.nc

The main quantity / data field is the column-average dry-air mole fraction of atmospheric carbon dioxide (CO_2), denoted XCO_2, as retrieved from the two satellite instruments SCIAMACHY/ENVISAT (*Burrows et al., 1995; Bovensmann et al., 1999*), TANSO-FTS/GOSAT (*Kuze et al., 2009*) and OCO-2 (*Crisp et al., 2004; Boesch et al., 2011*). XCO_2 is a dimensionless quantity (unit: mol/mol) defined as the vertical column of CO_2 divided by the vertical column of dry air (= all air molecules except water vapor) (see, e.g., *Buchwitz et al., 2005*, for details). For example, if XCO_2 is 0.0004 (i.e., 400 ppm, parts per million) at a given location this means that there are 400 CO_2 molecules above that location per 1 million air molecules (excluding water vapour molecules). Table 10 lists the main characteristics of this data product. See also *Reuter et al., 2020*, for an overview and additional details.

Table 10: Main characteristics of the XCO_2 Obs4MIPs v4.2 product.

CF variable name, units	Long name: column-average dry-air mole fraction of atmospheric carbon dioxide Standard name: dry_atmosphere_mole_fraction_of_carbon_dioxide Units: dimensionless (mol/mol) See also: CF Standard Name Table, Version 31, 08 March 2016 (http://cfconventions.org/Data/cf-standard-names/31/build/cf-standard-name-table.html)
Spatial resolution	5° equal angle
Temporal resolution	Monthly average, from January 2003–December 2019
Coverage	Global (2003 – mid 2009: land only)

Note that a resolution of 5°x5° has been selected (instead of, e.g., 1°x1°) to ensure better noise suppression (note that the underlying individual satellite retrievals are noisy and sparse due to very strict quality filtering).

The main variables as contained in the XCO_2 Obs4MIPs product file are:

xco2:
Satellite retrieved column-average dry-air mole fraction of atmospheric carbon dioxide
(Note: typical values are << 1.0 (typically close to 0.0004) and 1.0E20 = no data)

xco2_nobs:
Number of individual XCO_2 Level 2 observation (per 5^ox5^o grid cell) used to compute the reported Level 3 XCO_2 monthly average value (0 = no data)

xco2_stderr:
Reported uncertainty defined as standard error of the average including single sounding noise and potential seasonal and regional biases

xco2_stddev:
Average standard deviation of the underlying XCO_2 Level 2 observations

time:
Time in days since 1-Jan-1990

lat:
Center latitude in degrees north (-90.0 to +90.0)

lon:
Center longitude in degrees east (-180.0 to +180.0)

3.1.2 Obs4MIPS XCH_4 product format

The initial version of this product has been generated based on the GHG-CCI CRDP3 data set.

The product described in this document has the same format but is updated in terms of input Level 2 products and extension in time, i.e., it covers a longer time period.

The entire product is contained in a single file using this file name convention:

xch4_c3s_l3_v42_200301_201912.nc

The main quantity / data field is the column-average dry-air mole fraction of atmospheric methane (CH_4), denoted XCH_4, as retrieved from the two satellite instruments SCIAMACHY/ENVISAT (*Burrows et al., 1995; Bovensmann et al., 1999*) and TANSO-FTS/GOSAT (*Kuze et al., 2009*). XCH_4 is a dimensionless quantity (unit: mol/mol) defined as the vertical column of CH_4 divided by the vertical column of dry air (= all air molecules except water vapor) (see, e.g., *Buchwitz et al., 2005*, for details). For example, if XCH_4 is 0.0000018 (i.e., 1800 ppb, parts per billion) at a given location this means that there are 1800 CH_4 molecules above that location per 1 billion air molecules (excluding water vapour molecules). Table 11 lists the main characteristics of this data product. See also *Reuter et al., 2020*, for an overview and additional details.

Table 11: Main characteristics of the XCH_4 Obs4MIPs v4.2 product.

CF variable name, units	Long name: column-average dry-air mole fraction of atmospheric methane Standard name: dry_atmosphere_mole_fraction_of_methane Units: dimensionless (mol/mol) See also: CF Standard Name Table, Version 31, 08 March 2016 (http://cfconventions.org/Data/cf-standard-names/31/build/cf-standard-name-table.html)
Spatial resolution	5° equal angle
Temporal resolution	Monthly average, from January 2003–December 2019
Coverage	Global (November 2005 – March 2009: land only)

Note that a resolution of 5°x5° has been selected (instead of, e.g., 1°x1°) to ensure better noise suppression (note that the underlying individual satellite retrievals are noisy and sparse due to very strict quality filtering).

The main variables as contained in the XCH_4 Obs4MIPs product file are:

xch4:
Satellite retrieved column-average dry-air mole fraction of atmospheric methane
(Note: typical values are << 1.0 (typically close to 0.0000018) and 1.0E20 = no data)

xch4_nobs:
Number of individual XCH_4 Level 2 observation (per 5^ox5^o grid cell) used to compute the reported Level 3 XCH_4 monthly average value (0 = no data)

xch4_stderr:
Reported uncertainty defined as standard error of the average including single sounding noise and potential seasonal and regional biases

xch4_stddev:
Average standard deviation of the underlying XCH_4 Level 2 observations

time:
Time in days since 1-Jan-1990

lat:
Center latitude in degrees north (-90.0 to +90.0)

lon:
Center longitude in degrees east (-180.0 to +180.0)

3.2 Target requirements

Target requirements for satellite-derived XCO_2 and XCH_4 products are described in the Target Requirement Document (TRD) (*D4*). Although these requirements have been formulated for Level 2 products most of them are also valid for Level 3 products.

The Obs4MIPs products have been primarily generated for comparison with climate models, see, for example *Lauer et al., 2017*.

3.3 Data usage information

The Obs4MIPs products have been primarily generated for comparison with climate models, see, for example *Lauer et al., 2017*, but also for other applications (e.g., *Buchwitz et al., 2018; Reuter et al., 2020*).

4. Level 2 mid-tropospheric CO_2 and CH_4 data products

4.1 Product description

These products contain the IASI mid-tropospheric CO_2 and CH_4 mixing ratios and the AIRS mid-tropospheric CO_2 mixing ratio, i.e., the description given in this section is valid for these products:

- CO2_IASA_NLIS (product from IASI on Metop-A)
- CO2_IASB_NLIS (product from IASI on Metop-B)
- CH4_IASA_NLIS (product from IASI on Metop-A)
- CH4_IASB_NLIS (product from IASI on Metop-B)
- CO2_AIRS_NLIS (product from AIRS)

The format of these products is essentially identical as the Level 2 XCO_2 and XCH_4 data product format described in Sect. 2.

They only exceptions are:

- xco2 needs to be replaced by co2 (e.g., co2_quality_flag instead of xco2_quality_flag)
- xch4 needs to be replaced by ch4 (e.g., ch4_quality_flag instead of xch4_quality_flag)
- All other variable names are the same but note that some contain -999.0 for “no valid data” (e.g., some angles and uncertainty).

For additional details see the corresponding PUGS (see Sect. 9.5 for ANNEX E).

4.2 Target requirements

The target requirements for these products are described in the Target Requirement Document (TRD) (*D4*).

4.3 Data usage information

The data products can be used to study atmospheric trends and variability, for comparison with models and to obtain information on sources and sinks as shown in a number of publications such as *Chevallier et al., 2005, 2009a; Crevoisier et al., 2004, 2009, 2009b, 2013; Cressot et al., 2014.*

5. PUGS for existing GHG-CCI products

In this section a short overview about existing products is given. These products, which are not regenerated within C3S but made available for C3S and (for the XCO_2 and XCH_4 products) are used as input to generate the merged Level 2 EMMA and Level 3 OBS4MIPS C3S products.

5.1 CO2_SCI_BESD product

Product: XCO_2
Level: 2
Sensor: SCIAMACHY/ENVISAT

Reference:

- Reuter, M., H. Bovensmann, M. Buchwitz, J. P. Burrows, B. J. Connor, N. M. Deutscher, D. W. T. Griffith, J. Heymann, G. Keppel-Aleks, J. Messerschmidt, J. Notholt, C. Petri, J. Robinson, O. Schneising, V. Sherlock, V. Velazco, T. Warneke, P. O. Wennberg, and D. Wunch: "Retrieval of atmospheric CO_2 with enhanced accuracy and precision from SCIAMACHY: Validation with FTS measurements and comparison with model results" J. Geophys. Res., doi: 10.1029/2010JD015047, 2011.

The product is compliant with the GHG-CCI Product Specification Document for XCO_2 and XCH_4 Level 2 data products:

- Buchwitz, M., et al., ESA Climate Change Initiative (CCI) Product Specification Document (PSD) for the Essential Climate Variable (ECV) Greenhouse Gases (GHG), 6-June-2014, Version 3, 2014.

Product User Guide:

- Reuter, M., et al., ESA Climate Change Initiative (CCI) Product User Guide Version 4 (PUGv4) for the XCO_2 SCIAMACHY Data Product BESD for the Essential Climate Variable (ECV) Greenhouse Gases (GHG), 31-Aug-2016, 2016.

5.2 CO2_SCI_WFMD and CH4_SCI_WFMD products

Products: XCO_2 and XCH_4
Level: 2
Sensor: SCIAMACHY/ENVISAT

Reference:

- Schneising, O., Buchwitz, M., Reuter, M., Heymann, J., Bovensmann, H., and Burrows, J. P.: Long-term analysis of carbon dioxide and methane column-averaged mole fractions retrieved from SCIAMACHY, Atmos. Chem. Phys., 11, 2863-2880, doi:10.5194/acp-11-2863-2011, 2011.

The products are compliant with the GHG-CCI Product Specification Document for XCO_2 and XCH_4 Level 2 data products:

- Buchwitz, M., et al., ESA Climate Change Initiative (CCI) Product Specification Document (PSD) for the Essential Climate Variable (ECV) Greenhouse Gases (GHG), 6-June-2014, Version 3, 2014.

Product User Guide:

- Schneising, O., et al., ESA Climate Change Initiative (CCI) Product User Guide SCIAMACHY WFM-DOAS (WFMD) XCO_2 and XCH_4 for the Essential Climate Variable (ECV) Greenhouse Gases (GHG), 15-May-2016, version 4, 2016.

5.3 CH4_SCI_IMAP product

Product: XCH_4
Level: 2
Sensor: SCIAMACHY/ENVISAT

Reference:

- Frankenberg, C., Aben, I., Bergamaschi, P., et al., Global column-averaged methane mixing ratios from 2003 to 2009 as derived from SCIAMACHY: Trends and variability, J. Geophys. Res., doi:10.1029/2010JD014849, 2011.

The product is compliant with the GHG-CCI Product Specification Document for XCO_2 and XCH_4 Level 2 data products:

- Buchwitz, M., et al., ESA Climate Change Initiative (CCI) Product Specification Document (PSD) for the Essential Climate Variable (ECV) Greenhouse Gases (GHG), 6-June-2014, Version 3, 2014.

Product User Guide:

- Frankenberg, C., et al., ESA Climate Change Initiative (CCI) Product User Guide (PUG) for the IMAP-DOAS XCH4 SCIAMACHY Data Products (v7.2) for the Essential Climate Variable (ECV) Greenhouse Gases (GHG), 28-Aug-2016, version 4, 2016.

6. Data quality overview

In this section a short overview about the data quality is given. The summary is based on preliminary assessments.

Important: In this section only PRELIMINARY results are shown. Users of the C3S GHG satellite data set CRD4 (2003-2019) should consult the latest version of document PQAR (*D6*) for the final quality assessment results.

XCO_2 Level 2 products (see D6):

Figure 35 shows a summary of the achieved performance in terms of single measurement random error (precision), relative accuracy or systematic error in terms of spatial (lower value) and spatio-temporal (higher value) biases (i.e., neglecting a possible constant bias or global offset) and stability in terms of linear bias drift/trend as obtained from comparison with TCCON XCO_2.

XCO_2 Level 3 product (see D6):

Figure 36 shows a comparison of Level 3 product XCO2_OBS4MIPS with TCCON XCO_2. Based on these and related assessments (see *D6*) the validation of Level 3 product XCO2_OBS4MIPS can be summarized as follows: The overall monthly mean uncertainty is 1.2 ppm and the mean bias is -0.11 ppm. Relative systematic errors, i.e., spatial and temporal biases amount to 0.7±0.6 ppm. The computed linear drift of -0.07±0.20 ppm is small and not significant.

XCH_4 Level 2 products (see D6):

Figure 37 shows a summary of the achieved performance in terms of single measurement random error (precision), relative accuracy or systematic error in terms of spatial (lower value) and spatio-temporal (higher value) biases (i.e., neglecting a possible constant bias or global offset) and stability in terms of linear bias drift/trend as obtained from comparison with TCCON XCH_4.

XCH_4 Level 3 product (see D6):

Figure 38 shows a comparison of Level 3 product XCH4_OBS4MIPS with TCCON XCH_4.
Based on these and related assessments (see *D6*) the validation of Level 3 product XCH4_OBS4MIPS can be summarized as follows: The overall monthly mean uncertainty is 8.8 ppb and the mean bias is -3.3 ppb. Relative systematic errors, i.e., spatial and temporal biases amount to 5±6 ppb. The computed linear drift of 0.1±1.0 ppb is small and not significant.

Level 2 mid tropospheric products (see D6):

Summary quality IASI CO_2 products: The single measurement precision of product CO2_IASA_NLIS (from IASI on Metop-A) is 1 ppm. The mean bias (global offset) is 0.96 ppm. The estimated relative accuracy is around 1 ppm. The probability that the < 0.5 ppm user requirement is met has been estimated to 50% taking into account the uncertainty of the reference data and assessment method. The product is also very stable (0.06 +/- 0.10 ppm/year (1-sigma)) meeting the requirement for long-term drift stability. The performance of product CO2_IASB_NLIS (from IASI on Metop-B) seems to be similar.

Summary quality IASI CH_4 products: The single measurement precision of product CH4_IASA_NLIS (from IASI on Metop-A) is 12 ppb. The mean bias (global offset) is -3.4 ppb. The product appears to meet the “relative systematic error” requirement of better than 10 ppb: the estimated relative accuracy is 3.4 ppb. The product appears to be very stable but a quantitative analysis could not be carried out due to lack of reference data. The performance of product CH4_IASB_NLIS (from IASI on Metop-B) seems to be similar.

For product CO2_AIRS_NLIS (from project GHG-CCI) the estimated performance is: single measurement precision: 1.3 ppm, mean bias: -0.43 ppm.

Figure 35 - Overview data quality assessment results for Level 2 XCO_2 data products. The green bars refer to the “Quality Assessment / Quality control” (QA/QC) results as described in this document. The red bars refer to results obtained by the data providers (DPs), as described in separate Annexes (see Sect. 9). For “Accuracy” and “Stability” also the numerical values for the “Probability that TR is met” are given (computed as mean value if more than one value (bar) exists). Also listed (in grey on the right hand side) is the uncertainty of the reference data as used for the Target Requirement (TR) assessments.

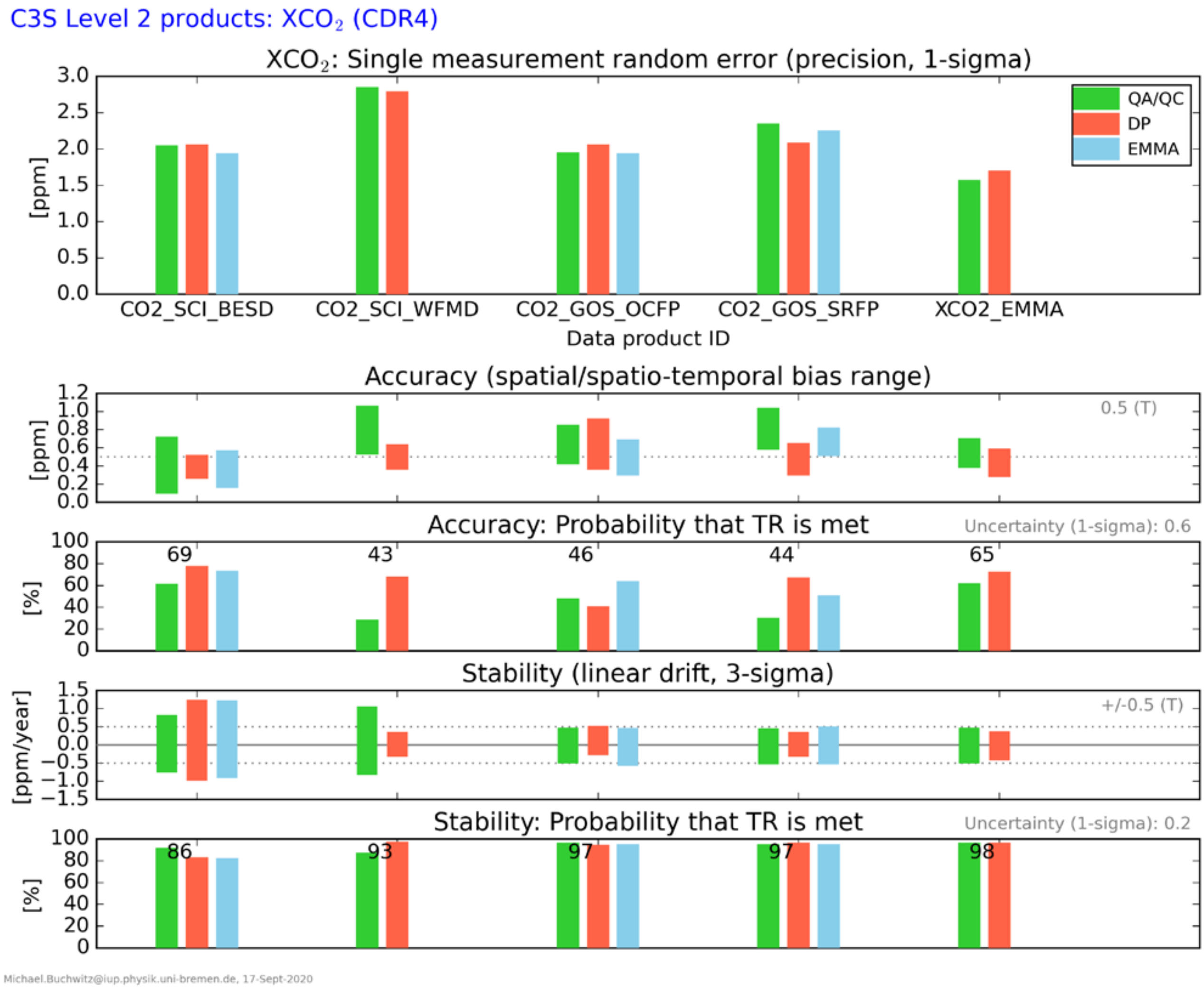

Figure 36 - Overview data quality assessment results for Level 3 XCO_2 Obs4MIPs format data product.

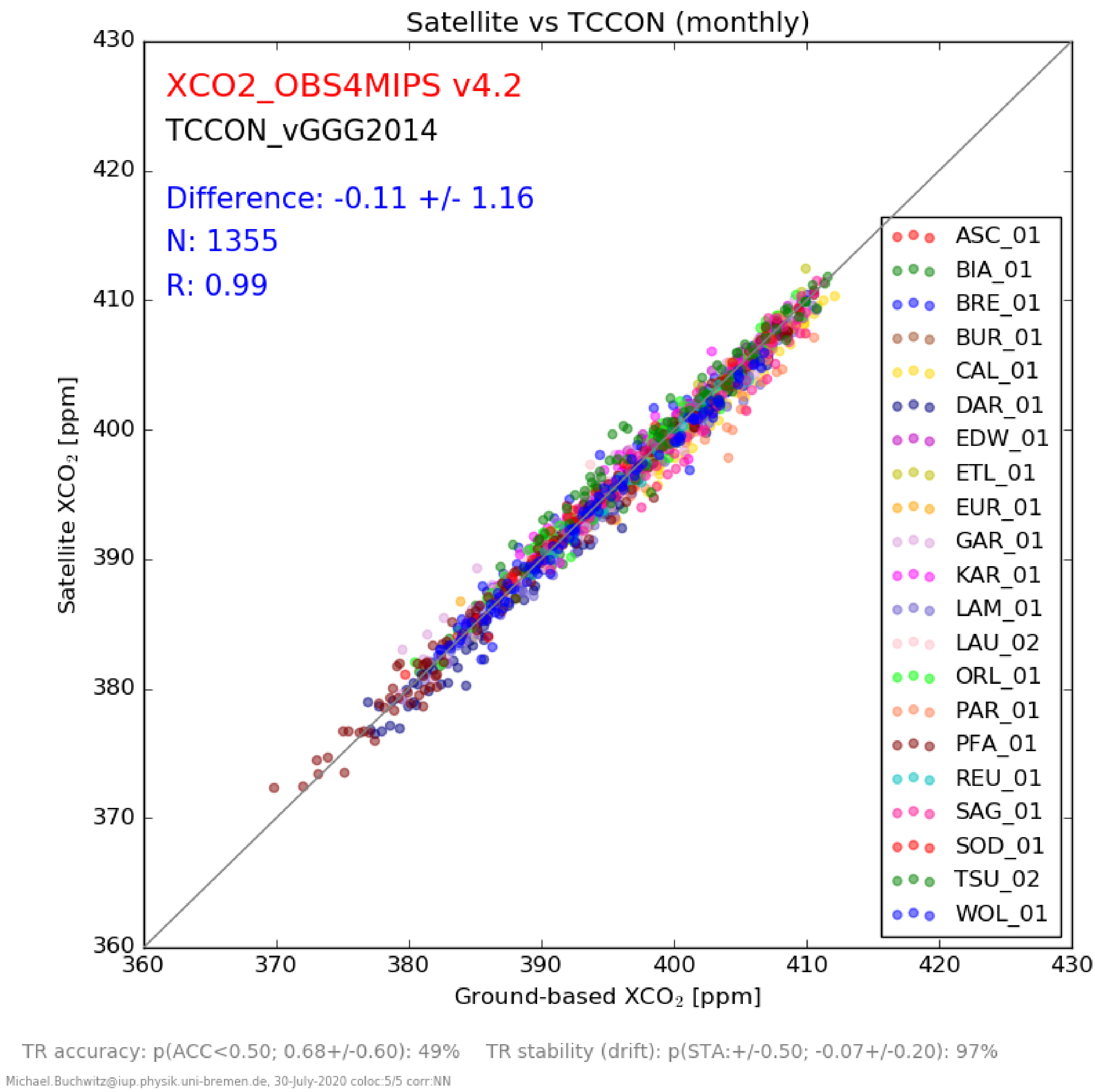

Figure 37 - Overview data quality assessment results for Level 2 XCH_4 data products. The green bars refer to the "Quality Assessment / Quality control" (QA/QC) results as described in this document. The red bars refer to results obtained by the data providers (DPs), as described in separate Annexes (see Sect. 9). For "Accuracy" and "Stability" also the numerical values for the "Probability that TR is met" are given (computed as mean value if more than one value (bar) exists). Also listed (in grey on the right hand side) is the uncertainty of the reference data as used for the Target Requirement (TR) assessments.

Figure 38 - Overview data quality assessment results for Level 3 XCH_4 Obs4MIPs format data product.

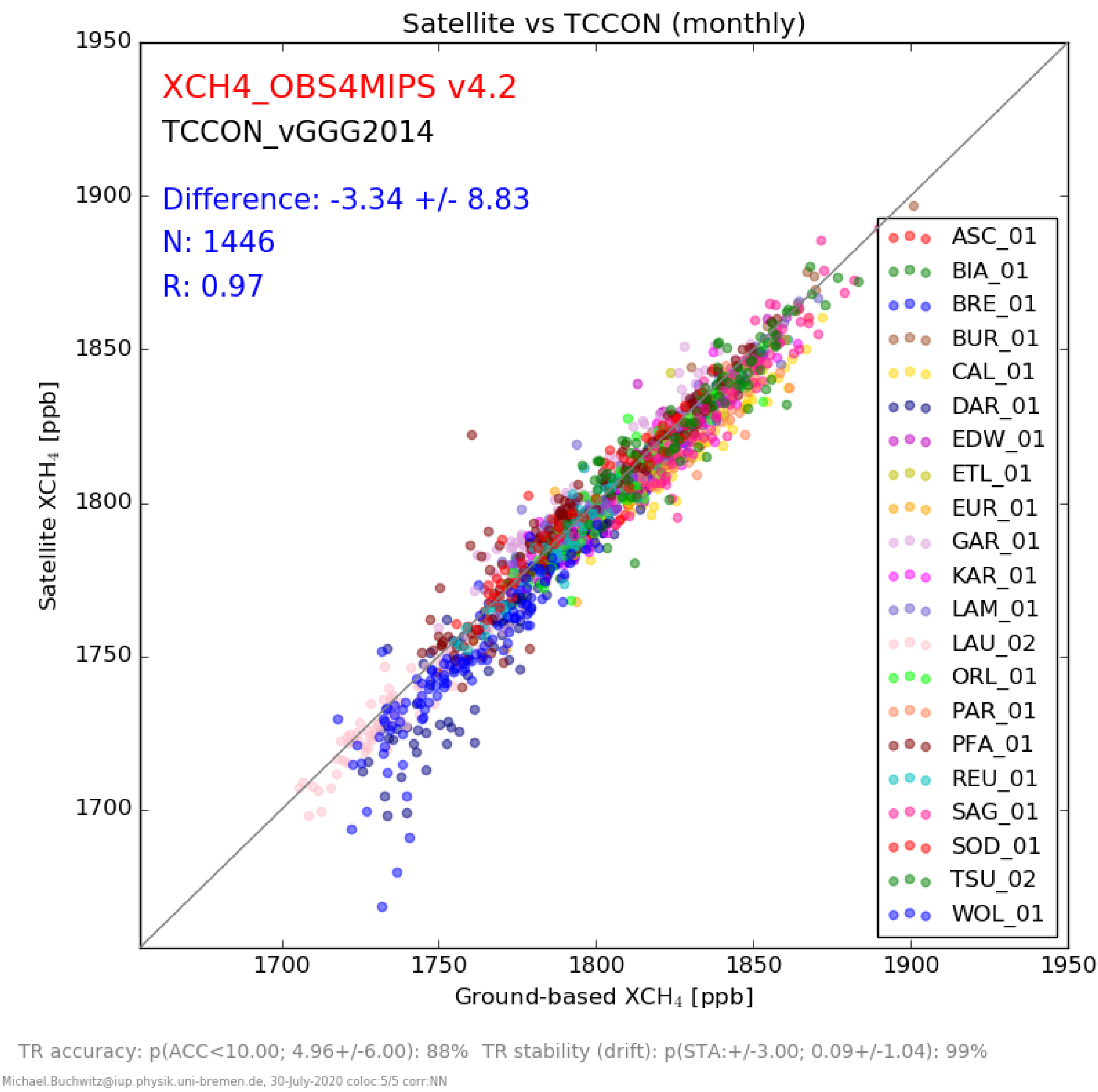

7. Data access information

The data products are / will be available via the Copernicus Climate Data Store (CDS):
[*https://cds.climate.copernicus.eu/#!/home*](https://cds.climate.copernicus.eu/#!/home)

See also Copernicus Climate Change Service (C3S):
[*https://climate.copernicus.eu/*](https://climate.copernicus.eu/)

References

Alexe et al., 2015: Alexe, M., P. Bergamaschi, A. Segers, R. Detmers, A. Butz, O. Hasekamp, S. Guerlet, R. Parker, H. Boesch, C. Frankenberg, R. A. Scheepmaker, E. Dlugokencky, C. Sweeney, S. C. Wofsy, and E. A. Kort, Inverse modeling of CH4 emissions for 2010–2011 using different satellite retrieval products from GOSAT and SCIAMACHY, Atmos. Chem. Phys., 15, 113–133, doi:10.5194/acp-15-113-2015, 2015.

ATBD GHG, 2017: Buchwitz, M., Aben, I., Anand, J., Armante, R., Boesch, H., Crevoisier, C., Detmers, R. G., Hasekamp, O. P., Reuter, M., Schneising-Weigel, O., Algorithm Theoretical Basis Document (ATBD) – Main document, C3S project C3S_312a_Lot6_IUP-UB – Greenhouse Gases, v1.1, 2017.

ATBD GHG, 2018: Buchwitz, M., Aben, I., Anand, J., Armante, R., Boesch, H., Crevoisier, C., Detmers, R. G., Hasekamp, O. P., Reuter, M., Schneising-Weigel, O., Algorithm Theoretical Basis Document (ATBD) – Main document, C3S project C3S_312a_Lot6_IUP-UB – Greenhouse Gases, v2.0, 2018.

ATBD GHG, 2019: Buchwitz, M., Aben, I., J., Armante, R., Boesch, H., Crevoisier, C., Di Noia, A., Hasekamp, O. P., Reuter, M., Schneising-Weigel, O., Wu, L.., Algorithm Theoretical Basis Document (ATBD) – Main document for Greenhouse Gas (GHG: CO_2 & CH_4) data set CDR 3 (2003-2018), C3S project C3S_312b_Lot2_DLR, v3.0, 2019.

ATBD GHG, 2020: Buchwitz, M., Aben, I., J., Armante, R., Boesch, H., Crevoisier, C., Di Noia, A., Hasekamp, O. P., Reuter, M., Schneising-Weigel, O., Wu, L.., Algorithm Theoretical Basis Document (ATBD) – Main document for Greenhouse Gas (GHG: CO_2 & CH_4) data set CDR 4 (2003-2019), C3S project C3S_312b_Lot2_DLR, v4.0, 2020.

Bergamaschi et al., 2009: Bergamaschi, P., Frankenberg, C., Meirink, J. F., Krol, M., Villani, M. G., Houweling, S., Dentener, F., Dlugokencky, E. J., Miller, J. B., Gatti, L. V., Engel, A., and Levin, I.: Inverse modeling of global and regional CH_4 emissions using SCIAMACHY satellite retrievals, J. Geophys. Res., 114, D22301, doi:10.1029/2009JD012287, 2009.

Bergamaschi et al., 2013: Bergamaschi, P., Houweling, H., Segers, A., et al., Atmospheric CH4 in the first decade of the 21st century: Inverse modeling analysis using SCIAMACHY satellite retrievals and NOAA surface measurements, J. Geophys. Res., 118, 7350-7369, doi:10.1002/jrgd.50480, 2013.

Boesch et al., 2011: Boesch, H., D. Baker, B. Connor, D. Crisp, and C. Miller, Global characterization of CO_2 column retrievals from shortwave-infrared satellite observations of the Orbiting Carbon Observatory-2 mission, Remote Sensing, 3 (2), 270-304, 2011.

Bovensmann et al., 1999: Bovensmann, H., Burrows, J. P., Buchwitz, M., Frerick, J., Noël, S., Rozanov, V. V., Chance, K. V., Goede, A. H. P. (1999), SCIAMACHY - Mission objectives and measurement modes, J. Atmos. Sci., 56 (2), 127-150, 1999.

Bovensmann et al., 2010: Bovensmann, H., Buchwitz, M., Burrows, J. P., Reuter, M., Krings, T., Gerilowski, K., Schneising, O., Heymann, J., Tretner, A., and Erzinger, J.: A remote sensing technique for global monitoring of power plant CO_2 emissions from space and related applications, Atmos. Meas. Tech., 3, 781-811, 2010.

Buchwitz et al., 2000: Buchwitz, M., Rozanov, V. V., and Burrows, J. P.: A near-infrared optimized DOAS method for the fast global retrieval of atmospheric CH_4, CO, CO_2, H_2O, and N_2O total column amounts from SCIAMACHY Envisat-1 nadir radiances, J. Geophys. Res. 105, 15,231-15,245, 2000.

Buchwitz et al., 2005: Buchwitz, M., R. de Beek, J. P. Burrows, H. Bovensmann, T. Warneke, J. Notholt, J. F. Meirink, A. P. H. Goede, P. Bergamaschi, S. Körner, M. Heimann, and A. Schulz, Atmospheric methane and carbon dioxide from SCIAMACHY satellite data: Initial comparison with chemistry and transport models, Atmos. Chem. Phys., 5, 941-962, 2005.

Buchwitz et al., 2007: Buchwitz, M., O. Schneising, J. P. Burrows, H. Bovensmann, M. Reuter, J. Notholt, First direct observation of the atmospheric CO_2 year-to-year increase from space, Atmos. Chem. Phys., 7, 4249-4256, 2007.

Buchwitz et al., 2013a: Buchwitz, M., M. Reuter, O. Schneising, H. Boesch, S. Guerlet, B. Dils, I. Aben, R. Armante, P. Bergamaschi, T. Blumenstock, H. Bovensmann, D. Brunner, B. Buchmann, J. P. Burrows, A. Butz, A. Chédin, F. Chevallier, C. D. Crevoisier, N. M. Deutscher, C. Frankenberg, F. Hase, O. P. Hasekamp, J. Heymann, T. Kaminski, A. Laeng, G. Lichtenberg, M. De Mazière, S. Noël, J. Notholt, J. Orphal, C. Popp, R. Parker, M. Scholze, R. Sussmann, G. P. Stiller, T. Warneke, C. Zehner, A. Bril, D. Crisp, D. W. T. Griffith, A. Kuze, C. O'Dell, S. Oshchepkov, V. Sherlock, H. Suto, P. Wennberg, D. Wunch, T. Yokota, Y. Yoshida, The Greenhouse Gas Climate Change Initiative (GHG-CCI): comparison and quality assessment of near-surface-sensitive satellite-derived CO_2 and CH_4 global data sets, *Remote Sensing of Environment*, doi:10.1016/j.rse.2013.04.024, 2013.

Buchwitz et al., 2013b: Buchwitz, M., Reuter, M., Bovensmann, H., Pillai, D., Heymann, J., Schneising, O., Rozanov, V., Krings, T., Burrows, J. P., Boesch, H., Gerbig, C., Meijer, Y., and Loescher, A.: Carbon Monitoring Satellite (CarbonSat): assessment of atmospheric CO_2 and CH_4 retrieval errors by error parameterization, Atmos. Meas. Tech., 6, 3477-3500, 2013.

Buchwitz et al., 2014: Buchwitz, M., et al.: ESA Climate Change Initiative (CCI) Product Specification Document (PSD) for the Essential Climate Variable (ECV) Greenhouse Gases (GHG), 6-June-2014, Version 3, 2014.

Buchwitz et al., 2015: Buchwitz, M., Reuter, M., Schneising, O., Boesch, H., Guerlet, S., Dils, B., Aben, I., Armante, R., Bergamaschi, P., Blumenstock, T., Bovensmann, H., Brunner, D., Buchmann, B., Burrows, J.P., Butz, A., Chédin, A., Chevallier, F., Crevoisier, C.D., Deutscher, N.M., Frankenberg, C., Hase, F., Hasekamp, O.P., Heymann, J., Kaminski, T., Laeng, A., Lichtenberg, G., De Mazière, M., Noël, S., Notholt, J., Orphal, J., Popp, C., Parker, R., Scholze, M., Sussmann, R., Stiller, G.P., Warneke, T., Zehner, C., Bril, A., Crisp, D., Griffith, D.W.T., Kuze, A., O'Dell, C., Oshchepkov, S., Sherlock, V., Suto, H., Wennberg, P., Wunch, D., Yokota, T., Yoshida, Y., The Greenhouse Gas Climate Change Initiative (GHG-CCI): comparison and quality assessment of near-surface-sensitive satellite-derived CO2 and CH4 global data sets. Remote Sens. Environ. 162:344–362, http://dx.doi.org/10.1016/j.rse.2013.04.024, 2015.

Buchwitz et al., 2016: Buchwitz, M., Reuter, M., Schneising, O., Hewson, W., Detmers, R. G., Boesch, H., Hasekamp, O. P., Aben, I., Bovensmann, H., Burrows, J. P., Butz, A., Chevallier, F., Dils, B., Frankenberg, C., Heymann, J., Lichtenberg, G., De Mazière, M., Notholt, J., Parker, R., Warneke, T., Zehner, C., Griffith, D. W. T., Deutscher, N. M., Kuze, A., Suto, H., and Wunch, D.:, Global satellite observations of column-averaged carbon dioxide and methane: The GHG-CCI XCO_2 and XCH_4 CRDP3 data, Remote Sensing of Environment (in press), Special Issue on Essential Climate Variables, DOI: 10.1016/j.rse.2016.12.027, (link: http://dx.doi.org/10.1016/j.rse.2016.12.027), 2016.

Buchwitz et al., 2016a: Buchwitz, M.; Reuter, M.; Aben, I.; Boesch, H.; Butz, A.; Detmers, R.G.; Frankenberg, C.; Hasekamp, O.P.; Parker, R.; Schneising, O.; Somkuti, P., ESA Greenhouse Gases Climate Change Initiative (GHG-CCI): Merged SCIAMACHY and GOSAT Level 3 gridded atmospheric column-average methane (XCH_4) product in Obs4MIPs format, Centre for Environmental Data Analysis, 10 October 2016, pp. 11, 2016.

Buchwitz et al., 2017: ESA Climate Change Initiative (CCI) Product Validation and Intercomparison Report (PVIR) for the Essential Climate Variable (ECV) Greenhouse Gases (GHG) for data set Climate Research Data Package No. 4 (CRDP#4), Version 5.0, 9. Feb. 2017, 2017.

Buchwitz et al., 2017a: Buchwitz, M.; Reuter, M.; Aben, I.; Boesch, H.; Butz, A.; Detmers, R.G.; Frankenberg, C.; Hasekamp, O.P.; Parker, R.; Schneising, O.; Somkuti, P., ESA Greenhouse Gases Climate Change Initiative (GHG-CCI): Merged SCIAMACHY and GOSAT Level 3 gridded atmospheric column-average methane (XCH_4) product in Obs4MIPs format version 2 (CRDP#4), Technical Note, pp. 11, 1 February 2017, 2017.

Buchwitz et al., 2018: Buchwitz, M., Reuter, M., Schneising, O., Noel, S., Gier, B., Bovensmann, H., Burrows, J. P., Boesch, H., Anand, J., Parker, R. J., Somkuti, P., Detmers, R. G., Hasekamp, O. P., Aben, I., Butz, A., Kuze, A., Suto, H., Yoshida, Y., Crisp, D., and O'Dell, C., Computation and analysis of atmospheric carbon dioxide annual mean growth rates from satellite observations during 2003-2016, Atmos. Chem. Phys., 18, 17355-17370, https://doi.org/10.5194/acp-18-17355-2018, 2018.

Burrows et al., 1995: Burrows, J. P., Hölzle, E., Goede, A. P. H., Visser, H., and Fricke, W., SCIAMACHY—Scanning Imaging Absorption Spectrometer for Atmospheric Chartography, Acta Astronaut., 35(7), 445–451, doi:10.1016/0094-5765(94)00278-t, 1995.

Butz et al., 2011: Butz, A., Guerlet, S., Hasekamp, O., et al., Toward accurate CO_2 and CH_4 observations from GOSAT, *Geophys. Res. Lett.*, doi:10.1029/2011GL047888, 2011.

Butz et al., 2012: Butz, A., Galli, A., Hasekamp, O., Landgraf, J., Tol, P., and Aben, I.: Remote Sensing of Environment, TROPOMI aboard Sentinel-5 Precursor : Prospective performance of CH_4 retrievals for aerosol and cirrus loaded atmospheres, 120, 267-276, doi:10.1016/j.rse.2011.05.030, 2012.

Chédin et al. 2003: Chédin, A., Saunders, R., Hollingsworth, A., Scott, N. A., Matricardi, M., Etcheto, J., Clerbaux, C., Armante, R. and Crevoisier, C.: The feasibility of monitoring CO_2 from high resolution infrared sounders. J. Geophys. Res., 108, ACH 6-1–6-19, doi: 10.1029/2001JD001443, 2003.

Chevallier et al., 2005: Chevallier, F., R. J. Engelen, and P. Peylin, The contribution of AIRS data to the estimation of CO_2 sources and sinks. Geophys. Res. Lett., 32, L23801, doi:10.1029/ 2005GL024229, 2005.

Chevallier et al., 2007: Chevallier, F., F.-M. Bréon, and P. J. Rayner, Contribution of the Orbiting Carbon Observatory to the estimation of CO_2 sources and sinks: Theoretical study in a variational data assimilation framework. J. Geophys. Res., 112, D09307, doi:10.1029/2006JD007375, 2007.

Chevallier et al., 2009a: Chevallier, F., R. J. Engelen, C. Carouge, T. J. Conway, P. Peylin, C. Pickett-Heaps, M. Ramonet, P. J. Rayner and I. Xueref-Remy, AIRS-based vs. surface-based estimation of carbon surface fluxes. J. Geophys. Res., 114, D20303, doi:10.1029/2009JD012311, 2009.

Chevallier et al., 2009b: Chevallier, F., S. Maksyutov, P. Bousquet, F.-M. Bréon, R. Saito, Y. Yoshida, and T. Yokota, On the accuracy of the CO_2 surface fluxes to be estimated from the GOSAT observations. Geophys. Res. Lett., 36, L19807, doi:10.1029/2009GL040108, 2009.

Chevallier et al., 2010: Chevallier, F., Feng, L., Boesch, H. Palmer, P., and Rayner, P., On the impact of transport model errors for the estimation of CO_2 surface fluxes from GOSAT observations, Geophys. Res. Let., 37, L21803, 2010.

Chevallier et al., 2014: Chevallier, F., Palmer, P.I., Feng, L., Boesch, H., O'Dell, C.W., Bousquet, P., Towards robust and consistent regional CO_2 flux estimates from in situ and space-borne measurements of atmospheric CO_2, Geophys. Res. Lett., 41, 1065-1070, DOI: 10.1002/2013GL058772, 2014.

Chevallier et al., 2016b: Chevallier, F., et al., Climate Assessment Report (CAR), ESA Climate Change Initiative (CCI) GHG-CCI project, Version 3, 3 May 2016, 2016.

Ciais et al., 2014: Ciais, P., Dolman, A. J., Bombelli, A., et al.: Current systematic carbon cycle observations and needs for implementing a policy-relevant carbon observing system, Biogeosciences, 11, 3547-3602, www.biogeosciences.net/11/3547/2014/, doi:10.5194/bg-11-3547-2014, 2014.

Ciais et al., 2015: Ciais, P., et al.: Towards a European Operational Observing System to Monitor Fossil CO_2 emissions - Final Report from the expert group, http://www.copernicus.eu/main/towards-european-operational-observing-system-monitor-fossil-co2-emissions, pp. 68, October 2015, 2015.

CMUG-RBD, 2010: Climate Modelling User Group Requirements Baseline Document, Deliverable 1.2, Number D1.2, Version 1.3, 2 Nov 2010.

Cogan et al., 2011: Cogan, A. J., Boesch, H., Parker, R. J., et al., Atmospheric carbon dioxide retrieved from the Greenhouse gases Observing SATellite (GOSAT): Comparison with ground-based TCCON observations and GEOS-Chem model calculations, *J. Geophys. Res.*, 117, D21301, doi:10.1029/2012JD018087, 2012.

Corbin et al., 2008: Corbin, K. D., A. S. Denning, L. Lu, J.-W. Wang, and I. T. Baker, Possible representation errors in inversions of satellite CO_2 retrievals, J. Geophys. Res., 113, D02301, doi:10.1029/2007JD008716, 2008.

Cressot et al., 2014: Cressot, C., F. Chevallier, P. Bousquet, et al., On the consistency between global and regional methane emissions inferred from SCIAMACHY, TANSO-FTS, IASI and surface measurements, Atmos. Chem. Phys., 14, 577-592, 2014.

Crevoisier et al., 2004: Crevoisier, C., S. Heilliette, A. Chédin, S. Serrar, R. Armante, and N. A. Scott, Midtropospheric CO_2 concentration retrieval from AIRS observations in the tropics, Geophys. Res. Lett., 31, L17106, doi:10.1029/2004GL020141, 2004.

Chevallier et al., 2005: Chevallier, F., R. J. Engelen, and P. Peylin, The contribution of AIRS data to the estimation of CO_2 sources and sinks. Geophys. Res. Lett., 32, L23801, doi:10.1029/ 2005GL024229, 2005.

Crevoisier et al., 2004: Crevoisier, C., S. Heilliette, A. Chédin, S. Serrar, R. Armante, and N. A. Scott, Midtropospheric CO_2 concentration retrieval from AIRS observations in the tropics, Geophys. Res. Lett., 31, L17106, doi:10.1029/2004GL020141, 2004.

Crevoisier et al., 2009: Crevoisier, C., Chédin, A., Matsueda, H., et al., First year of upper tropospheric integrated content of CO_2 from IASI hyperspectral infrared observations, *Atmos. Chem. Phys.*, 9, 4797-4810, 2009.

Crevoisier et al. 2009b: Crevoisier, C., Nobileau, D., Fiore, A., Armante, R., Chédin, A., and Scott, N. A.: Tropospheric methane in the tropics – first year from IASI hyperspectral infrared observations, Atmos. Chem. Phys., 9, 6337–6350, doi:10.5194/acp-9-6337-2009, 2009b.

Crevoisier et al., 2013: Crevoisier, C., Nobileau, D., Armante, R., et al., The 2007–2011 evolution of tropical methane in the mid-troposphere as seen from space by MetOp-A/IASI, *Atmos. Chem. Phys.*, 13, 4279-4289, 2013.

Crisp et al., 2004: Crisp, D., Atlas, R. M., Breon, F.-M., Brown, L. R., Burrows, J. P., Ciais, P., Connor, B. J., Doney, S. C., Fung, I. Y., Jacob, D. J., Miller, C. E., O'Brien, D., Pawson, S., Randerson, J. T., Rayner, P., Salawitch, R. S., Sander, S. P., Sen, B., Stephens, G. L., Tans, P. P., Toon, G. C., Wennberg, P. O., Wofsy, S. C., Yung, Y. L., Kuang, Z., Chudasama, B., Sprague, G., Weiss, P., Pollock, R., Kenyon, D., and Schroll, S.: The Orbiting Carbon Observatory (OCO) mission, Adv. Space Res., 34, 700-709, 2004.

Detmers et al., 2015: Detmers, R. G., O. Hasekamp, I. Aben, S. Houweling, T. T. van Leeuwen, A. Butz, J. Landgraf, P. Koehler, L. Guanter, and B. Poulter, Anomalous carbon uptake in Australia as seen by GOSAT, Geophys. Res. Lett., 42, doi:10.1002/2015GL065161, 2015.

Dils et al., 2014: B. Dils, M. Buchwitz, M. Reuter, O. Schneising, H. Boesch, R. Parker, S. Guerlet, I. Aben, T. Blumenstock, J. P. Burrows, A. Butz, N. M. Deutscher, C. Frankenberg, F. Hase, O. P. Hasekamp, J. Heymann, M. De Mazière, J. Notholt, R. Sussmann, T. Warneke, D. Griffith, V. Sherlock, D. Wunch :The Greenhouse Gas Climate Change Initiative (GHG-CCI): Comparative validation of GHG-CCI SCIAMACHY/ENVISAT and TANSO-FTS/GOSAT CO_2 and CH_4 retrieval algorithm products with measurements from the TCCON network, Atmos. Meas. Tech., 7, 1723-1744, 2014.

ESA-CCI-GHG-URDv2.1: Chevallier, F., et al., User Requirements Document (URD), ESA Climate Change Initiative (CCI) GHG-CCI project, Version 2.1, 19 Oct 2016, 2016.

Frankenberg et al., 2011: Frankenberg, C., Aben, I., Bergamaschi, P., et al., Global column-averaged methane mixing ratios from 2003 to 2009 as derived from SCIAMACHY: Trends and variability, *J. Geophys. Res.*, doi:10.1029/2010JD014849, 2011.

GCOS-154: Global Climate Observing System (GCOS): SYSTEMATIC OBSERVATION REQUIREMENTS FOR SATELLITE-BASED DATA PRODUCTS FOR CLIMATE - 2011 Update - Supplemental details to the satellite-based component of the "Implementation Plan for the Global Observing System for Climate in Support of the UNFCCC (2010 Update)", December 2011, prepared by World Meteorological Organization (WMO), Intergovernmental Oceanographic Commission, United Nations Environment Programme (UNEP), International Council for Science, Doc.: GCOS 154, link: http://cci.esa.int/sites/default/files/gcos-154.pdf, 2011.

GCOS-200: The Global Observing System for Climate: Implementation Needs, World Meteorological Organization (WMO), GCOS-200 (GOOS-214), pp. 325, link:

http://unfccc.int/files/science/workstreams/systematic_observation/application/pdf/gcos_ip_10oct2016.pdf, 2016.

Guerlet et al., 2013: Guerlet, S., S. Basu, A. Butz, M. Krol, P. Hahne, S. Houweling, O. P. Hasekamp and I. Aben, Reduced carbon uptake during the 2010 Northern Hemisphere summer from GOSAT, Geophys. Res. Lett., doi: 10.1002/grl.50402, 2013.

Hayman et al., 2014: Hayman, G. D., O'Connor, F. M., Dalvi, M., Clark, D. B., Gedney, N., Huntingford, C., Prigent, C., Buchwitz, M., Schneising, O., Burrows, J. P., Wilson, C., Richards, N., Chipperfield, M., Comparison of the HadGEM2 climate-chemistry model against in-situ and SCIAMACHY atmospheric methane data, Atmos. Chem. Phys., 14, 13257-13280, doi:10.5194/acp-14-13257-2014, 2014.

Hollmann et al., 2013: Hollmann, C.J. Merchant, R. Saunders, C. Downy, M. Buchwitz, A. Cazenave, E. Chuvieco, P. Defourny, G. de Leeuw, R. Forsberg, T. Holzer-Popp, F. Paul, S. Sandven, S. Sathyendranath, M. van Roozendael, W. Wagner, The ESA Climate Change Initiative: satellite data records for essential climate variables, Bulletin of the American Meteorological Society (BAMS), 0.1175/BAMS-D-11-00254.1, pp. 12, 2013.

Houweling et al., 2004: Houweling, S., Breon, F.-M., Aben, I., Rödenbeck, C., Gloor, M., Heimann, M. and Ciais, P.: Inverse modeling of CO_2 sources and sinks using satellite data: A synthetic inter-comparison of measurement techniques and their performance as a function of space and time, Atmos. Chem. Phys., 4, 523-538, 2004.

Houweling et al., 2005: Houweling, S., Hartmann, W., Aben, I., Schrijver, H., Skidmore, J., Roelofs, G.-J., and Breon, F.-M.: Evidence of systematic errors in SCIAMACHY-observed CO_2 due to aerosols, Atmos. Chem. Phys., 5, 3003–3013, 2005.

Houweling et al., 2015: Houweling, S., D. Baker, S. Basu, H. Boesch, A. Butz, F. Chevallier, F. Deng, E. J. Dlugokencky, L. Feng, A. Ganshin, O. Hasekamp, D. Jones, S. Maksyutov, J. Marshall, T. Oda, C.W. O'Dell1, S. Oshchepkov, P. I. Palmer, P. Peylin, Z. Poussi, F. Reum, H. Takagi, Y. Yoshida, and R. Zhuravlev, An intercomparison of inverse models for estimating sources and sinks of CO_2 using GOSAT measurements, J. Geophys. Res. Atmos., 120, 5253–5266, doi:10.1002/2014JD022962, 2015.

Hu et al., 2018: Hu, H., J. Landgraf, R. Detmers, T. Borsdorff, J. Aan de Brugh, I. Aben, A. Butz, O. Hasekamp, Toward Global Mapping of Methane With TROPOMI: First Results and Intersatellite Comparison to GOSAT, Geophys. Res. Lett, Vol. 45, Issue 8, 3682-3689, https://doi.org/10.1002/2018GL077259, 2018.

Hungershoefer et al., 2010: Hungershoefer, K., Breon, F.-M., Peylin, P., Chevallier, F., Rayner, P., Klonecki, A., Houweling, S., and Marshall, J., Evaluation of various observing systems for the global monitoring of CO_2 surface fluxes, Atmos. Chem. Phys., 10, 10503-10520, 2010.

IPCC, 2013: Climate Change 2013: The Physical Science Basis, Working Group I Contribution to the Fifth Assessment Report of the Intergovernmental Report on Climate Change, http://www.ipcc.ch/report/ar5/wg1/, 2013.

JCGM, 2008: JCGM/WG 1, Working Group 1 of the Joint Committee for Guides in Metrology, Evalutation of measurement data – Guide to the expression of uncertainty in measurement, http://www.bipm.org/utils/common/documents/jcgm/JCGM_100_2008_E.pdf, 2008.

Kirschke et al., 2013: Kirschke, S., Bousquet, P., Ciais, P., et al.: Three decades of global methane sources and sinks, Nat. Geosci., 6, 813–823, doi:10.1038/ngeo1955, 2013.

Kuze et al., 2009: Kuze, A., Suto, H., Nakajima, M., and Hamazaki, T. (2009), Thermal and near infrared sensor for carbon observation Fourier-transform spectrometer on the Greenhouse Gases Observing Satellite for greenhouse gases monitoring, Appl. Opt., 48, 6716–6733, 2009.

Kuze et al., 2014: Kuze, A., Taylor, T., Kataoka, F., Bruegge, C., Crisp, D., Harada, M., Helmlinger, M., Inoue, M., Kawakami, S., Kikuchi, N., Mitomi, Y., Murooka, J., Naitoh, M., O'Brien, D., O'Dell, C., Ohyama, H., Pollock, H., Schwandner, F., Shiomi, K., Suto, H., Takeda, T., Tanaka, T., Urabe, T., Yokota, T., and Yoshida, Y. (2014), Long-term vicarious calibration of GOSAT short-wave sensors: techniques for error reduction and new estimates of radiometric degradation factors, IEEE T. Geosci. Remote, 52, 3991–4004, doi:10.1109/TGRS.2013.2278696, 2014.

Kuze et al., 2016: Kuze, A., Suto, H., Shiomi, K., Kawakami, S., Tanaka, M., Ueda, Y., Deguchi, A., Yoshida, J., Yamamoto, Y., Kataoka, F., Taylor, T. E., and Buijs, H. L.: Update on GOSAT TANSO-FTS performance, operations, and data products after more than 6 years in space, Atmos. Meas. Tech., 9, 2445-2461, doi:10.5194/amt-9-2445-2016, 2016.

Lauer et al., 2017: Lauer, A., Eyring, V., Righi, M., Buchwitz, M., Defourny, P., Evaldsson, M., Friedlingstein, P., de Jeu, R., de Leeuw, G., Loew, A., Merchant, C. J., Mueller, B., Popp, T., Reuter, M., Sandven, S., Senftleben, D., Stengel, M., Van Roozendael, M., Wenzel, S., and Willen, U.: Benchmarking CMIP5modelswith a subset of ESA CCI Phase 2 data using the ESMValTool, Remote Sensing of Environment 203, 9-39, http://dx.doi.org/10.1016/j.rse.2017.01.007, 2017.

Machida et al. 2008: Machida, T., Matsueda, H., Sawa, Y., Nakagawa, Y., Hirotani, K., Kondo, N., Goto, K., Nakazawa, T., Ishikawa, K., and Ogawa, T.: Worldwide measurements of atmospheric CO_2 and other trace gas species using commercial airlines, J. Atmos. Ocean. Tech., 25(10), 1744–1754, doi:10.1175/2008JTECHA1082.1, 2008.

Massart et al., 2016: Massart, S., A. Agustí-Panareda, J. Heymann, M. Buchwitz, F. Chevallier, M. Reuter, M. Hilker, J. P. Burrows, N. M. Deutscher, D. G. Feist, F. Hase, R. Sussmann, F. Desmet, M. K. Dubey, D. W. T. Griffith, R. Kivi, C. Petri, M. Schneider, V. A. Velazco, Ability of the 4-D-Var analysis of the GOSAT BESD XCO_2 retrievals to characterize atmospheric CO_2 at large and synoptic scales, Atmos. Chem. Phys., 16, 1653-1671, doi:10.5194/acp-16-1653-2016, 2016.

Matsueda et al. 2008: Matsueda, H., Machida, T., Sawa, Y., Nakagawa, Y., Hirotani, K., Ikeda, H., Kondo, N., and Goto, K.: Evaluation of atmospheric CO_2 measurements from new flask air sampling of JAL airliner observation, Pap. Meteorol. Geophys., 59, 1–17, 2008.

McNorton et al., 2016: McNorton, J., E. Gloor, C. Wilson, G. D. Hayman, N. Gedney, E. Comyn-Platt, T. Marthews, R. J. Parker, H. Boesch, and M. P. Chipperfield, Role of regional wetland emissions in atmospheric methane variability, Geophys. Res. Lett., 43, doi:10.1002/2016GL070649, 2016.

Meirink et al., 2006: Meirink, J.-F., Eskes, H. J., and Goede, A. P. H., Sensitivity analysis of methane emissions derived from SCIAMACHY observations through inverse modelling, Atmos. Chem. Phys., 6, 1275-1292, 2006.

Membrive et al. 2016: Membrive, O., Crevoisier, C., Sweeney, C., Danis, F., Hertzog, A., Engel, A., Bönisch, H., and Picon, L.: AirCore-HR: A high resolution column sampling to enhance the vertical description of CH_4 and CO_2, Atmos. Meas. Tech. Discuss., doi:10.5194/amt-2016-236, 2016.

Miller et al., 2007: Miller, C. E., Crisp, D., DeCola, P. L., et al.: Precision requirements for space-based XCO2 data, J. Geophys. Res., 112, D10314, doi:10.1029/2006JD007659, 2007.

Nisbet et al., 2014: Nisbet, E., Dlugokencky, E., and Bousquet, P.: Methane on the rise – again, Science, 343, 493–495, doi:10.1126/science.1247828, 2014.

Pandey et al., 2016: Pandey, S., S. Houweling, M. Krol, I. Aben, F. Chevallier, E. J. Dlugokencky, L. V. Gatti, E. Gloor, J. B. Miller, R. Detmers, T. Machida, T. Roeckmann, Inverse modeling of GOSAT-retrieved ratios of total column CH_4 and CO_2 for 2009 and 2010, Atmos. Chem. Phys., 16, 5043–5062, doi:10.5194/acp-16-5043-2016, 2016.

Parker et al., 2011: Parker, R., Boesch, H., Cogan, A., et al., Methane Observations from the Greenhouse gases Observing SATellite: Comparison to ground-based TCCON data and Model Calculations, *Geophys. Res. Lett.*, doi:10.1029/2011GL047871, 2011.

Parker et al., 2016: Parker, R. J., H. Boesch, M. J. Wooster, D. P. Moore, A. J. Webb, D. Gaveau, and D. Murdiyarso, Atmospheric CH4 and CO2 enhancements and biomass burning emission ratios derived from satellite observations of the 2015 Indonesian fire plumes, Atmos. Chem. Phys., Atmos. Chem. Phys., 16, 10111-10131, doi:10.5194/acp-16-10111-2016, 2016.

Pillai et al., 2016: Pillai, D., Buchwitz, M., Gerbig, C., Koch, T., Reuter, M., Bovensmann, H., Marshall, J., and Burrows, J. P.: Tracking city CO_2 emissions from space using a high resolution inverse modeling approach: A case study for Berlin, Germany, Atmos. Chem. Phys., 16, 9591-9610, doi:10.5194/acp-16-9591-2016, 2016.

PQAR GHG, 2017: Buchwitz, M., Aben, I., Anand, J., Armante, R., Boesch, H., Crevoisier, C., Detmers, R. G., Hasekamp, O. P., Reuter, M., Schneising-Weigel, O., et al., Product Quality Assessment Report (PQAR) – Main document, C3S project C3S_312a_Lot6_IUP-UB – Greenhouse Gases, v1.1, 2017.

PQAR GHG, 2018: Buchwitz, M., Aben, I., Anand, J., Armante, R., Boesch, H., Crevoisier, C., Detmers, R. G., Hasekamp, O. P., Reuter, M., Schneising-Weigel, O., et al., Product Quality Assessment Report (PQAR) – Main document, C3S project C3S_312a_Lot6_IUP-UB – Greenhouse Gases, v2.0, 2018.

PQAR GHG, 2019: Buchwitz, M., Aben, I., J., Armante, R., Boesch, H., Crevoisier, C., Di Noia, A., Hasekamp, O. P., Reuter, M., Schneising-Weigel, O., Wu, L.., Product Quality Assessment Report (PQAR) – Main document for Greenhouse Gas (GHG: CO_2 & CH_4) data set CDR 3 (2003-2018), C3S project C3S_312b_Lot2_DLR, v3.0, 2019.

PQAR GHG, 2020: Buchwitz, M., Aben, I., J., Armante, R., Boesch, H., Crevoisier, C., Di Noia, A., Hasekamp, O. P., Reuter, M., Schneising-Weigel, O., Wu, L.., Product Quality Assessment Report (PQAR) – Main document for Greenhouse Gas (GHG: CO_2 & CH_4) data set CDR 4 (2003-2019), C3S project C3S_312b_Lot2_DLR, v4.0, 2020.

Rayner and O'Brien, 2001: Rayner, P. J., and O'Brien, D.M.: The utility of remotely sensed CO_2 concentration data in surface inversions, Geophys. Res. Lett., 28, 175-178, 2001.

Reuter et al. 2011: Reuter, M., Bovensmann, H., Buchwitz, M., Burrows, J. P., Connor, B. J., Deutscher, N. M., Griffith, D.W. T., Heymann, J., Keppel-Aleks, G., Messerschmidt, J., and et al.: Retrieval of atmospheric CO_2 with enhanced accuracy and precision from SCIAMACHY: Validation with FTS measurements and comparison with model results., Journal of Geophysical Research, 116, doi:10.1029/2010JD015047, URL http://dx.doi.org/10.1029/2010JD015047, 2011.

Reuter et al., 2013: Reuter, M. H. Bösch, H. Bovensmann, A. Bril, M. Buchwitz, A. Butz, J. P. Burrows, C. W. O'Dell, S. Guerlet, O. Hasekamp, J. Heymann, N. Kikuchi, S. Oshchepkov, R. Parker, S. Pfeifer, O. Schneising, T. Yokota, and Y. Yoshida, A joint effort to deliver satellite retrieved atmospheric CO_2 concentrations for surface flux inversions: The ensemble median algorithm EMMA, Atmos. Chem. Phys., 13, 1771-1780, 2013.

Reuter et al., 2014a: Reuter, M., M. Buchwitz, A. Hilboll, A. Richter, O. Schneising, M. Hilker, J. Heymann, H. Bovensmann and J. P. Burrows, Decreasing emissions of NOx relative to CO_2 in East Asia inferred from satellite observations, Nature Geoscience, 28 Sept. 2014, doi:10.1038/ngeo2257, pp.4, 2014.

Reuter et al., 2014b: Reuter, M., M. Buchwitz, M. Hilker, J. Heymann, O. Schneising, D. Pillai, H. Bovensmann, J. P. Burrows, H. Bösch, R. Parker, A. Butz, O. Hasekamp, C. W. O'Dell, Y. Yoshida, C. Gerbig, T. Nehrkorn, N. M. Deutscher, T. Warneke, J. Notholt, F. Hase, R. Kivi, R. Sussmann, T. Machida, H. Matsueda, and Y. Sawa, Satellite-inferred European carbon sink larger than expected, Atmos. Chem. Phys., 14, 13739-13753, doi:10.5194/acp-14-13739-2014, 2014.

Reuter et al., 2016: Reuter, M.; Buchwitz, M.; Aben, I.; Boesch, H.; Butz, A.; Detmers, R.G.; Hasekamp, O.P.; Heymann, J.; Parker, R.; Schneising, O.; Somkuti, P., ESA Greenhouse Gases Climate Change Initiative (GHG_cci): Merged SCIAMACHY and GOSAT Level 3 gridded atmospheric column-average carbon dioxide (XCO_2) product in Obs4MIPs format. Centre for Environmental Data Analysis, 10 October 2016, doi:10.5285/3FAE8371-0CBB-4B21-9EA6-7A1FC293C4A2pp. 11, 2016.

Reuter et al., 2017: Reuter, M., M. Buchwitz, M. Hilker, J. Heymann, H. Bovensmann, J. Burrows, S. Houweling, Y. Liu, R. Nassar, F. Chevallier, P. Ciais, J. Marshall, and M. Reichstein, 2016: How much CO_2 is taken up by the European terrestrial biosphere ?, Bull. Amer. Meteor. Soc. doi:10.1175/BAMS-D-15-00310.1, 24 April 2017, 665-671, 2017.

Reuter et al., 2017a: Reuter, M.; Buchwitz, M.; Aben, I.; Boesch, H.; Butz, A.; Detmers, R.G.; Hasekamp, O.P.; Heymann, J.; Parker, R.; Schneising, O.; Somkuti, P., ESA Greenhouse Gases Climate Change Initiative (GHG-CCI): Merged SCIAMACHY and GOSAT Level 3 gridded atmospheric column-average carbon dioxide (XCO_2) product in Obs4MIPs format version 2 (CRDP#4), Technical Note, pp. 11, 1 February 2017, 2017.

Reuter et al., 2020: Reuter, M., Buchwitz, M., Schneising, O., Noel, S., Bovensmann, H., Burrows, J. P., Boesch, H., Di Noia, A., Anand, J., Parker, R. J., Somkuti, P., Wu, L., Hasekamp, O. P., Aben, I., Kuze, A., Suto, H., Shiomi, K., Yoshida, Y., Morino, I., Crisp, D., O'Dell, C. W., Notholt, J., Petri, C., Warneke, T., Velazco, V. A., Deutscher, N. M., Griffith, D. W. T., Kivi, R., Pollard, D. F., Hase, F., Sussmann, R., Te, Y. V., Strong, K., Roche, S., Sha, M. K., De Maziere, M., Feist, D. G., Iraci, L. T., Roehl, C. M., Retscher, C., and Schepers, D.: Ensemble-based satellite-derived carbon dioxide and methane column-averaged dry-air mole fraction data sets (2003-2018) for carbon and climate applications, Atmos. Meas. Tech., 13, 789-819, https://doi.org/10.5194/amt-13-789-2020, 2020.

Rodgers, 2000: Rodgers C. D.: Inverse Methods for Atmospheric Sounding: Theory and Practice, World Scientific Publishing, 2000.

Ross et al., 2013: Ross, A. N., Wooster, M. J., Boesch, H., Parker, R., First satellite measurements of carbon dioxide and methane emission ratios in wildfire plumes, Geophys. Res. Lett., 40, 1-5, doi:10.1002/grl.50733, 2013.

Schaefer et al., 2016: Schaefer, H., Mikaloff Fletcher, S. E., Veidt, C., Lassey, K. R., Brailsford, G. W., Bromley, T. M., Dlugokencky, E. J., Michel, S. E., Miller, J. B., Levin, I., Lowe, D. C., Martin, R. J., Vaughn, B. H., and White, J. W. C.: A 21st-century shift from fossil-fuel to biogenic methane emissions indicated by $^{13}CH_4$, Science, Vol. 352, Issue 6281, pp. 80-84, doi 10.1126/science.aad2705, 2016.

Shindell et al., 2013: Shindell, D. T., Pechony, O., Voulgarakis, A., et al. (2013), Interactive ozone and methane chemistry in GISS-E2 historical and future climate simulations, Atmos. Chem. Phys., 13, 2653–2689, doi:10.5194/acp-13-2653-2013, 2013.

Schepers et al., 2012: Schepers, D., Guerlet, S., Butz, A., Landgraf, J., Frankenberg, C., Hasekamp, O., Blavier, J.-F., Deutscher, N. M., Griffith, D. W. T., Hase, F., Kyro, E., Morino, I., Sherlock, V., Sussmann, R., Aben, I. (2012), Methane retrievals from Greenhouse Gases Observing Satellite (GOSAT) shortwave infrared measurements: Performance comparison of proxy and physics retrieval algorithms, J. Geophys. Res., 117, D10307, doi:10.1029/2012JD017549, 2012.

Schneising et al., 2011: Schneising, O., Buchwitz, M., Reuter, M., et al., Long-term analysis of carbon dioxide and methane column-averaged mole fractions retrieved from SCIAMACHY, *Atmos. Chem. Phys*., 11, 2881-2892, 2011.

Schneising et al., 2014a: Schneising, O., Reuter, M., Buchwitz, M., Heymann, J., Bovensmann, H., and Burrows, J. P., Terrestrial carbon sink observed from space: variation of growth rates and seasonal cycle amplitudes in response to interannual surface temperature variability, Atmos. Chem. Phys., 14, 133-141, 2014.

Schneising et al., 2014b: Schneising, O., Burrows, J. P., Dickerson, R. R., Buchwitz, M., Reuter, M., Bovensmann, H., Remote sensing of fugitive methane emissions from oil and gas production in North American tight geologic formations, Earth's Future, 2, DOI: 10.1002/2014EF000265, pp. 11, 2014.

TRD GHG, 2017: Buchwitz, M., Aben, I., Anand, J., Armante, R., Boesch, H., Crevoisier, C., Detmers, R. G., Hasekamp, O. P., Reuter, M., Schneising-Weigel, O., Target Requirement Document, Copernicus Climate Change Service (C3S) project on satellite-derived Essential Climate Variable (ECV) Greenhouse Gases (CO_2 and CH_4) data products (project C3S_312a_Lot6), Version 1.3, 20-October-2017, pp. 53, 2017.

TRD GAD GHG, 2020: Buchwitz, M., Aben, I., Armante, R., Boesch, H., Crevoisier, C., Hasekamp, O. P., Wu, L.., Reuter, M., Schneising-Weigel, O., Target Requirement and Gap Analysis Document, Copernicus Climate Change Service (C3S) project on satellite-derived Essential Climate Variable (ECV) Greenhouse Gases (CO_2 and CH_4) data products (project C3S_312b_Lot2), Version 2.11, 9-April-2020, pp. 80, 2020.

Turner et al., 2015: Turner, A. J., D. J. Jacob, K. J. Wecht, J. D. Maasakkers, S. C. Biraud, H. Boesch, K. W. Bowman, N. M. Deutscher, M. K. Dubey, D. W. T. Griffith, F. Hase, A. Kuze, J. Notholt, H. Ohyama, R. Parker, V. H. Payne, R. Sussmann, V. A. Velazco, T. Warneke, P. O. Wennberg, and D. Wunch, Estimating global and North American methane emissions with high spatial resolution using GOSAT satellite data, Atmos. Chem. Phys., 15, 7049-7069, doi:10.5194/acp-15-7049-2015, 2015.

Turner et al., 2016: Turner, A. J., D. J. Jacob, J. Benmergui, S. C. Wofsy, J. D. Maasakkers, A. Butz, O. Hasekamp, and S. C. Biraud, A large increase in U.S. methane emissions over the past decade inferred from satellite data and surface observations, Geophys. Res. Lett., 43, 2218–2224, doi:10.1002/2016GL067987, 2016.

Veefkind et al. 2012: Veefkind, J. P., Aben, I., McMullan, K., Förster, H., De Vries, J., Otter, G., Claas, J., Eskes, H. J., De Haan, J. F., Kleipool, Q., Van Weele, M., Hasekamp, O., Hoogeveen, R., Landgraf, J., Snel, R., Tol, P.,Ingmann, P., Voors, R., Kruizinga, B., Vink, R., Visser, H., and Levelt, P. F.: TROPOMI on the ESA Sentinel-5 Precursor: A GMES mission for global observations of the atmospheric composition for climate, air quality and ozone layer applications. Rem. Sens. Environment, 120:70–83, 2012.

Velazco et al. 2011: Velazco, V. A., Buchwitz, M., Bovensmann, H., Reuter, M., Schneising, O., Heymann, J., Krings, T., Gerilowski, K., and Burrows, J. P.: Towards space based verification of CO2 emissions from strong localized sources: fossil fuel power plant emissions as seen by a CarbonSat constellation, Atmos. Meas. Tech., 4, 2809-2822, 2011.

Wofsy et al. 2012: Wofsy, S. C., Daube, B. C., Jimenez, R., et al.: HIPPO Merged 10-second Meteorology, Atmospheric Chemistry, Aerosol Data (R 20121129), Carbon Dioxide Information Analysis Center, Oak Ridge National Laboratory, Oak Ridge, Tennessee, USA, release 29 November 2012), 2012.

Wunch et al. 2010: Wunch, D., Toon, G. C., Wennberg, P. O., Wofsy, S. C., Stephens, B. B., Fischer, M. L., Uchino, O., Abshire, J. B., Bernath, P., Biraud, S. C., Blavier, J.-F. L., Boone, C., Bowman, K. P., Browell, E. V., Campos, T., Connor, B. J., Daube, B. C., Deutscher, N. M., Diao, M., Elkins, J. W., Gerbig, C., Gottlieb, E., Griffith, D. W. T., Hurst, D. F., Jiménez, R., Keppel-Aleks, G., Kort, E. A., Macatangay, R., Machida, T., Matsueda, H., Moore, F., Morino, I., Park, S., Robinson, J., Roehl, C. M., Sawa, Y., Sherlock, V., Sweeney, C., Tanaka, T., and Zondlo, M. A.: Calibration of the Total Carbon Column Observing Network using aircraft profile data, Atmospheric Measurement Techniques, 3, 1351–1362, doi:10.5194/amt-3-1351-2010, URL http://www.atmos-meas-tech.net/3/1351/2010/, 2010.

Wunch et al. 2011: Wunch, D., Toon, G. C., Blavier, J.-F. L., Washenfelder, R. A., Notholt, J., Connor, B. J., Griffith, D. W. T., Sherlock, V., and Wennberg, P. O.: The Total Carbon Column Observing Network (TCCON), Philosophical Transactions of the Royal Society of London, Series A: Mathematical, Physical and Engineering Sciences, 369, 2087–2112, doi:10.1098/rsta.2010.0240, 2011.

Wunch et al. 2015: Wunch, D., Toon, G.C., Sherlock, V., Deutscher, N.M., Liu, X., Feist, D.G., Wennberg, P.O., The Total Carbon Column Observing Network's GGG2014 Data Version. Carbon Dioxide Information Analysis Center, Oak Ridge National Laboratory, Oak Ridge, Tennessee, USA (available at: doi:10.14291/tccon.ggg2014.documentation.R0/1221662), 2015.

Yoshida et al. 2013: Yoshida, Y., Kikuchi, N., Morino, I., Uchino, O., Oshchepkov, S., Bril, A., Saeki, T., Schutgens, N., Toon, G. C., Wunch, D., Roehl, C. M., Wennberg, P. O., Griffith, D. W. T, Deutscher, N. M., Warneke, T., Notholt, J., Robinson, J., Sherlock, V., Connor, B., Rettinger, M., Sussmann, R., Ahonen, P., Heikkinen, P., Kyrö, E., Mendonca, J., Strong, K., Hase, F., Dohe, S., and Yokota, T.: Improvement of the retrieval algorithm for GOSAT SWIR XCO_2 and XCH_4 and their validation using TCCON data, Atmos. Meas. Tech., 6, 1533–1547, doi:10.5194/amt-6-1533-2013, 2013.

8. Acknowledgement

We acknowledge previous funding by the European Space Agency (ESA) via Climate Change Initiative (CCI) project GHG-CCI. This funding significantly enhanced the quality of the retrieval algorithms and related documentation. This resulted in more mature data products as needed for an operational project such as the Copernicus Climate Change Service (C3S). We also acknowledge the availability of GOSAT data products via the ESA GOSAT Third Party Mission (TPM) archive.

We are also very grateful to the GOSAT team in Japan comprising the Japan Aerospace Exploration Agency (JAXA), the National Institute for Environmental Studies (NIES), and the Ministry of the Environment (MOE) for providing access to the GOSAT Level 1 and Level 2 data products via the GOSAT Data Archive Service (GDAS) hosted by NIES.

We also acknowledge the availability of OCO-2 Level 1 and Level 2 (XCO_2) data products from NASA, which have been used for the generation on the XCO2_EMMA and XCO2_OBS4MIPS products. These products also include OCO-2 XCO_2 retrieved at Univ. Bremen with the FOCAL algorithm. The FOCAL activities would not have been possible without funding from University of Bremen, from the EU H2020 projects CHE (grant agreement ID: 776186) and VERIFY (Grant agreement ID: 776810) and from ESA via project GHG-CCI+.

Last but not least we acknowledge the availability of TCCON data via the TCCON data archive (https://tccondata.org/).

9. List of ANNEXes

The ANNEXes to this main document are the following ANNEXes A – E:

9.1 ANNEX A: PUGS for products CO2_GOS_OCFP, CH4_GOS_OCFP and CH4_OCPR

Describes the GOSAT XCO_2 and XCH_4 Level 2 products generated by University of Leicester, UK.

9.2 ANNEX B: PUGS for products CO2_GOS_SRFP and CH4_GOS_SRFP

Describes the GOSAT XCO_2 and XCH_4 Full Physics (FP) Level 2 products generated by SRON, The Netherlands.

9.3 ANNEX C: PUGS for product CH4_GOS_SRPR

Describes the GOSAT XCH_4 Proxy (PR) Level 2 product generated by SRON, The Netherlands.

9.4 ANNEX D: PUGS for XCO2_EMMA, XCH4_EMMA, XCO2_OBS4MPIS, XCH4_OBS4MIPS

Describes the multi-sensor multi-algorithms merged XCO_2 and XCH_4 Level 2 and 3 products generated by University of Bremen, Germany.

9.5 ANNEX E: PUGS for IASI CO_2 and CH_4 and AIRS CO_2 products

Describes the mid-tropospheric CO_2 and CH_4 products from the IASI instrument series and AIRS generated by LMD/CNRS, France.

These ANNEXes and the corresponding data products are / will be available via the Copernicus Climate Data Store (CDS):
https://cds.climate.copernicus.eu/#!/home

See also Copernicus Climate Change Service (C3S):
https://climate.copernicus.eu/

Copernicus Climate Change Service

ECMWF - Shinfield Park, Reading RG2 9AX, UK

Contact: info@copernicus-climate.eu

climate.copernicus.eu copernicus.eu ecmwf.int